Differentially regulated proteins in breast cancer chemotherapy

A thesis presented to Massey University in partial fulfilment of the requirement for the degree of Doctor of Philosophy in Biochemistry

Henning Koehn

2005

Acknowledgements

First and foremost I would like to thank my supervisors Dr Kathryn Stowell and Dr Richard Isaacs for their support and encouragement during the course of my thesis work. Furthermore, I would also like to express my gratitude to Dr Kathryn Stowell for giving me the opportunity to undertake my studies in her laboratory.

I would also like to thank Massey University for its financial assistance by providing me with a doctoral scholarship.

Moreover, I would very much like to thank all those in the IMBS who have helped with so many different aspects of my research project. Also, I would like to express my appreciation to Dr Fran Wolber and Dr. Bruce Lockett for going the extra mile in helping me with my work.

I very much feel indebted to a few people who have helped make my stay in New Zealand so wonderful and a true Kiwi-experience, including Jamie, Santanu, Amram, Stu, Uwe, Verena, Mark, the Thirsties, and the members of the Twilight zone. Moreover, I am especially grateful to Mathias, Heiko, and Paul, who have proven that distance is not a barrier for friendship.

I would especially like to thank my parents for their relentless support, without whom this would have never been possible.

And a very special thank you goes to my best friend Melanie, for her patience, her help, and her friendship and making sure that the English language did not suffer undue distress in preparation of this thesis.

Abstract

Intrinsic or acquired drug resistance of tumours is a major problem for successful therapy of breast cancer patients. The efficacy of doxorubicin, one of the most important and commonly used drugs in chemotherapy, can be severely compromised by a variety of unspecific mechanisms rendering tumours drug resistant. Little is known however, about the specific events taking place in response to doxorubicin treatment, which may repair doxorubicin-induced damage, leading to drug resistance.

Doxorubicin is a topoisomerase II poison, which interferes with topoisomerase II enzymes during DNA replication, resulting in DNA double-strand breaks. Topoisomerase II enzymes mediate the passage of DNA strands by introducing transient DNA breaks, and are essential for changes in DNA topology during replication. The DNA lesions induced by the combination of topoisomerase II and doxorubicin can be repaired by either non homologous end-joining or homologous recombination repair, as both pathways are specifically responsible for the repair of DNA double-strand breaks. The DNA-dependent protein kinase catalytic subunit in non homologous end-joining and Rad51 in homologous recombination repair are essential for each of these pathways. If it was possible to specifically target these proteins or other antagonistic mechanisms of doxorubicin-induced cell death, which may be activated in response to doxorubicin treatment, chemosensitivity of tumours could be restored and chemotherapy made more effective. Hence it was the purpose of this study to investigate proteome-wide changes in protein expression in response to drug treatment, as well as specifically analysing alterations in the protein levels of the DNA-dependent protein kinase catalytic subunit and Rad51.

Global changes in protein regulation of breast and breast cancer cells were investigated using mass spectrometric and electrophoretic analysis techniques. These experiments however, could not reproducibly identify any genuine drug-induced changes in protein levels, as only proteins of relatively high abundance could be analysed. Immunoblotting results however, showed that Rad51 was differentially regulated in a cell line- and drug dosage-dependent manner, while levels of the DNA-dependent protein kinase catalytic subunit remained largely unchanged. Furthermore, increased levels of topoisomerase II alpha protein were also detected. In addition, immunohistochemical analysis demonstrated that both Rad51 and the DNA-dependent protein kinase catalytic subunit could be independently overexpressed in breast tumours and therefore may represent potential targets for selectively enhancing chemosensitivity of breast cancers.

Abbreviations

ABC	ATP-binding cassette
AcN	Acetonitrile
ATP	Adenosine triphosphate
ATPase	Adenosine triphosphatase
BSA	Bovine serum albumin
°C	Degrees Celsius
CAV2	Caveolin-2
CCND1	Cyclin D1 encoding gene
cDNA	Synthetic DNA, generated from RNA
CHAPS	3-[(3-Cholamidopropyl)dimethylamino]-1-propanesulphonate
CHCA	alpha-cyano-4-hydroxycinnamic acid
dCTP	deoxycytidine-triphosphate
DIGE	Differential gel electrophoresis
DMEM	Dulbecco's modified eagle's media
DMSO	Dimethyl sulfoxide
DNA	Deoxyribonucleicacid
DNA-DSB	DNA double-strand break
DNA-PK	DNA-dependent protein kinase
DNA-PKcs	DNA-dependent protein kinase catalytic subunit
DTT	Dithiothreitol
2DGE	Two dimensional gel electrophoresis
EDTA	Ethylene diamine tetra-acetic acid
EGF	Epidermal growth factor
EGFR	Epidermal growth factor receptor
ER	Estrogen receptor
ESI	Electro spray ionization
FACS	Fluorescence activated cell sorting
FCS	Foetal calf serum
Fig.	Figure
HEPES	N-[2-hydroxyethyl]piperazine-N'-[2-ethane sulfonic acid]
HRR	Homologous recombination repair
HSP	Heat shock protein

ICAT	Isotope-coded affinity tagging
IEF	Isoelectric focusing
IPG	Immobilized pH gradient
kDa	Kilo Dalton
LC	Liquid chromatography
MALDI-MS	Matrix-assisted laser desorption ionisation mass spectrometry
MCE	Multi compartment electrophoresis
MCF12A	Mammary epithelial cell line
MCF7	Mammary epithelial carcinoma cell line
MDA MB 231	Mammary epithelial carcinoma cell line
MDR	Multidrug resistance
MDR1	Multidrug resistance gene
MEM	Eagle's minimal essential media
MRP	Multidrug resistance-associated protein
MS	Mass spectrometry
MS/MS	Tandem mass spectrometry
MudPIT	Multidimensional protein identification technology
MXP	Mitoxantrone resistance associated protein
Mw	Molecular weight
MWCO	Molecular weight cut-off
m/z	Mass per charge
NHEJ	Non homologous end-joining
OC	Over-confluent
PAGE	Polyacrylamide gel electrophoresis
PBS	Phosphate buffered saline
PBSE	Phosphate buffered saline plus EDTA
P-gp	P-glycoprotein
PIKK	Phosphatidylinositol 3-kinase-like kinase
PR	Progesterone receptor
p53	Tumour suppressor protein p53
R	resistant
RP-HPLC	Reversed-phase high performance liquid chromatography
RNase	Ribonuclease
RT	Room temperature

SCX	Strong cation exchange
SDS	Sodium dodecyl sulphate
SELDI-MS	Surface-enhanced laser desorption ionization mass spectrometry
T	Tyrosine
TBST	Tris buffered saline tween 20
TCA	Trichloroacetic acid
TEMED	N,N,N',N'-Tetramethylethylenediamine
TFA	Trifluoroacetic acid
TGF	Transforming growth factor
Topo II alpha	topoisomerase II alpha
T 25, 75, 300	Filter top tissue culture flask of 25, 75, 300 cm^2
2-TCEP	Tris (2-carboxyethyl) phosphine
Xrcc4	X-ray repair cross-complementing protein 4)

List of tables

List of figures

Table of contents

Chapter Two: Materials and Methods

Chapter Seven: Summary and Discussion

Chapter One
Introduction

1.1 Breast Cancer

Breast cancer is the second most common cancer of women worldwide and the leading cause of cancer-related death. The majority of affected women develop breast cancer without a family history of the disease. The chance that a woman will develop invasive breast cancer during her lifetime is 1 in 12 in New Zealand, with incidences increasing with age. The latest reports in New Zealand also predict a future increase in reported breast cancers, while the mortality rate is expected to drop. Although breast cancer can also occur in males, the incidence is extremely low in comparison to the occurrence in females. Chemotherapy is one of the most important and effective ways of killing tumours and curing the patient. Hence, inherent or acquired drug resistance is one of the biggest problems in successful breast cancer chemotherapy today, as the presence of drug resistant tumours is often fatal. As tumours can be resistant to treatment for a variety of reasons it is important to understand these resistance mechanisms so that they can be overcome to improve patient survival (Ministry of Health, New Zealand, 2002).

1.2 Breast Cancer Treatment

The extent of breast cancer is generally classified in four stages (I - IV), with increasing stage reflecting an increased extent of disease. Treatment options (e.g. radiation, hormonal, surgical, chemotherapy or alternative) depend largely on the stage of the cancer. In recent years, major advances in breast cancer therapy have been made with the introduction of tamoxifen, a hormonal treatment, and trastuzumab (herceptin), an anti-erbB2 antibody.

1.2.1 Hormone Treatment

Hormones play a key role in the development of breast cancer, as well as therapy selection. The female sex hormones, estrogen and progesterone, are well-established endocrine steroid regulators that activate their nuclear receptors, (the estrogen receptor (ER) and progesterone receptor (PR), respectively). The activated hormone receptors directly modulate the transcription of their target genes, which include growth factors (such as transforming growth factor alpha, epidermal growth factor, and erbB2), components for cell cycle progression (such as different cyclin proteins), and genes responsible for chromatin structure and general transcription (such as histones). These hormones are also amongst the most serious risk

factors for acquiring breast cancer, when present at elevated levels. ER expression is found in about 60% of primary breast cancers, while only present in 6-10% of normal breast cells, where it controls development and growth. ER expression also serves as a marker for tumour aggressiveness (Dickson and Stancel, 2000; Hanstein *et al.*, 2004; Duffy, 2005).

Breast tumours often differ in estrogen receptor status, which consequently determines the appropriate treatment options. Hormonal treatment "inactivates" the estrogen receptor, which is at the centre of a complex regulatory mechanism promoting tumour growth in malignant cells, and can be particularly effective, as it disrupts proliferation-promoting pathways. Estrogen receptor expressing tumours are the prime target in tamoxifen treatment, which is also used in cancer prevention for women at high risk of developing breast cancer. Tamoxifen presumably inactivates the ER by blocking the interaction of co-activators with the receptor (Jordan and Morrow, 1999; Thiebaud and Secrest, 2001; Hanstein *et al.*, 2004).

1.2.2 Immunotherapy of erbB2

Much of the recent research has focused on erbB2, a transmembrane receptor protein. ErbB2 is a member of the epidermal growth factor receptor family (EGFR), capable of mediating the lateral signal transduction of all EGFRs (Graus-Porta *et al.*, 1997) (Fig. 1.1). These receptors are involved in cancer development as well as tumour proliferation, and survival (Yu and Hung, 2000; Holbro *et al.*, 2003). In particular, erbB2 overexpression plays an important role in cancer progression, and increases tumour aggressiveness, as well as metastatic potential (Yu *et al.*, 1993; Looi *et al.*, 1997; Tan M, 1997). Gene amplification and resultant overexpression of the *erbB2* gene is found in 25-30% of all primary breast cancers. In addition, overexpression of *erbB2* has been found to significantly lower the overall survival rate in breast and ovarian cancer patients (Slamon *et al.*, 1987; Meden *et al.*, 1998). A major breakthrough in recent years however, has been achieved with the development of the recombinant anti-erbB2 antibody, trastuzumab (herceptin). Antibody binding triggers a variety of mechanisms which result in the destruction of the tumour cell, including the down-regulation of *erbB2* expression and erbB2 degradation, as well as triggering an immune cell response, and enhancing sensitivity towards chemotherapy (Sliwkowski *et al.*, 1999). The administration of trastuzumab has led to significantly increased survival rates in patients with erbB2 overexpressing tumours, using trastuzumab alone (Vogel *et al.*, 2001) or in combination with chemotherapeutic drugs (Slamon *et al.*, 2001; Pegram *et al.*, 2004).

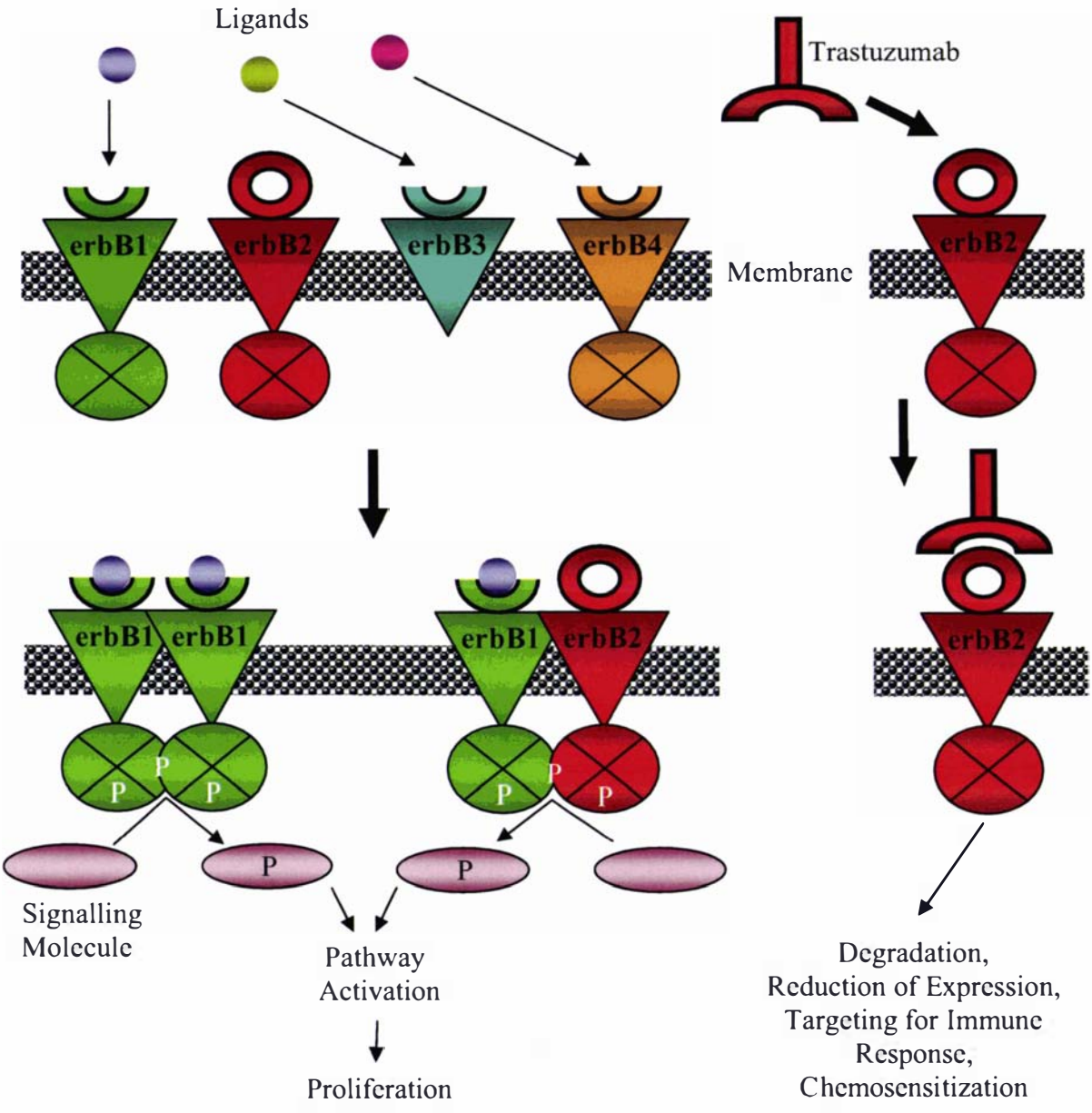

Fig. 1.1: ErbB2 signalling

The epidermal growth factor receptor (EGFR) family consists of four different receptors, erbB1, erbB2, erbB3, and erbB4. Signal transduction by erbB receptors is mediated by ligand specific binding to the extra-cellular receptor domain, which initiates dimerization (only shown for erbB1). As erbB2 does not have a specific ligand it requires the formation of heterodimers with any of the other activated erbB receptors. Indeed erbB2 is the preferred dimerization partner of all other erbB receptors. After activation the intracellular tyrosine kinase domain undergoes autophosphorylation, and subsequently phosphorylates (P) signalling molecules, which leads to the activation of proliferative pathways. The ErbB3 tyrosine kinase is impaired and hence requires erbB2 as dimerization partner for signalling activity. Trastuzumab is an erbB2 specific antibody which inhibits erbB2-mediated signal transduction.

1.3 Chemotherapy

Chemotherapy is one of the most potent forms of cancer therapy. Some of the most common chemotherapeutic agents are cyclophosphamide, taxol, fluorouracil, epirubicin and doxorubicin. Since heterogeneity is a common feature of tumours, treatment usually involves a mixture of these chemotherapeutic drugs most suited to patient requirements. This ensures that a wide range of cancer cells with different susceptibilities can be attacked simultaneously. Generally, a drug-target interaction stimulates a cascade of events, ultimately resulting in apoptosis. This complex pathway will usually involve some type of sensor that detects a death-inducing signal, a signal transduction network, and execution machinery, together mediating the process of cell death.

1.3.1 Drug Categories

Chemotherapeutic agents fall into several categories; alkylators, antimetabolites, topoisomerase II poisons, and microtubulin spindle poisons. The following summarizes the mechanisms of action of these agents and indicates clinical situations in which they may be used.

Alkylators affect cancer cells by crosslinking DNA molecules, blocking DNA repair and replication. Cyclophosphamide is the most commonly used alkylating agent and is employed for the treatment of lung, prostate and cervical cancers, to name a few. Antimetabolites (e.g. Fluorouracil) act as false building blocks in nucleic acid synthesis, causing cell death during division. Antimetabolites may also interfere with DNA and/or RNA synthesis by inhibiting enzymes essential for nucleotide biosynthesis, such as dihydrofolate reductase and thymidilate synthase (Longley *et al.*, 2003). Fluorouracil is used in the treatment of a number of cancers, including breast, liver, colon and pancreas. Topo II poisons include potent inhibitors of DNA replication, which cause DNA damage. Doxorubicin is the most commonly used drug in this category which is utilized to treat a variety of cancers, and plays a pivotal role in breast cancer chemotherapy. Mitotic spindle poisons comprise of two groups: taxanes (such as paclitaxel) stabilize the microtubules; and vinca alkaloids (such as vinorelbine), which inhibit tubulin polymerization (Abal *et al.*, 2003; Zhou and Giannakakou, 2005). Both poisons are used in breast cancer, as well as non small cell lung cancer.

1.3.2 Topoisomerase II Poisons

The first topoisomerase II (topo II) poisons in clinical use, the anthracyclines daunorubicin and its derivative doxorubicin are natural products produced by the Streptomyces species. Anthracycline drugs belong to the most important class of drugs used in chemotherapy, with a wider range of clinical use than any of the other categories of agents. Furthermore, these topo II poisons are relatively easy to combine with other drugs and are therefore often incorporated in combination chemotherapy regimens. In particular doxorubicin, also known as adriamycin, was found to have an extremely broad range of therapeutic activity against tumours and still remains the most important and widely used topo II poison. Other topo II poisons used in chemotherapy include indarubicin, epirubicin, etoposide and mitoxantrone.

Topo II poisons can act as DNA intercalating agents causing single and double-strand DNA breaks, or can form reactive free radicals inflicting oxidative damage upon cellular proteins. As DNA intercalating agents they induce the formation of a covalent topo II-DNA complex, arresting the enzyme-DNA complex in what is known as the cleavable complex, and thus transforming the enzyme into a cellular toxin. Topo II enzymes exert their function by inducing transient double-strand breaks in the DNA molecule allowing for strand passage. This involves binding of the 5'phosphate end by the enzyme, which in the case of a drug intercalating the DNA is shifted relative to the 3'OH end of the DNA during formation of the cleavable complex. The helix unwinding caused by intercalation supposedly leads to the misalignment of the cleavable complex and results in DNA strand breaks. It is also possible for the drug to stabilize the cleavable complex, preventing DNA religation, and to induce collisions with proteins tracking along the DNA, such as polymerases, which results in irreversible DNA double-strand breaks (Fig. 1.2) (Robert and Larsen, 1998; Kellner *et al.*, 2002). The accumulation of these irreversible DNA double-strand breaks eventually activates a series of cellular processes, resulting in cell necrosis or apoptosis (Topcu, 2001)

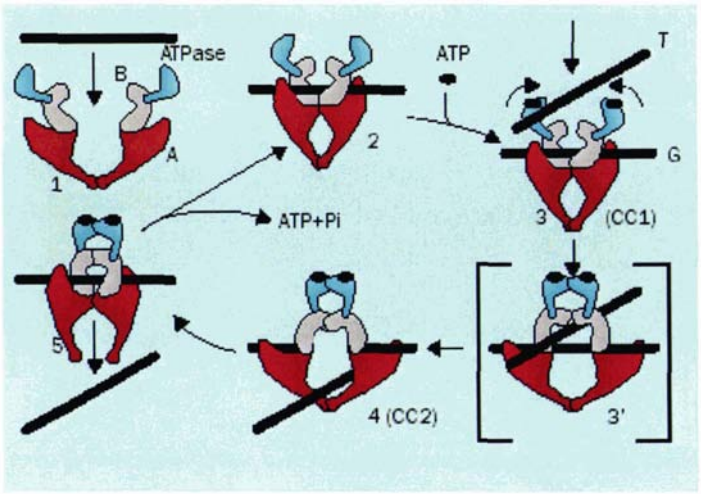

Fig. 1.2: Proposed structure and catalytic cycle of topoisomerase II

One DNA strand 'G' (gate) is cleaved during cleavable complex formation (CC1 and CC2), allowing the passage of another intact DNA strand 'T' (transport). The enzyme is a homodimer consisting of three functional segments, an ATPase (top), a cleavage (B), and a C-terminal (A) domain. The topoisomerase-II poisons act by stabilising stage 3 or 4, where the DNA strand is cleaved. (Taken from Kellner *et al.*, 2002)

1.4 Resistance Mechanisms

Resistance to chemotherapeutic drugs can be either intrinsic or acquired. Indeed, about 50% of tumours either do not respond to chemotherapy or re-emerge after treatment (Chu, 2001). One of the most well characterized intrinsic resistance mechanisms against anti-cancer drugs is conferred by P-glycoprotein (P-gp). The phenomenon of drug efflux from the cell, mediated by P-gp as well as other factors, is called multi-drug resistance (MDR). P-gp belongs to a class of proteins termed ATP-binding cassette (ABC) transporters, which control traffic of biological molecules across cell membranes. Other ABC transporter proteins involved in MDR are known as multi-drug resistance associated proteins (MRP) and mitoxantrone resistance associated protein (MXP). Other factors, such as differential expression of certain genes, can also confer drug resistance on cancer cells. Prominent examples of this kind of resistance mechanism are erbB2 (Fig. 1.1) and topoisomerase II alpha (Fig. 1.2).

1.4.1 P-Glycoprotein Mediated Multi-Drug Resistance

Keld Dano (1972) was the first to describe an active outward transport of anthracyclines from tumour cells and thus detected what is now known as MDR. The efflux of anthracyclines was

later traced back to an overexpression of a membrane protein named P-glycoprotein and was the first human ABC protein shown to export drugs from the cell (Litman *et al.*, 2001). The gene encoding P-gp was named *mdr-1* (Ueda *et al.*, 1986). The broad substrate recognition pattern of P-gp makes it a very potent resistance mechanism against a wide variety of agents, including anticancer agents (Varadi *et al.*, 2002; Leslie *et al.*, 2005). For many years P-gp was believed to be the major cause of drug resistance in chemotherapeutic treatment of cancers. Nowadays, it is more obvious that drug resistance in cancer cells is a multifactorial process that can involve different ABC transporters, such as MRP and MXP, which transport a wider variety of substrates than P-gp alone (Filipits *et al.*, 1996).

1.4.2 Multi-Drug Resistance Associated Protein

In 1992, 20 years after Dano's work, Cole discovered the MDR associated protein (MRP), a second major ABC transporter involved in MDR. This protein showed a 15% homology to P-gp and is present in tumour tissues at elevated levels (Litman *et al.*, 2001). Although MRP transports different drugs than P-gp, MRP conferred drug resistance has also been detected in cells exposed to doxorubicin and other reagents. MRP is ubiquitously present in most cell and tumour types, but elevated levels of MRP mRNA are found in most human cancer types (Nooter *et al.*, 1995; Ito *et al.*, 1998). MRP1-3 have been shown to be involved in doxorubicin transport, thus mediating drug resistance. Studies focusing on the correlation of expression levels and survival are however, yet to yield any conclusive results. Approximately 30% of primary breast cancer cases have been shown to exhibit significant MRP expression and presumably confer an increased risk of treatment failure (Nooter *et al.*, 1997; Burger *et al.*, 2003). A different study, however, did not find data to sustain this conclusion (Ferrero *et al.*, 2000). Hence, the role of MRP in clinical drug resistance still remains to be determined.

1.4.3 Mitoxantrone Resistance Associated Protein

More recently, a novel drug resistance conferring protein has been detected in the plasma membrane (Doyle *et al.*, 1998; Scheffer *et al.*, 2000; Schellens *et al.*, 2000) of different cancer cell lines and termed MXP, for mitoxantrone resistance associated protein. It was shown to be expressed in breast cancer cells (MCF7) which had been treated by combining adriamycin and verapamil (a P-gp inhibitor), to select for resistance mechanisms other than P-gp (Ross *et al.*, 1999). Although elevated MXP levels have been observed in breast carcinomas (Diestra *et al.*, 2002), they could not be linked to conferring anthracycline resistance (Faneyte *et al.*, 2002).

1.4.4 Glutathione-S-transferase

Detoxification of doxorubicin occurs in the liver, where CYP450 enzymes are responsible for metabolizing doxorubicin into inactive derivatives (Stearns *et al.*, 2004). Another important mechanism of detoxification is the attachment of glutathione to drug molecules by the glutathione-S-transferases (alpha, mu, and pi), which leads to the deactivation of chemotherapeutic agents. Increased expression of glutathione-S-transferases has been implicated in enhanced therapy resistance of a variety of tumours including those of the breast (Perquin *et al.*, 2001; Su *et al.*, 2003). Although glutathione-S-transferase-mediated drug resistance contributes to the multi-drug resistant phenotype of tumour cells it does not appear to have the same broad drug interaction spectrum typical of the ABC transporters. It is known that doxorubicin, for example, does not undergo significant glutathione conjugation, and hence should remain relatively unaffected by glutathione-S-transferase expression levels (Gaudiano *et al.*, 2000).

1.4.5 erbB2

erbB2 is a transmembrane receptor protein which is overexpressed in about 30% of all breast cancers (section 1.2.2). It is not only a potent oncogene, but can also render cancer cells drug resistant. Several clinical trials have revealed that overexpression of *erbB2* makes cancer cells less responsive or even resistant to certain types of chemotherapeutic treatment (Gusterson *et al.*, 1992; Yu *et al.*, 1998), but the underlying mechanism of action remains elusive (Yu and Hung, 2000).

1.4.6 Topoisomerase II Alpha and Beta

The topoisomerase II enzymes, designated topo II alpha and beta, are typically responsible for the interconversion of topological states of DNA molecules. In particular, topo II alpha has been shown to be essential for the replication process and cell survival (Holm *et al.*, 1985). Over the years many drugs have been developed targeting these enzymes, such as anthracyclines (doxorubicin and daunorubicin), epipodophyllotoxins (etoposide) and anthracene-diones (mitoxantrone), to name a few. The main aim of many of these drugs is to stabilize the cleavable complex, which is formed during DNA replication and represents a state in which temporary double-strand nicked DNA is bound to the enzyme (Fig. 1.2). Stabilization of this complex eventually renders the cell incapable of replication and induces cell death (Robert and Larsen, 1998).

Although many tumour types display elevated levels of both topoisomerase II isoforms it has been found that drug resistance is conferred on cells exhibiting decreased enzyme levels (Deffie *et al.*, 1989). The topo II alpha expression level depends on the cell cycle state, with low amounts usually present during the G0/G1-phase (Sullivan *et al.*, 1987; Woessner *et al.*, 1991). Enzyme levels increase during the S-phase, reaching their maximum in the G2/M-phase, at which point the cell is most susceptible to topo II drugs, as there is a high number of cleavable complexes present (Tanoguchi *et al.*, 1998). Conversely, reduced topo II alpha levels result in fewer cleavable complexes, making cells relatively drug resistant. Moreover, two additional mechanisms have been reported for cells carrying deletions of nuclear localization signals (Feldhoff *et al.*, 1994). It has been hypothesised that in these cells cytoplasmic topo II alpha could act as a drug sump by reducing the amount of drug molecules effectively entering the nucleus and being able to bind to nuclear topo II alpha (Withoff *et al.*, 1996). Furthermore, the decreased levels of nuclear topo II, which are due to delocalized nuclear topo II in the cytoplasm, can generate fewer cleavable complexes, thus contributing to drug resistance (Fig. 1.3).

It has also been suggested that the beta form of topo II, which has been shown to be decreased or absent in several resistant cell lines (Evans *et al.*, 1994; Harker *et al.*, 1995), can interact with the same DNA sequences as the alpha form and may therefore be a primary cause for drug resistance (Marsh *et al.*, 1996).

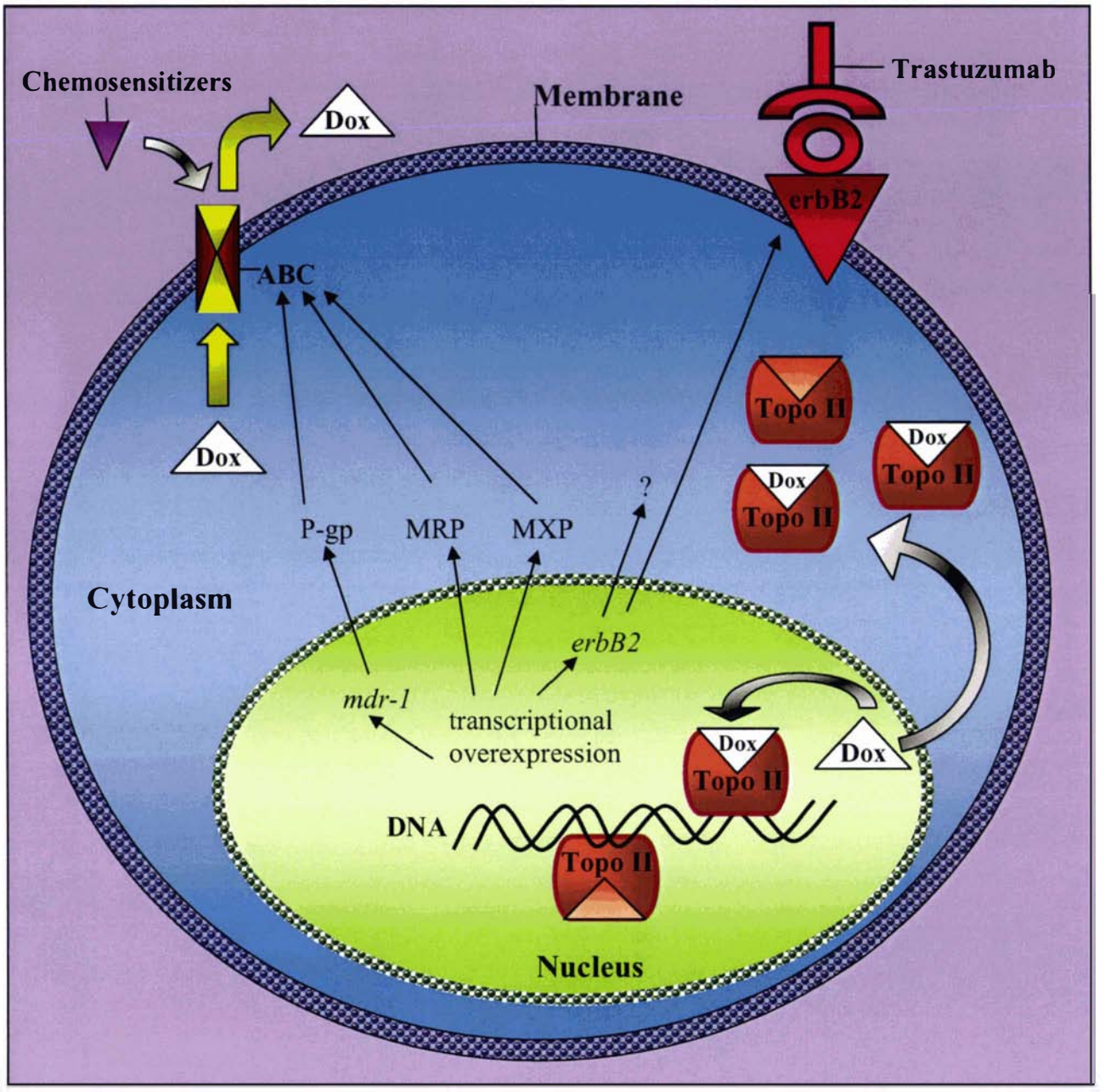

Fig. 1.3: Mechanisms of drug resistance

mdr-1 overexpression increases the synthesis of P-gp (ABC transporter protein), enhancing drug efflux from the cell. MRP and MXP are also ABC transporter proteins, increasing drug efflux from the cell when present at elevated levels. Chemosensitizers target such multi-drug resistance mechanisms to stop drug efflux and restore drug sensitivity. *erbB2* gene overexpression contributes to drug resistance by an unknown mechanism (?). Trastuzumab, an erbB2 specific antibody is used to kill erbB2 overexpressing tumours. Reduced nuclear levels of topo II alpha and/or beta lead to a decreased number of cleavable complexes available to be targeted by drug molecules such as doxorubicin (Dox). This results in less DNA damage, thus increasing the chances of cell survival. Increased amounts of cytoplasmic topo II alpha binding to drug molecules, such as doxorubicin also promotes drug resistance, by decreasing the number of drug molecules entering the nucleus.

1.5 New Therapeutic Agents and Reversal of Drug Resistance

Overcoming mechanisms conferring multi-drug resistance will always be of utmost importance, in order to ensure drug efficacy, even if other molecules are the actual chemotherapeutic target. As more than 50% of cancer patients do not respond to chemotherapy or relapse and eventually die from the disease, it is necessary to improve current therapy strategies as well as discovering new, more potent drugs. Historically, an empiric approach has been used for drug discovery, but with new insights into the molecular mechanisms and cellular signalling pathways, drug discovery efforts have become more focused. Currently, multiple strategies are being investigated to enable more efficient treatment of cancer patients. Some of these are summarized below.

1.5.1 Chemosensitizers

One promising strategy of increasing the efficacy of current anti-cancer agents is to reverse mechanisms associated with multi-drug resistance, such as P-glycoprotein-mediated drug efflux. Although a significant number of such agents, also called chemosensitizers, are available which can overturn MDR-mediated drug resistance; toxicity, adverse effects, and poor solubility at required doses, render most unsuitable for clinical application. In addition, effective chemosensitizers need to be specific for tumour cells, with little or no effect on normal cells. They must also enhance drug efficacy without altering pharmacokinetic properties (Peer *et al.*, 2004). Although it is unlikely that a single chemosensitizer alone will be applicable in all clinical situations given the diversity of different tumours, a number of molecules with chemoresistant potential have been identified and are currently undergoing clinical trials, such as the P-gp inhibitors tariquidar (XR9576) (Agrawal *et al.*, 2003; Pusztai *et al.*, 2005) and zosuquida (LY335979) (Shepard *et al.*, 2003; Sandler *et al.*, 2004).

1.5.2 Tumour Suppressors and Proto-Oncogenes

A different approach to therapy targets genes and their products which are at the very basis of breast cancer development. It is widely accepted that accumulation of multiple genetic aberrations are required for cancer development. Such malignant genetic changes are usually the result of oncogene activation (for example c-*Myc, erbB2* and *CCND1*) via mutation, translocation, or amplification, coupled with the inactivation of tumour-suppressor genes (for example *BRCA1, BRCA2, p53,* and *PTEN*). In tumour cells, mutations in oncogenes and tumour suppressor genes, as well as the lack of proper control mechanisms responsible for growth regulation, differentiation, DNA repair, and apoptosis, can result in dysfunctional or

overabundant gene-products. In addition to disease initiation and development, many of the affected gene products can render tumours drug resistant, or favour the development of drug resistance mechanisms. One aim of counteracting these aberrations for therapeutic purposes is to reverse detrimental effects by re-establishing tumour suppressor function, or by decreasing the activity of overexpressed oncogene products. One approach is to complement defective cells with functional tumour suppressor proteins for example in p53 mutated cells, using viral (Mujoo *et al.*, 1996; Lebedeva *et al.*, 2001; Wen *et al.*, 2003) or non-viral strategies (Xu *et al.*, 2001; Kim *et al.*, 2003) in order to restore tumour suppressor activity.

Viral strategies usually use a replication deficient adenovirus system, for example ad-p53 SCH 58500, to express the gene of interest, in this case p53. This strategy has been tested successfully for a variety of tumours including breast (Dummer *et al.*, 2000). Non-viral strategies, such as liposome-mediated gene transfer for example, utilize liposome-bound ligands. These ligands bind to specific receptors on the cell surface, which mediate endocytosis. Because liposomes form spontaneous complexes with naked DNA, such as plasmid vectors, these expression systems can be released during endocytosis and expressed, once they have found their way into the nucleus (Xu *et al.*, 2001). This system also allows systematic targeting of tumours overexpressing receptors which mediate endocytosis upon ligand binding, such as folate or transferrin receptors.

A different strategy is to either inhibit oncogene expression or to target the oncogene product. RNA interference has successfully been used to knock down the expression of *CCND1* (cyclin D1 encoding gene) stably transfected cells, which has resulted in increased chemosensitivity of tumour cells (Kornmann *et al.*, 1998; Kornmann *et al.*, 1999; Nakashima and Clayman, 2000). Selective targeting of tumours overexpressing the erbB2 oncogene product for example, is possible using a specific antibody (trastuzumab) (section 1.2.2).

The critical step in chemotherapy of tumour cells is the induction of apoptotic pathways. Molecules involved in mechanisms influencing this decision, such as DNA repair, cell cycle checkpoint, and growth regulation, represent particularly interesting targets for enhancing treatment efficacy. In general, little is known about the immediate cellular response to particular agents used in chemotherapy. Understanding the cellular activation of response mechanisms due to treatment with specific chemotherapeutic agents however, may expose

mechanisms which contribute to cell survival, as well as drug resistance towards a particular agent, and could hence be specifically targeted to increase treatment efficacy of that drug.

1.6 Gene Expression Analysis

Gene expression profiling utilizing cDNA microarray technology has been used to discover additional genes involved in mechanisms of drug resistance. Levels of gene expression in different cells (e.g. normal and cancer cells, or drug-treated and untreated cells) have been compared with the aim of finding new potential targets for cancer treatment. Such expression analyses have identified differentially regulated genes. Nonetheless, they have not resulted in any major breakthrough in helping to understand new mechanisms of drug resistance.

In a study conducted by Kudoh *et al.* in 2000 it was found that MCF-7 breast cancer cells displayed a 2-30 fold increase in transcription of some genes in a time-dependent manner when transiently exposed to doxorubicin. These authors also found that some of the genes that were overexpressed during transient drug treatment were also overexpressed in drug resistant MCF7 cancer cells. In a different study Sotiriou *et al.* (2002) used microarrays to evaluate gene expression in response to chemotherapy and found that breast tumours which were susceptible to therapy showed a different expression profile than those which were not. Genes overexpressed in both studies comprised of transcription factors, protein kinases and phosphatases, cell cycle regulators, proteases, apoptotic and antiapoptotic factors, and metabolic genes.

Although these and other studies provide a global view of the complex response of breast cancer cells to drugs, and proof of numerous biological pathways being altered, they fail to show actual effects on end products of affected pathways and changes at the protein level in general. Microarray analyses cannot predict the actual effects of altered gene expression on specific protein levels, protein (-protein) interactions, or post-translational modifications (Luker *et al.*, 2001).

1.7 Posttranslational Protein Modification

One example that highlights the importance of post-translational protein modification, and the necessity to understand the effects of such alterations on the cell, is the phosphorylation of the *mdr-1* gene product P-gp. Loo and Clarke (1999) discovered that contrary to common belief, P-gp unlike other ABC proteins, is not functional immediately after synthesis, but requires a

maturation process for the glycosylated core protein to be fully functional. These authors hypothesized that for the successful maturation of the protein, the presence of drug substrates is required in order to remove certain barriers blocking the maturation process. Earlier experiments have revealed that P-gp is probably phosphorylated by phospholipase C when exposed to stress (e.g. heat shock, drug treatment), possibly regulating and increasing the proteins transport function (Yang *et al.*, 1995).

Moreover, protein phosphorylation is also an integral mechanism of signal transduction networks, which are activated in response to cellular stress and damage, and determine subsequent cellular events. One prominent example for phosphorylation-mediated signal transduction is the phosphorylation of p53 in response to DNA damage, which may result in cell cycle arrest, DNA repair, or apoptosis (Kim *et al.*, 1999).

These examples underscore the importance of investigating post-translational and protein interaction events in response to drug treatment, as an integral part of understanding resistance mechanisms in cancer and discovering new potential targets for drug therapy or therapy regimen.

1.8 Project Background

Since gene expression analysis, using microarray technology for example, cannot provide a complete picture of the events, effects, and consequences that occur at the post-translational level of cell physiology in response to drug exposure, it is necessary to employ additional techniques that allow for these events to be examined in more detail. Changes in transcriptional activity are non-linear and do not correspond to a 1:1 gene expression: protein synthesis ratio. Transcriptional alterations thus cannot be used to predict changes at the protein level (Dutt and Lee, 2000; Wulfkuhle *et al.*, 2001; Godovac-Zimmermann *et al.*, 2005). Moreover, proteins are often highly interactive and regulate specific molecular pathways. The expression of other proteins (e.g. transcription factors and pathway regulators) can hence influence certain pathways, which in turn will exert changes on other proteins or gene expression. It is therefore very likely that different and additional changes will be encountered at the protein level than at the transcriptional level, as a consequence of drug treatment.

Several studies have used proteomic strategies to investigate changes in protein expression in drug sensitive compared to drug resistant breast cancer cell lines. In particular, the MCF7 cell line has been utilized, because a doxorubicin resistant subpopulation has been isolated, MCF7/Adr, which allows a direct comparison of drug sensitive and resistant cells. Two dimensional gel electrophoresis (2DGE) as well as surface-enhanced laser desorption ionization mass spectrometry (SELDI-MS) and liquid chromatography mass spectrometry based strategies have been used for this type of analysis. It is unclear at this stage however, if the observed differences between drug sensitive and resistant cell lines are phenotypical or associated with doxorubicin treatment (Hathout *et al.*, 2002; Brown and Fenselau, 2004; Gehrmann *et al.*, 2004; Gehrmann *et al.*, 2004; Hathout *et al.*, 2004). Moreover, differences between breast cancer cell lines, such as MCF7 cells and MDA MB 231 cells, have also been observed using these techniques (Hathout *et al.*, 2004).

More immediate changes in protein regulation in breast cancer cell lines have also been studied in response to doxorubicin exposure. Again 2DGE and SELDI-MS were used for analysis, and although a few proteins appeared to be differentially regulated, only three different isoforms of the heat shock protein 27 (HSP27), which were down-regulated after doxorubicin treatment, were identified (Chen *et al.*, 2002). Earlier studies have linked HSP27 expression specifically to doxorubicin resistance in breast cancer cells (Ciocca *et al.*, 1992; Oesterreich *et al.*, 1993). The mechanism by which resistance is rendered on cells however, remains unclear. In light of this, the functional consequences of HSP27 down-regulation after doxorubicin treatment are also not understood. In the study conducted by Chen and his co-workers (2002), cells were exposed to a low concentration (0.1 μM) of doxorubicin, which consequently may have limited the degree of change in protein regulation. In another study, a high concentration (10 μM) of doxorubicin was utilized, but only a very small range of proteins (2-5 kDa and 15-20 kDa) were analysed (Mian *et al.*, 2003), dramatically limiting the chances of detecting differentially regulated proteins. Nevertheless, these studies have underscored the possibility of using proteomic techniques for detecting differentially regulated proteins in response to doxorubicin treatment.

1.9 Aim of Project

Resistance to chemotherapeutic drugs is one of the most severe problems occurring during treatment of cancer patients. The aim of this study was to investigate mechanisms which may contribute to cancer cells becoming resistant during drug treatment, by monitoring changes in

protein expression profiles, which could ultimately provide information to help improve current therapeutic strategies.

To this end human breast cells (MCF12A) and the breast cancer cell lines (MCF7 and MDA MB 231) were treated with a commonly used chemotherapeutic drug (doxorubicin) and analysed for changes in protein expression compared to untreated control cells. Unlike other studies however, which maintained cells in drug-spiked media (Chen *et al.*, 2002; Mian *et al.*, 2003), doxorubicin was removed from the media after one hour, to mimic the clinical situation of doxorubicin metabolism and removal. Furthermore, an ER positive (MCF7) and an ER negative (MDA MB 231) cell line were used in this study because the ER receptor status of breast tumours can have an impact on drug resistance (Zampieri *et al.*, 2002).

One approach of detecting candidate proteins which were up- or down-regulated in response to drug exposure was to monitor changes of the whole proteome using two dimensional gel electrophoresis (2DGE) and surface-enhanced laser desorption ionization mass spectrometry (SELDI-MS). Differentially regulated proteins could then be identified by peptide mass fingerprinting and cellular functions determined (Chapters 3-5).

A second approach was to specifically investigate changes in proteins which are likely to be involved in the repair of doxorubicin-induced damage. Because doxorubicin is known to cause DNA-damage, two proteins involved in independent DNA repair pathways were specifically monitored for drug-induced alterations in protein expression (Chapter 6).

Chapter Two
Materials and Methods

2.1 Materials

MCF12A, MCF7, and MDA MB 231 cell lines were all purchased from the American Type Culture Collection.

DMSO and sodium bicarbonate were tissue culture grade from Sigma Chemical Company, St. Louis, MO, USA. Opti MEM, Penicillin (5000 U/mL), Streptomycin (5000 μg/mL), 2.5% trypsin, and foetal calf serum were from Invitrogen Life Technologies Inc., New Zealand. Cryotubes were from Nunc INC., IL, USA. Media sterilization filters were Supor Acrodisc 32 0.2 μM filters from Gelman Sciences, MI, USA. T25 and T75 Nunc filter cap easy flasks were from Invitrogen, New Zealand. T300 filter cap flasks and 380 mm x 25mm cell scrapers were from TPP, Medica Pacifica Ltd., New Zealand. 12-well plates with lids were from Corning Costar Corporation, MA, USA. Doxorubicin (2 mg/mL, Upjohn & Pharmacia) was a gift from Richard Isaacs, Palmerston North Hospital. Propidium iodide and thymidine were from Sigma Chemical Company, St. Louis, MO, USA.

Benzonase® and Tergitol NP-4 were from Sigma, St. Louis, IL, USA. Swinnex® membrane holders and 0.65 μm Durapore® membranes were from Millipore, MA, USA. The IPGphor® and Hoefer SE 600 Ruby standard dual cooled basic gel electrophoresis unit, immobilized pH gradient dry strips (IPG strips) pH 4-7 and 3-10, plus one® dry strip cover fluid, and IPG buffer were from Amersham Pharmacia Biotech AB, Uppsala, Sweden. Phoretix 2D Evolution gel analysis software was from Nonlinear Dynamics, England.

Lubricated micro-centrifuge tubes were from Corning Costar Corporation, MA, USA. Reversed-phase C_{18} ZipTips® were from Millipore, MA, USA and nitrocellulose from Bio Rad Laboratories, CA, USA. Angiotensin I was a kind gift from David Lun, Massey University. Alpha-cyano-4-hydroxycinnamic acid (CHCA) and 2,5,Dihydroxybenzoic acid (gentisic acid) were from Sigma Chemical Company, St. Louis, MO, USA.

Bradford reagent, acrylamide (40%), and SDS-PAGE broad range molecular weight standards were from Bio Rad Laboratories, CA, USA. The Roche Complete™ mini protease inhibitors, the Chemiluminescence Blotting Substrate (POD) Kit, and nylon membrane (positively

charged) were from Roche Molecular Biochemicals, Mannheim, Germany. Nylon membrane (positively charged) was also used from Gelman Sciences, MI, USA. 3 MM paper was from Whatman, England.

DNA-PKcs (H-163,) (rabbit polyclonal, N-terminal human DNA-PKcs), Rad51 (H-92) (rabbit polyclonal, C-terminal human Rad51), and topo II alpha (K-19) (goat polyclonal, C-terminal human topo II alpha) antibodies were from Santa Cruz Biotechnology, CA, USA. Alpha tubulin (anti-alpha tubulin clone DM 1A), and the IgG horse radish peroxidase conjugates of anti-mouse, anti-human, and anti-goat antibodies were from Sigma Chemical Company, St. Louis, MO, USA. The X-ray film, developer, and fixer were from Eastman Kodak, NY, USA.

Trifluoroacetic acid (TFA), formic acid, and acetonitrile were gradient grade quality from Romil, England. 0.22 μm Ultrafree-MC® filters and 0.2 μm filter membranes were from Millipore, MA, USA. Jupiter C4 250 mm x 4.6 mm, 300 Å, 5 μm, column, security guard column, and widepore C4 (Butyl) cartridges were from Phenomenex, New Zealand. The ultrafiltration membranes Vivaspin® 2 mL, 5 kDa (MWCO); Centricon® SR-3, 3 kDa (MWCO); Macrosep®, 10 kDa (MWCO); were from Vivascience, Germany; Millipore, MA, USA; and Pall, England, respectively.

2.2 Methods

2.2.1 Cell Culture

2.2.1.1 Cell Maintenance

All handling of cells, other than harvesting, was carried out under aseptic conditions using a laminar air flow unit (Crossflow 1800 with HEPA filter, Westinghouse). Media was filter-sterilized using a 0.2 μm acro cap filter (Pall), stored at 4°C, and warmed up to RT just prior to use. MDA MB 231 and MCF7 cells were grown in Opti-MEM (GibcoBRL) supplemented with 2% foetal calf serum (FCS) (GibcoBRL), 2.4 mg/mL sodium bicarbonate, and 50 units/mL of penicillin and streptomycin (GibcoBRL). MCF12A were cultured in a 1:1 mixture of Ham's F12 (Sigma) and DMEM (Sigma) supplemented with 2.4 mg/mL sodium bicarbonate (Sigma), 20 ng/mL epidermal growth factor (Sigma), 500 ng/mL hydrocortisone (Sigma), 5% horse serum (GibcoBRL), and 50 units/mL of penicillin and streptomycin (GibcoBRL). MCF7 and MCF12A were grown in media containing 10 μg/mL insulin (Roche). All cells were grown in humid conditions at 37°C in a 5% CO_2 incubator and experiments were carried out during exponential growth phase unless otherwise indicated.

2.2.1.2 Cell Passaging

1 x trypsin (0.25%) (GibcoBRL) was obtained by diluting 1 mL of 10 x concentrated trypsin with 9 mL of PBSE (0.14 M NaCl, 2.7 mM KCl, 4.3 mM $NaHPO_4.2H_2O$ pH 7.2 plus 0.5 mM EDTA) under aseptic conditions. After removing the old cell media, 1 x trypsin was added to the flasks at a ratio of 1 mL/40 cm^2. The cells were monitored under an inverted light microscope (Olympus CK2) and the trypsin solution removed as soon as the cells started rounding up. Flasks were vigorously tapped on the side several times to facilitate dislodging of the cells. The cells were aspirated in fresh media which was evenly distributed to new flasks. Fresh media was added to the new flasks to a final concentration of 0.125 mL/cm^2 before being placed in the incubator. Generally, filter top flasks were used ranging from 25 cm^2 (T25) (Nunc) for growing cells from frozen stocks to 75 cm^2 (T75) (Nunc, Invitrogen) and 300 cm^2 (T300) (TPP) which were used for drug exposure experiments.

2.2.1.3 Freezing and Thawing of Cell Stocks

After trypsin treatment, cells were taken up in 1 mL of FCS and 10% DMSO. The cells were then transferred to cryo tubes (Nunc) and wrapped in tissue paper before being stored at -70°C. After 24 h, the cells were transferred to a liquid nitrogen container where they were stored indefinitely. When starting a new batch of cells from frozen stocks they were first removed from the container and quickly defrosted by holding the tube in the hand. The cells were then transferred to a sterile 15 mL nunc tube and 5 mL of appropriate growth media added before being pelleted at 480 x g. The supernatant was removed and the cells resuspended in 5 mL of fresh media. The suspension was than transferred to a T25 flask (Nunc) for cell propagation.

2.2.1.4 Drug Exposure

Cells were seeded at 25-30% confluence and left undisturbed for 24 h before exposure to doxorubicin (Pharmacia & Upjohn, New Zealand) for 1 h. The medium was then replaced with doxorubicin-free conditioned media and cells left undisturbed until harvested. When selecting for "resistant" cells, the culture was left undisturbed for 4 days, after 80-90% of the cells had died, the media was replaced. The culture was allowed to re-establish growth before being passaged, and re-exposed to doxorubicin an additional two times before harvesting.

2.2.1.5 Cell Viability Assay

Cells were seeded at 1 x 10^5 (MDA MB 231 and MCF12A) and 5 x 10^4 (MCF7) per well in 12 well plates (Nunc). For analyses, growth media and trypsinized cells were collected and centrifuged at 480 x g for 5 min. Cell pellets were resuspended in PBS (0.14 M NaCl, 2.7 mM KCl, 10.1 mM Na_2HPO_4, 1.8 mM KH_2PO_4 pH 7.2) and diluted 1:1 with erythrosin B (1 mg/mL) to distinguish between viable and dead cells, and counted using a hemocytometer (Neubauer).

2.2.1.6 Harvesting Cells

Old media was discarded and cell cultures were repeatedly washed with ice-cold PBS to remove extracellular proteases and plasma proteins. Flasks were scraped thoroughly, cells were repeatedly collected in 10 mL ice cold PBS and pooled into 50 mL Nunc® tubes. The cell suspension was then centrifuged at 480 x g at 4°C for 5-10 minutes and the supernatant discarded. The tube was weighed to estimate the protein concentration which is roughly 5% of the wet weight (Taylor, 2003) before snap freezing the cell pellet in liquid nitrogen and storing at -70°C.

2.2.2 Protein Handling

2.2.2.1 Protein Extraction for 2D Analysis

Cell pellets obtained by harvesting three T80 flasks or one T300 were lysed using 270 µL of extraction buffer (8 M urea, 4% (w/v) CHAPS (3-[(3-Cholamidopropyl)dimethylamino]-1-propanesulphonate), 1 x Complete™ mini, 40 mM tris pH 9), to which 5 mM 2-TCEP was added, and vortexed vigorously. As the suspension turned viscous 2 µL of Benzonase® (Sigma) was added and the solution vortexed for an additional minute, observing an immediate decrease in sample viscosity. After 5 min 1 mM EDTA and 2 M thiourea were added. Once the thiourea had dissolved, the lysis buffer was completed by adding 0.75 µL of 4-Vinylpyridine (95% solution) to a final concentration of 20 mM and left to stand at RT for 90 minutes, occasionally inverting the tube.

2.2.2.2 TCA Precipitation

Trichloroacetic acid (TCA) was added to a final concentration of 15%, for protein precipitation, and incubated on ice for 1h. After centrifugation at 13000 rpm at 4°C for 15 min, the protein pellet was repeatedly washed with 300 µL of ice-cold acetone and centrifuged. The protein pellet was subsequently dissolved in 100 µL extraction buffer (8 M

urea, 2 M thiourea, 4% CHAPS, 40 mM tris pH 9, and 1 x Roche Complete™ mini) which had been prefiltered using Swinnex® (Millipore) membrane holders with a 0.65 μm Durapore® membrane (Millipore), by vortexing for 1h.

2.2.2.3 Ultracentrifugation

Samples were transferred to ultracentrifugation tubes (Beckman) and centrifuged at 1 x 10^5 x g at 15°C for 30 min in a Beckman TL-100 tabletop ultracentrifuge to remove nucleic acids from protein extracts obtained without Benzonase® treatment. The supernatant was subsequently transferred to a fresh tube.

2.2.2.4 Storing of Protein Extracts

Protein extracts were divided into aliquots (30 μl) and snap frozen in liquid nitrogen before being transferred to -70°C for storage.

2.2.2.5 Bradford Assay

BSA (New England Biolabs, 10 mg/mL) was diluted with Milli Q water to give standard concentrations of 0 (Milli Q only) 0.1, 0.25, 0.5, 0.75, 1, and 2 μg/μL. Protein samples were diluted 5, 10, 20, 50, and 100 fold with Milli Q water. 5 μL of each sample and BSA solution were transferred to a 96-well microtiter plate (Nunc). Bradford protein assay dye reagent concentrate (Bio Rad) was diluted 1:4 in Milli Q water and 195 μL added and left standing for 5 min. Each dilution was carried out in triplicate and shaken for 10 sec at medium speed before the absorption was measured at 595 nm using an anthos htII spectrometer (Sci Tech). A standard curve was constructed utilizing the BSA standards of known concentration, allowing the determination of protein concentration in the samples.

2.2.2.6 Reversed-Phase High Performance Liquid Chromatography

RP-HPLC was conducted using a DIONEX system (ASI-100 sample injector, 580 Pump, STH585 column oven, and a UVD340S detector) and data analysed using DIONEX chromeleon client 6.40 software. All reagents were filtered using a 0.2 μm filter (Millipore) and H_2O was initially charcoal filtered. Protein extracts were filtered prior to analysis using 0.22 μm Ultrafree-MC filters (Millipore). Different amounts of protein extracts were loaded onto a Jupiter C4 250 mm x 4.6 mm, 300 Å, 5 μm column (Phenomenex), which had a security guard column containing two widepore C4 (Butyl) cartridges, attached. Prior to any analysis the column was routinely equilibrated with acetonitrile and the trendline monitored

on the computer. Once the trendline had stabilized and no changes were observed for at least 10 min the column was subsequently equilibrated with 0.1% trifluoroacetic acid (TFA) in H_2O, until no more trendline-changes were observed for at least 10 min. Different amounts of protein sample were then injected onto the column which was followed by a wash H_2O (0.1% TFA), before eluting proteins off the column using different concentrations of AcN and 0.1% TFA in H_2O. The samples were collected in 15 mL test tubes and kept on ice.

2.2.2.7 Speed Vac

The protein fractions (approximately 5 mL) were transferred from the test tubes to lubricated micro-centrifuge tubes (Costar®) and dried in a speed vac (SpeedVac SC100, Pierce) at a medium drying rate. When 70% of the sample had evaporated, it was reconstituted to the original volume by adding more fractionated protein solution. This process was repeated 10-15 times until all of the fractionated sample solutions were used up, at which stage the samples were dried to completeness. The dried protein fractions were then dissolved in protein extraction buffer.

2.2.2.8 Ultrafiltration

All ultrafiltration devices were used according to the manufacturer's recommendations. Protein fractions containing an AcN concentration exceeding the manufacturer's recommendations were diluted to recommended levels using protein extraction buffer. In general the protein fractions were filtered at least three times and diluted with prefiltered extraction buffer between filtering spins to dilute the AcN. Ultrafiltration devices and molecular weight cut-off values (MWCO) were as follows: Vivaspin® 2 mL (Vivascience), 5 kDa (MWCO); Centricon® SR-3 (Amicon), 3 kDa (MWCO); Macrosep® (Pall), 10 kDa (MWCO).

2.2.2.9 Freeze Drying

After RP-HPLC the protein fractions were collected in 15 mL tubes (Nunc), snap frozen in liquid nitrogen, and stored at -70°C for 24 h. The fractions were then dried in a lyophilizer and reconstituted in filtered extraction buffer.

2.2.3 Two Dimensional Electrophoresis

2.2.3.1 Isoelectric Focusing (IEF)

Samples consisting of 75 µg of protein in 300 µL of extraction buffer containing 0.01% Coomassie brilliant blue, 0.5% IPG buffer, and 0.001% tergitol NP-4 were transferred into the middle of an 18 cm strip holder. The cover of either pH 4-7 or 3-10 immobilised pH gradient IPG strips (Amersham Biosciences) was carefully removed and the strip placed gel-side down in the correct orientation onto the strip holder, ensuring no air bubbles were trapped underneath the strip. Approximately 2 mL of Plus one® cover oil (Amersham Biosciences) was applied on top of the strip to avoid sample evaporation. Strips were focused in 7 subsequent steps which had been programmed into the IPGphor® (Amersham Biosciences) apparatus as follows:

1. 30 V for 13 h
2. 250 V for 1 h
3. 500 V for 1 h
4. 750 V for 1 h
5. 2500 V for 1h
6. 5000 V for 1 h
7. 8000 V for 9 h

2.2.3.2 Polyacrylamide Gel Casting

Acrylamide stock solution (30.8% T, 2.6% C) was prepared by adding 29.22 g of acrylamide and 0.87 g of Bisacrylamide to 100 mL of Milli Q water and stored in the dark at 4°C. 10-15% gradient gels were cast using 12.9 mL of both heavy and light solution which were prepared as follows:

Reagent	Light solution 10%	Heavy solution 15%
Acrylamide	10 mL	15 mL
4 x Resolving buffer	7.5 mL	7.5 mL
Milli Q water	12 mL	4.6 mL
10% SDS	0.3 mL	0.3 mL
Sucrose	none	4.5 g
20% APS (Ammonium persulfate)*	81.3 µL	25 µL
TEMED*	4.2 µL	4.2 µL

* Were added to the 12.9 ml of solution already in the mixing chamber

The Hoefer SG100 mixing chamber (Amersham Biosciences) and a Bio-Rad Econo Pump were used for pouring the gels. First the heavy solution was transferred into the chamber labelled "H" and the tap of the L chamber was opened to allow the heavy solution to force any air out of the connection tube. Once the tubing was filled with heavy solution the tap was closed and the light solution filled into the "L" labelled chamber. APS and TEMED were added as indicated and mixed well using stir bars at a stirrer setting of 6 (medium fast). The stir bar in the "L" chamber was removed before starting to pour the gel, by opening the tap of the "H" chamber by 3 half turns to the left. The pump was then switched on at a flow rate of 2.4 mL/min. Once the front of the heavy solution had reached the pump, the tap of the light chamber was opened by 3 half turns to the left to allow the mixing of the two solutions. A needle attached to the end of the rubber hosing was placed in the middle of the assembled glass plates and gradually moved upwards in sueh a way as to maintain a distance of about 1 cm between the needle tip and the gel front. Immediately after finishing casting, the gel was overlaid with a thin layer of about 300 µL of water-saturated butanol. After allowing to stand at RT for at least 1 h, the gel was covered in wet paper towels, wrapped in plastic wrap and stored at 4°C overnight to ensure proper polymerization.

2.2.3.3 Second Dimension and Strip Transfer

After IEF, the focused strips were washed 3 times in SDS running buffer (25 mM tris base, 192 mM glycine, 0.1% (w/v) SDS). Focused strips of protein samples extracted according to the protocol of (Berkelman and Stenstedt, 1998) were subsequently transferred to SDS equilibration buffer (6 M urea, 30% glycerol, 2% SDS, 10 mg/mL DTT) for 20 min before being placed in alkylating buffer (6 M urea, 30% glycerol, 2% SDS, 25 mg/mL iodoacetamide) for 20 min. Protein samples which had been alkylated prior to IEF were transferred to SDS equilibration buffer without DTT for 20 min. All strips were then placed onto filter paper for 5 min. The strips were then cut at the cathodic end and the blue anodic end to an appropriate size for transfer onto the polyacrylamide gel. After lubricating the strips in running buffer (25 mM tris base, 192 mM glycine, 0.1% (w/v) SDS), they were placed on the second dimensional gel with the plastic-side against the glass and overlaid with agarose (0.5% agarose with a trace of Coomassie blue) to facilitate protein transfer from the first to the second dimension. The gels were then placed into the Hoefer SE 600 Ruby gel tank (Amersham Biosciences). The gel tank was connected to a circulating water bath for temperature control, maintaining 20°C. Electrophoresis was carried out at 10 mA for 20 min,

before increasing the current to 20 mA and then continued until the Coomassie blue dye front reached the gel bottom, which typically took 16 h.

2.2.3.4 Silver Staining

The silver staining protocol was a kind gift from Zhou-Zhan Liu, Institute of Molecular Biosciences, Massey University. Milli Q water was used for all solutions which were 250 mL/gel unless stated otherwise. Gels were transferred to glass bowls containing 50% ethanol and 10% acetic acid, and placed on a shaker at RT overnight. They were then rinsed in 5% ethanol and 1% acetic acid for 15 min, before being washed 3 times for 5 min each wash. For sensitisation purposes the gels were transferred to a 40 mg sodium thiosulfate solution for 2 min, after which they were washed for 5 min, and then placed in a 0.4 g silver nitrate solution for 20 min. After being washed twice for 20 sec. in 400 mL of water, the gels were washed with 50 mL of developer solution containing 60 g/l sodium carbonate, 0.5 mL 37% formaldehyde and 20 mL 0.2 g/l sodium thiosulfate. The gels were then left in fresh developer solution until the desired staining had been achieved, which usually took 5-6 min. The solution was then replaced with 5% cold acetic acid for 10 min before repeatedly rinsing the gels with water. Gels were stored in a 35% methanol, 3% glycerol solution and sealed in laminating cover sheets.

2.2.3.5 Image Acquisition

Stained gels were placed on a glass tray in the Fuji FLA 1000 dark box which was set to DIA and digitizing mode for image acquisition. Pictures were obtained with the Image Reader 1000 program using automatic exposure. Saved images were exported as tiff files and manually analysed for differences in protein concentration and spot patterns using Adobe Photoshop.

2.2.3.6 Phoretix 2D Software Analysis

Image analysis was performed using the manufacturer's (Nonlinear) recommended settings. Gel images were aligned to match spots between different gels. This was achieved by gel warping, a process by which the areas surrounding prominent and easily identifiable proteins spots on different gels are matched. This procedure was particularly important for gels showing slight protein migration differences which otherwise would have prevented accurate spot matching. Spot detection was performed automatically by the software. Results were checked and corrected manually where necessary to ensure correct spot matching. Only spots

exceeding a signal intensity of 0.04 units were used for analysis in order to facilitate spot matching and to reduce data ambiguity. Background subtraction was performed in accordance with the manufacturer's recommendations, but additional options were utilized when data confirmation was considered necessary. A protein spot had to be up- or down-regulated 1.7 fold between samples to be considered as a potential candidate.

2.2.4 Immunoblotting

2.2.4.1 Protein Extraction

After harvesting, the cells were lysed in 40 mM Hepes pH 7.9, 0.4 M KCl, 1 mM DTT, 10% glycerol, 1 mM EDTA, and 1 x Roche Complete™ mini using 4 freeze-thaw cycles in liquid nitrogen. Aliquots were snap frozen and stored at -70°C and protein quantification carried out by Bradford assay as described in section 2.2.2.5.

2.2.4.2 Western Blots

A Bio-Rad mini gel system was used for 1D SDS-PAGE, and to transfer the proteins onto a membrane following the manufacturer's recommendations. Samples containing 20 μg of protein were boiled in 1 x SDS loading buffer (SDS, glycerol, 2-β-mercaptoethanol, bromophenol-blue) for 5 min, and transferred onto ice for 5 min, before being loaded onto 5-10% gradient SDS-PAGE mini gels. The gels were run in SDS electrophoresis buffer (25 mM Tris, 192 mM Glycine, 0.1% w/v SDS in H_2O) at 200 V until the dye front reached the bottom of the gel.

Proteins were transferred to a nitrocellulose membrane (Pall, Roche) in electrotransfer buffer (25 mM Tris, 192 mM glycine in H_2O) at a constant current of 450 mM for 1 hour. Roche BM chemiluminescence Blotting Substrate (POD) was used for immuno detection according to the manufacturer's recommendations. Membranes were cut into the appropriate molecular weight regions where applicable or transferred whole into TBST (0.5 M Tris, 150 mM NaCl, 0.1% v/v Tween 20) including 1% blocking reagent for 1 h at RT. The proteins were immunolabeled using 1:250 Rad51 (H-92) (Santa Cruz) and 1:4000 DNA-PKcs (H-163) (Santa Cruz), 1:250 topo II alpha (K-19) (Santa Cruz), and 1:2000 alpha tubulin (DM 1A) (Sigma) primary antibodies in TBST including 0.5% blocking reagent for 1 h. The membranes were then washed twice in TBST and twice in TBST plus 0.5% blocking reagent for 10 min each, before adding the appropriate amount of horseradish conjugated secondary antibody (anti-rabbit, 1:2500; anti-goat and anti-mouse, 1:5000 (Sigma)) in TBST including

0.5% blocking reagent for 1 h at RT. Subsequently, the membranes were washed in TBST three times for 15 min before being bathed in detection solution (99 parts solution A, 1 part solution B) for 2 min.

Images were captured using X-ray film (Kodak X-Omat K film) and a 100 Plus™ automatic X-ray film processor from All-pro Imaging (Hicksville, New York 11801). Additional images were acquired using the Fuji Las 1000 intelligent dark box according to the manufacturer's recommendations for immunoblots. Images were saved as tiff files.

2.2.4.3 Densitometry

Densitometric analysis was performed using ImageJ software according to the manufacturer's recommendations. Gel images to be analysed using ImageJ software were used as tiff files. First, one lane was marked using the rectangular tool from the menu. Each subsequent lane was then marked with a new rectangle, with the same dimensions as the first rectangle. After the final lane which was to be included in the analysis had been marked, the results for each lane were displayed in a plot profile. The higher a band was located on the lane of the gel, the further left the corresponding peak appeared. The height of the peak corresponded to the densitometric value (protein concentration) of the gel band (section 6.8, Fig. 6.4). Individual peaks were then selected and the densitometric value of each peak/band summarized in a list, which allowed the determination of the relative concentration of proteins in each sample.

2.2.5 Matrix-Assisted Laser Desorption Ionization Mass Spectrometry (MALDI-MS)

2.2.5.1 Farmer's Reagent Destaining (Gharahdaghi *et al.*, 1999)

The protein band of interest was excised from the gel and cut up into small cubes (approximately 1 mm^2). A fresh solution of 30 mM potassium ferricyanide and 100 mM sodium thiosulfate was prepared at a ratio of 1:1. The gel slices were place in a 650 µL centrifuge tube and covered in this solution, typically a volume of 30-50 µL was sufficient. The tube was gently vortexed until the brownish colour disappeared from the gel cubes. At this point the solution was removed and 25 mM ammonium bicarbonate (pH 8) added, and vortexed for 10 min. The solution was then discarded and fresh 25 mM ammonium bicarbonate (pH 8) was added. The slices were then treated as described in section 2.2.5.3.

2.2.5.2 Hydrogen Peroxide Destaining

The excised protein band was cut into small cubes, placed in a centrifuge tube and repeatedly washed in water for 5 min. The cubes were then repeatedly treated with 25 mM ammonium bicarbonate (pH 8) for 5 min. 1% H_2O_2 in 25 mM ammonium bicarbonate (pH 8) was then added and removed once the cubes appeared clear, which typically took less than 10 minutes. They were then rinsed in water twice for 5 min, before adding a 1% formic acid solution. After 5 min, the solution was replaced by a 1% formic acid/acetonitrile solution with a ratio of 1:1. The solution was replaced by acetonitrile 5 min later and cubes were ready for in-gel digestion after a further 10 min.

2.2.5.3 In-Gel Protein Digestion

After completely drying the gel cubes using a speed-vac (SpeedVac SC100, Pierce) pump they were submersed in 100 µL of 2 mM Tris (2-carboxyethyl) phosphine (TCEP), in 25 mM ammonium bicarbonate and incubated at 37°C for 15 min, occasionally agitating the tube. The supernatant was then replaced by adding 100 µL of 20 mM iodoacetamide in 25 mM ammonium bicarbonate and incubated at 37°C in the dark for 30 min. The supernatant was then discarded and the gel cubes washed three times with 200 µL of 25 mM ammonium bicarbonate for 15 minutes under constant shaking. The gel slices were then completely dried using a speed vac and transferred to a lubricated micro-centrifuge tube (Costar®). The cubes were subsequently rehydrated in 5-10 µL of trypsin solution (0.05 µg/µL sequencing grade modified trypsin (Roche) in 40 mM ammonium bicarbonate containing 0.1% w/v n-octylglucoside for 1 h. After this period, an additional 50 µL of trypsin solution was added and the gel slices incubated at 37°C overnight. The solution was then centrifuged and the supernatant transferred to a new lubricated centrifuge tube. In the subsequent step, the sample volume was reduced to 10-20 µL using a speed vac.

2.2.5.4 ZipTip® Sample Concentration

In general, all samples which had been silver stained were further concentrated and desalted after in-gel digestion using reversed-phase C_{18} ZipTips® (Millipore) according to the manufacturer's recommendations. After wetting the resin with acetonitrile, the tip was equilibrated using 0.1% TFA. Prior to loading, TFA was added to the sample to a final concentration of 0.1%. After aspirating the sample ten times, the bound peptides were washed twice in 0.1% TFA, and once in 5% ethanol and 0.1% TFA. Peptides were eluted in 2 µL of

0.1% TFA and 50% AcN, mixed with a matrix (see 2.2.2.5 and 2.2.2.6), and loaded onto the MALDI-MS target plate.

2.2.5.5 Dried Droplet Method

10 mg/mL of alpha-cyano-4-hydroxycinnamic acid (CHCA) in 1 vol acetontile and 2 vol 0.1% trifluoroacetic acid (TFA) were vortexed for 30 seconds to solubilize the matrix. The solution was quickly centrifuged and the supernatant transferred to a new tube. The supernatant was then mixed in a ratio of 1:1 with the protein sample to be analysed. 1 µL of this mixture was then applied to the target plate and allowed to dry in a laminar flow hood before analysis. In some cases this step was repeated in order to increase the amount of detectable peptides.

2.2.5.6 Fast Evaporation Method (Vorm *et al.*, 1994)

40 mg/mL of CHCA was dissolved in acetone and vortexed briefly. Insoluble material was removed by transferring the supernatant to a new tube after centrifugation. A 10 mg/mL solution of nitrocellulose (Bio-Rad) in acetone/isopropanol (1:1) was mixed in a ratio of 1:4 with the CHCA/acetone solution. 1 µL of matrix solution was deposited on the target plate and allowed to dry. 0.5 µL of 5% formic acid was then placed on top of the dried matrix. 0.5 µL of sample solution was then injected immediately into the drop of formic acid on the target plate and allowed to dry in a laminar flow hood. As an optional step samples were rinsed three times by depositing 5-10 µL of water on the probe and then immediately removing it. The samples were then analysed in the mass spectrometer.

2.2.5.7 MALDI-MS Analysis

The peptides on the target plate were ionized and analysed on a micromass® TofSpec 2E/M@LDI™. After loading of the target plate, subsequent mass spectra were either obtained manually by moving the crosshair and selecting different areas for ionization within a target circle, or automatically using the software. The amount of laser energy required for optimal sample signals needed to be determined empirically for each analysis. Angiotensin I was added to one target well and analysed prior to any sample data collection to ensure correct calibration of the mass spectrometer. If the monoisotopic angiotensin I signal deviated from its known mass ([M+H]+ = 1296.6853), the mass spectrometer was adjusted and calibrated accordingly. The average sample signal intensities of ten laser shots were recorded using

Mass Lynx v.3.5 software. The list of mass spectra generated was subsequently used for peptide mass fingerprinting analysis.

2.2.5.8 Peptide Mass Fingerprinting

The lists of peptide peaks generated by MALDI-MS were searched against the Mascot protein data base for protein identification using the Mascot Peptide Mass Fingerprint program (www.matrixscience.com). The following parameters were used for identifying the protein using the peptide list obtained from MALDI-MS: The Swiss-Prot and Matrixscience database (MSDB) were selected as the protein databases. The search was restricted to the mammalian taxa, and trypsin specified as the enzyme used for proteolytic cleavage of the protein, allowing 1 missed cleavage site. No modifications were selected from the menu (default) when searching a database. Peptide mass tolerance was set to 1 Da (default) and MH+ and monoisotopic mass selected from the mass values menu. The list of peptide peaks obtained from MALDI-MS was entered in the query field and searched against either the Swiss-Prot or Matrixscience database. Results included the degree of sequence coverage (in percent), the number of matched and unmatched peptide peaks, and a score indicating the likelihood of having identified the protein in question.

2.2.5.9 Target Plate Maintenance

Cleaning of target plates was carried out according to the manufacturer's recommendations. The target plate was scrubbed in 2% Decon 90 using a tooth brush and rinsed with distilled water followed by soaking for 15 min in trichloroethylene. This was followed by sonication for 30 min in 2% Decon 90. Plates were then rinsed extensively with HPLC-grade water, followed by rinsing with HPLC-grade acetonitrile and allowed to dry before use.

2.2.6 FACS (Fluorescence-activated Cell Sorter) Analysis

Cells were trypsinized and pelleted at 480 x g at 4°C for 10 min, before determining the cell concentration using a hemocytometer (Neubauer). Approximately 1 x 10^6 cells were used for FACS analysis and were resuspended in 50 µL PBS and fixed with 600 µL 70% ethanol at 4°C for at least 1 h, or stored for up to 1 week at 4°C. Cells were then washed in PBS twice before adding 100 µL of 1 mg/mL RNase for 15 min at RT, and staining in 200 µL of 100 µg/mL propidium iodide for 2-24 h. FACS analysis was performed on a Becton Dickinson FACScalibur (BD Biosciences, NSW, Australia), counting at least 1 x 10^5 cells per sample.

The data analysis was performed by Dr Fran Wolber, Institute for Food, Nutrition and Human Health, Massey University.

2.2.7 Immunohistochemistry

All immunohistochemistry procedures were performed at MedLabCentral, Palmerston North Hospital and analysis conducted by Dr Bruce Lockett, Palmerston North Hospital.

2.2.7.1 Cell Blocks

Harvested MDA MB 231 cells were fixed in 10% formaldehyde and transferred to MedLabCentral at 4°C. Cell blocks for immunohistochemical analysis were prepared by washing the fixed cells in isotonic saline (0.85%) three times and collecting the cell pellet by centrifugation. Cells were then resuspended in 5 drops of normal human plasma followed by the addition of 5 drops of activated thrombin mixture and 3 drops of 25 mM CaCl. The forming clot was then placed onto a histology cassette and immersed in 70% ethanol. The clot was then embedded in paraffin and 2 μm thick slices cut from the block and placed on a silanized glass slide. Slides had previously been placed in a silane solution (2% silane in acetone) for 2 min and washed in two changes of distilled water before being dried.

2.2.7.2 Histological Staining

Staining of the tissue specimens was performed at MedLabCentral, Palmerston North Hospital by Dr Bruce Lockett, using an autostainer. At first, tissue slides were deparaffinised in xylene and rehydrated with tap water, before treating the tissue with 33% H_2O_2 for 10 min. Antigen retrieval was performed by placing the slide in 0.25 M Tris base, pH 9, for 10 min, after which the slides were rinsed extensively in tap water, distilled water, and placed in PBS containing 0.05% tween. The next step was to apply DNA-PK (1:1200) and Rad51 (1:90) antibodies to the slide and incubate at 25°C for 30 min on a rotator. The slides were then rinsed three times with PBS and placed into Powervision solution, a commercial antibody detection complex. 45 min later the slides were rinsed three times with PBS, and then twice with distilled water. The slides were then submersed in DAB Chromogen (DAKO) for 5 min, and rinsed with tap water before being placed in copper sulphate for 1 min. After rinsing with water, the slides were counterstained by dipping them into haematoxylin five times, rinsing in water and dipping them in ammonia ten times. The slides were then rinsed in distilled water and dehydrated. Finally, the slides were examined under a light microscope and the degree of immunohistological staining determined using the semi-quantitative H-score methodology

(McCarthy *et al.*, 1985). Images were acquired using a 4 megapixel digital camera mounted to a light-microscope.

Chapter Three
SELDI-MS

3.1 Surface-Enhanced Laser Desorption Ionization Mass Spectrometry (SELDI-MS)

Surface-enhanced laser desorption mass spectrometry was used to determine the feasibility of detecting differentially regulated proteins, using the drug treatment regime described below and to compare these data to data obtained from two dimensional gel electrophoresis. SELDI-MS is a technology which combines the use of chromatographic surfaces with mass spectrometric analysis, and according to the manufacturer has a sensitivity limit comparable to other mass spectrometers (femto to atto mol range), and can detect proteins of over 500 kDa in size (Grus *et al.*, 2003). Samples are applied directly onto protein chips, each of which features a unique protein binding property, for example: hydrophobic, hydrophilic, anion exchange or cation exchange, thereby effectively fractionating the sample prior to analysis. The initial binding of proteins to the chip surface is followed by a wash step to eliminate any contaminants which may interfere with analysis. After drying the sample, a matrix consisting of energy absorbing molecules is used to overlay the bound sample, to facilitate desorption and ionization for subsequent mass spectrometric analysis. Molecules which have been ionized by laser shots are analysed by the time of flight detector and their masses subsequently displayed as a mass-to-charge ratio (m/z). Ionisation of a 2000 Da protein for example usually results in the addition of one proton which results in an m/z value of 2001 ($[M+H]^{1+}$). If two protons were added during ionization, the resulting m/z value would be 1001 ($[M+2H]^{2-}$). The resulting spectra display the relative intensity of each protein peak compared to the strongest signal/peak, which is set at 100 units. For instance, if a protein passes the detector ten times fewer than the most abundant molecule, the resulting signal for this protein would be 10 units.

3.2 Cell Lines and Protein Extracts

Three cell lines commonly used in breast cancer research were chosen for analyses of potentially differentially expressed proteins in response to doxorubicin treatment: MCF12A (normal breast tissue), MCF7 (breast cancer, estrogen receptor positive and wild-type p53), and MDA MB 231 (breast cancer, epidermal growth factor receptor and transforming growth factor receptor alpha positive, BRCA1 and p53 mutated, more aggressive than MCF7 (Xie *et al.*, 2002). These cells were grown to approximately 80% confluence, as growth inhibitory effects due to space limitation should not have been present at that stage. Cells were then

either harvested (0 h) or exposed to 5 μM doxorubicin for 1 h, after which the media was changed. Drug exposed cells were then harvested 2 h and 24 h after initial exposure, thereby allowing the analysis of immediate and prolonged changes in protein expression. These parameters were chosen as a previous study revealed that a drug concentration of 5 μM would allow only resistant cells to survive, while avoiding total annihilation of the cell culture (Allen, 2003). Drug exposure time was limited to 1 h to ensure clinical relevance of the experiment, as doxorubicin has only a short half-life in treated patients (Pharmacia & Upjohn). Harvested cells were lysed using a nuclear extraction buffer (section 2.2.4.1) and quantified using the Bradford method (section 2.2.2.5). Protein extracts were snap frozen in liquid nitrogen and stored on dry ice for shipment to Ciphergen in Brisbane, Australia, where the SELDI-MS analysis was conducted.

SELDI-MS was used to analyze 8 of the 9 protein samples: the 0, 2, and 24 h samples of MCF7 and MDA MB 231, as well as the 0 h and 24 h samples of MCF12A. The remaining sample, MCF12A 2 h, had to be omitted from analysis, as the protein chips used contained only 8 sample loading spots. Extracts were loaded onto different complementary protein chips.

3.3 Results

Of the three cell lines analysed by SELDI-MS, 7 differentially regulated proteins were detected in response to doxorubicin exposure. Up-regulated protein expression was observed in MCF7 (Fig. 3.1 and Fig. 3.3), MDA MB 231 (Fig. 3.2 and Fig. 3.3), and MCF12A (Fig. 3.2) after drug exposure, while down-regulated proteins were found only in MDA MB 231 and MCF12A cells (Fig. 3.2). The results were subsequently summarized and are shown in table 3.1. Unfortunately, SELDI analysis had to be discontinued as it was offered by Ciphergen for promotional purposes only, and additional analyses were beyond the budget of this research.

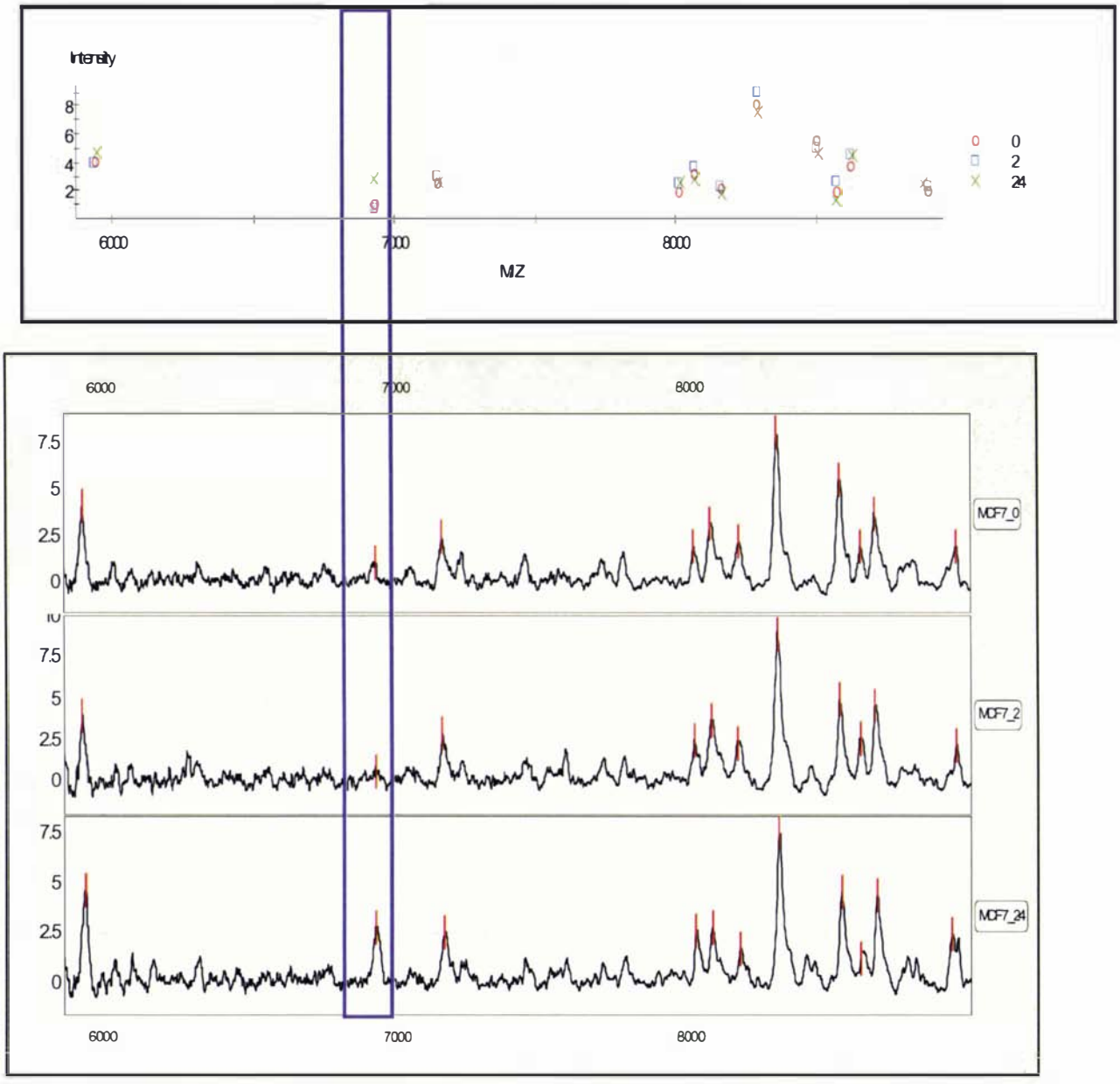

Fig. 3.1: SELDI analysis of a protein up-regulated in MCF7 cells

Before conducting the analysis samples were overlaid with a matrix consisting of energy absorbing molecules to allow protein desorption and ionization. A schematic (top) and peak-flow chart (bottom) representation highlighting a 5-10 fold increase in signal intensity of a 6929 Da protein, which was up-regulated in MCF7 cells 24 h after drug exposure (blue rectangle).

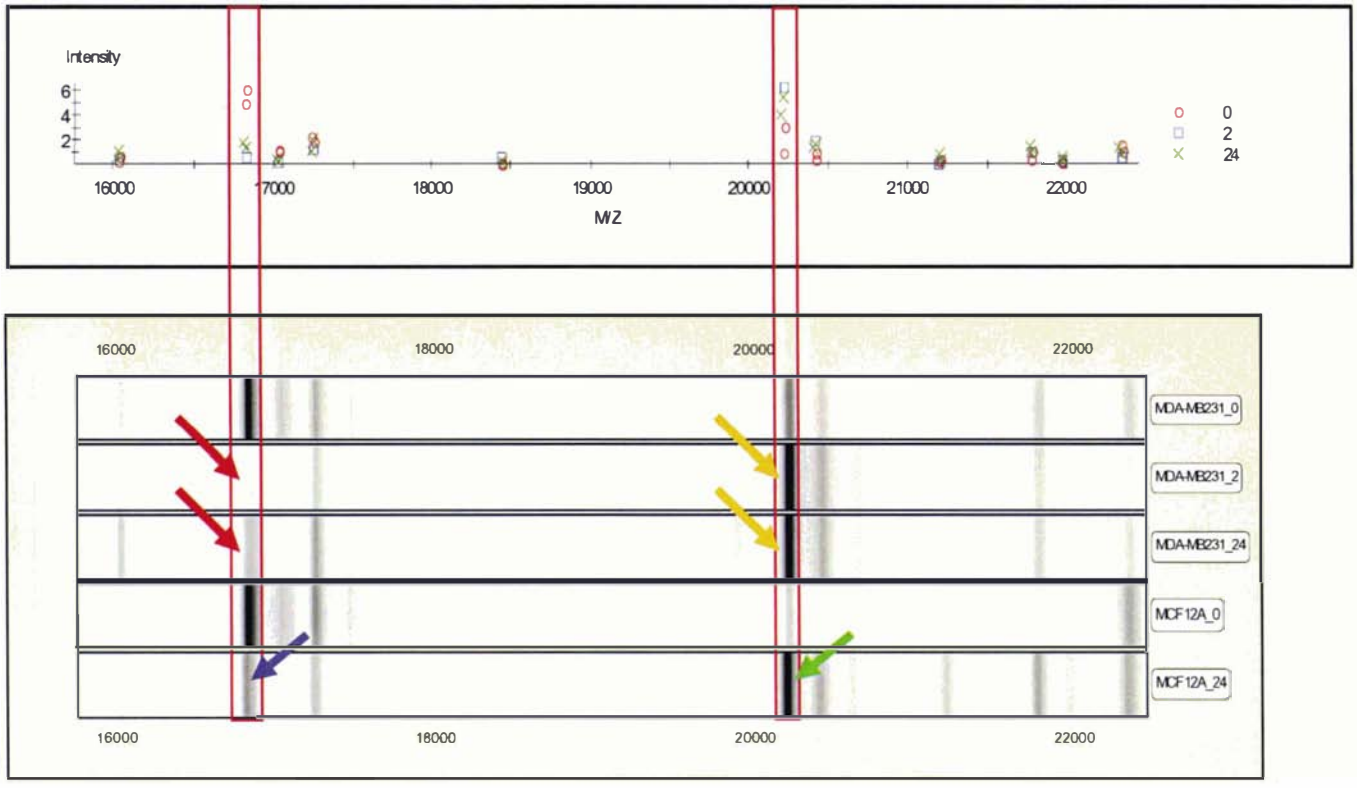

Fig. 3.2: Gel view of differentially regulated proteins in MDA MB 231 and MCF12A cells

Prior to analysis samples were overlaid with a matrix consisting of energy absorbing molecules to allow protein desorption and ionization. SELDI-MS analysis software allowed viewing of data either in standard peak-flow, schematic (top) or gel view mode (bottom). In the latter, increasing signal intensity was represented by increasing blackness of the corresponding band. A 16.828 kDa protein, which corresponds in molecular weight to Caveolin-2 (16828.51 Da), was found to be down-regulated approximately five fold in MDA MB 231 (red arrows) and MCF 12A (blue arrow) after drug treatment. Furthermore, post-treatment up-regulation of a 20.223 kDa protein was detected in MDA MB 231 (yellow arrows) and MCF 12A (green arrow).

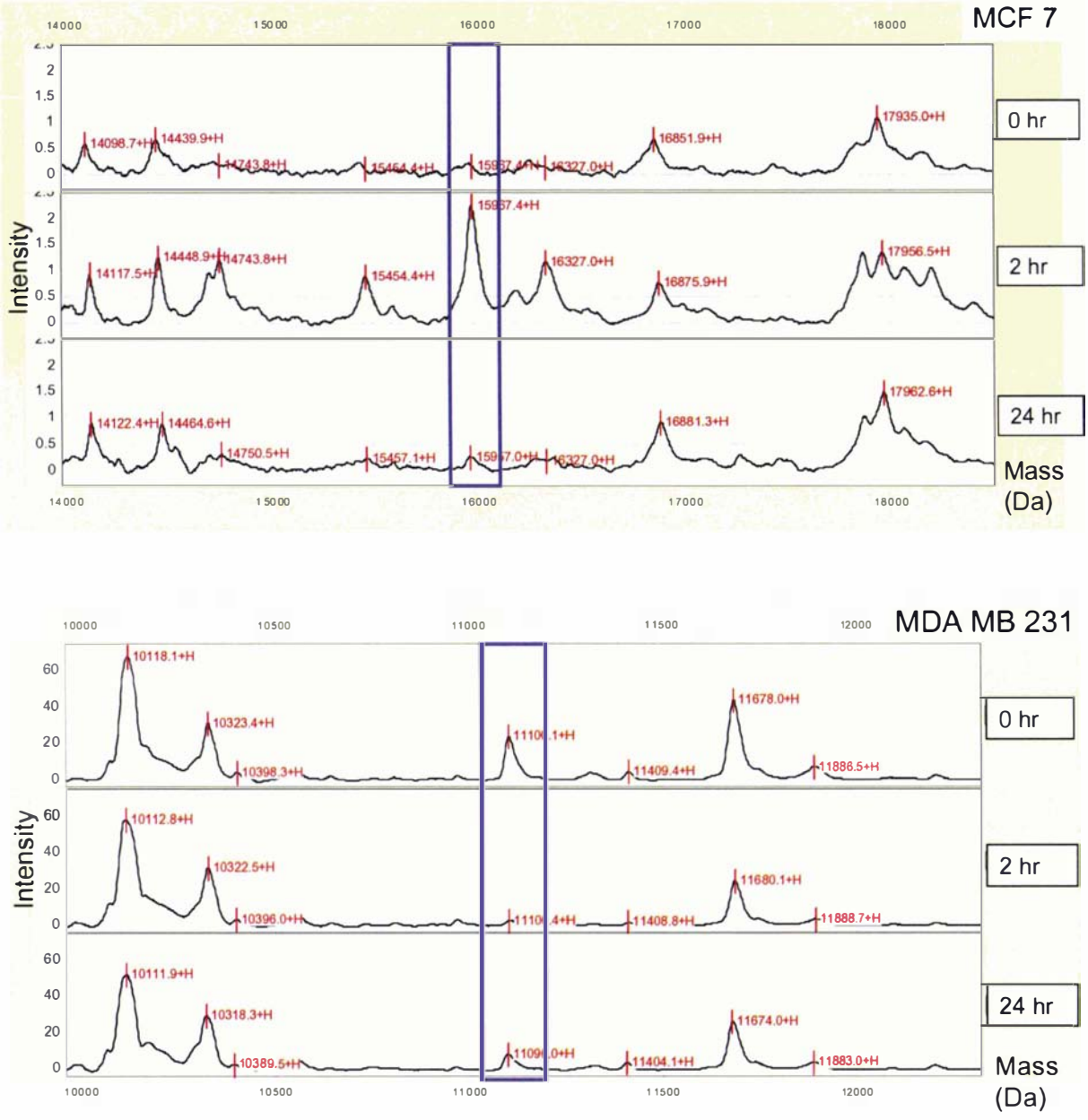

Fig. 3.3: Peak flow diagram of candidate proteins of MCF7 and MDA MB 231 cells

Prior to analysis samples were overlaid with a matrix consisting of energy absorbing molecules to allow protein desorption and ionization. A protein of 15.957 kDa was found to be up-regulated by more than 10 fold in MCF7 cells 2 h after drug exposure only. In MDA MB 231 cells an 11.100 kDa protein showed a 10 fold down-regulation in response to doxorubicin treatment.

	Down	Up
MDA MB	11.100	9.220
231	**16.828**	**20.223**
MCF12A	**16.828**	16.845
		20.223
MCF7		6.929
		15.957

Table 3.1: Summary of candidate proteins

The molecular weight (kDa) of proteins which appeared up- or down-regulated due to drug exposure in the three cell lines tested, according to SELDI-MS analysis, are shown. Bold numbers indicate candidate proteins which were differentially expressed in both MDA MB 231 and MCF12A cell lines.

3.4 Protein Mass Identification

In order to identify those proteins differentially regulated in response to drug treatment using the mass value only, the Swiss-Prot database was searched using TagIdent (http://au.expasy.org/tools/tagident.html). Once a protein mass and deviation range was entered, the program searched the Swiss-Prot database for matching protein masses, which were subsequently recorded in a list. To ensure only relevant matches were displayed, the search was limited to human proteins. The accuracy of protein masses as determined by SELDI-MS was within 1 Da according to Cyphergen. Consequently, when searching the database for putative candidates using protein mass, a deviation of +/- 2 Da was used to allow for rounding since most of the actual protein masses did not contain any decimals. For example 6926 Da may actually be 6926.9 Da in which case a 1 Da deviation would result in an actual rounded mass of 6928 Da. A search against the molecular weight of the 7 differentially regulated candidate proteins, using the TagIdent search engine against the Swiss-Prot database, only retrieved one result: Caveolin-2 (16828.51 Da) matched the 16.828 kDa protein which was found to be down-regulated in both MDA MB 231 and MCF12A cells after doxorubicin treatment.

Caveolin-2 has been suggested to act as a scaffolding protein within caveolar membranes and also to functionally regulate the activity of the alpha subunit of G-proteins. It is expressed in

endothelial cells, smooth muscle cells, skeletal myoblasts, and fibroblasts and has been found to be up-regulated in lung cancer cells after doxorubicin exposure (Belanger *et al.*, 2003). Furthermore, cDNA analyses have shown that the caveolin-2 (CAV2) gene is overexpressed in lung cancers (Bianchi *et al.*, 2004) and that increased protein levels coincide with shorter survival (Wikman *et al.*, 2004). On the contrary, suppressed CAV2 expression coinciding with lower protein levels has been reported in human breast cancers compared to normal tissue indicating a potential role of caveolin-2 in tumour progression (Sagara *et al.*, 2004).

3.5 Discussion

Interestingly, the results described here demonstrated that some proteins of identical molecular weight showed a similar response to drug treatment, in two different cell lines i.e. MDA MB 231 and MCF12A. This consistency provided support that the observed differences in protein levels were a genuine response to drug exposure and were not merely coincidental. The high degree of similarity in signal intensity of proteins from different samples further underscored this notion. Furthermore, SELDI-MS provided data of differentially regulated proteins and their masses. Ideally, all experiments would have been conducted in triplicate in order to confirm the reproducibility of any changes in protein expression. As a next step, SELDI-MS integrated software analysis could then have been employed to determine the statistical significance of observed differences. Since it was not possible to analyse any additional samples the reproducibility of these results could not be confirmed. The data base search demonstrated however, that these data are only of very limited use in trying to identify proteins in question, as the mass value alone is not sufficient for positively identifying unknown proteins. Post-translational changes are common for proteins, altering their molecular weight, and can be expected especially of proteins involved in signalling pathways, which are likely to be activated in response to drug treatment. As the search program (TagIdent) does not have the ability to consider changes in molecular weight due to post-translational modifications, the protein can no longer be correctly matched to the data base entry. Furthermore, false positive identification of proteins is also a concern, as any number of modifications may result in the same molecular weight of two entirely different proteins. For this reason, peptide fingerprints of candidate proteins are usually necessary to unambiguously identify unknown proteins.

The size limit for proteomic analysis (protein mixture) of whole proteins is roughly 2 - 40 kDa (Adam *et al.*, 2002). Although the analysis of proteins beyond this size is possible, they

become increasingly more difficult to ionize with increasing molecular weight. In practice this means that unless a large protein is highly abundant its chances of being ionized, and hence detected, are very slim compared to smaller proteins. For this reason, proteins which were identified as being differentially regulated after drug treatment in this research using SELDI-MS, were below 30 kDa in size.

One potential candidate which was down-regulated after doxorubicin treatment in MDA MB 231 and MCF12A cells was matched to Caveolin-2 by searching the Swiss-Prot protein database. It is unclear at this point if the differentially regulated protein of 16.828 kDa is indeed caveolin-2, and whether or not it plays a functional role in response to doxorubicin exposure. Contrary to the observation made here, caveolin-2 has been reported to be up-regulated in lung tumour cells after doxorubicin treatment. At present there are no data available that may explain this discrepancy. It is not uncommon however, for a protein to respond differently to drug-induced cellular stress in different tissues or cell lines (Bourgarel-Rey *et al.*, 2000).

Overall, the SELDI-MS results presented here succeeded in demonstrating the feasibility of the approach used in the current study, providing evidence that differentially regulated proteins could be detected in response to doxorubicin exposure in MDA MB 231, MCF12A, and MCF7 cells.

Chapter Four

Establishing a Methodology for the Separation and Identification of Unknown Proteins

4.1 Introduction

First introduced by O'Farrell (O'Farrell, 1975), two dimensional gel electrophoresis (2DGE) has remained one of the most popular techniques employed to study changes in protein expression. Protein samples are first separated on a small gel strip by means of isoelectric focusing (IEF) taking advantage of differing isoelectric point values. An immobilized pH gradient (IPG) gel strip is created by covalently incorporating a gradient of basic and acidic acrylamido buffering groups into a polyacrylamide gel. The concentrations of different acidic and basic buffers used for casting the gel determine the final range and shape of the IPG strips. Proteins are focused in gel regions where their net charge is zero. The gel strip containing the focused proteins is then transferred to the second dimension, an SDS-PAGE gel, which separates the proteins according to their molecular weight. 2DGE allows the study of whole protein extract expression profiles of different samples (e.g. cancerous and normal cells), that can subsequently be compared and scrutinized for differentially expressed proteins. This method had already been used successfully in other breast cancer studies focusing on monitoring drug-induced alterations in protein expression in cancer cells (Chen *et al.*, 2002; Moller *et al.*, 2002), post-translational modifications (Dwek *et al.*, 2001), and analysing differences between malignant and normal tissues (Stastny *et al.*, 1984). In this study 2DGE was used in an attempt to analyse and identify proteins differentially regulated in response to doxorubicin treatment using the same experimental design as that utilized for SELDI-MS analysis.

4.2 Optimisation for Two Dimensional Gel Electrophoresis

Initially cells were lysed and proteins extracted as previously described (section 2.2.4.1). These protein extracts were then mixed with rehydration buffer (8 M urea, 2% (w/v) CHAPS, 0.5% IPG buffer, 2.8 mg/mL DTT, bromophenol blue) (Berkelman and Stenstedt, 1998) to a final protein amount of 120 µg, which was used for IEF. Isoelectric focusing was ineffective however, as the tracking dye actually migrated towards the anode instead of the cathode. This was a consequence of the high salt concentrations generated from the potassium-chloride in the extraction buffer. In order to circumvent the problem of high salt concentration a suitable extraction protocol incorporating a 2DGE extraction buffer, was developed. Widely used

extraction buffers for 2DGE usually contain for example: 8 M urea, 4% (w/v) CHAPS, 40 mM tris base, 5 mM DTT, 1 x Roche Complete™ mini, 0.5% IPG buffer (carrier ampholytes), and a trace of bromophenol blue (Berkelman and Stenstedt, 1998). While this buffer omitted salts, its use resulted in increased sample viscosity necessitating the use of ultracentrifugation to remove residual DNA and RNA from the sample. While the 2DGE buffer allowed IEF to proceed, detectable spot numbers were low (data not shown). Therefore, a number of alterations were subsequently made to improve the protocol. To enhance protein solubility, thiourea was added as this has been reported to significantly increase the number of spots detectable on 2D gels (Rabilloud, 1998). Thiourea had an added advantage as it creates an inhibitory effect on proteolysis, even exceeding that measured for protease inhibitors, such as Roche Complete™ mini (Castellanos-Serra and Paz-Lago, 2002). Bromophenol blue was substituted by Coomassie brilliant blue, which was documented to improve spot resolution (Vilain *et al.*, 2001). Finally, tergitol was added as it has been reported to reduce the detrimental effects produced by salt ions, improving spot resolution, reducing horizontal smearing, and minimizing strip burns (Laoudj-Chenivesse et al, 2002). This new running buffer (8 M urea, 4% CHAPS, 1 x Complete™ mini, 40 mM tris base, 2 mM DTT, 1 mM EDTA, 2 M thiourea, 0.01% Coomassie brilliant blue, 0.5% IPG buffer, and 0.001% tergitol NP-4) resulted in the generation of the first comparable 2D gels (Fig. 4.1).

4.3 Two Dimensional Gels

Protein samples, extracted 0, 2, and 24 h after doxorubicin treatment, from normal breast cells (MCF12A) and from breast cancer cells (MCF 7 and MDA MB 231), were separated on 13% 2D SDS-PAGE gels using the improved 2D extraction buffer protocol. Some of these gels displayed potentially differentially regulated proteins (Fig. 4.1).

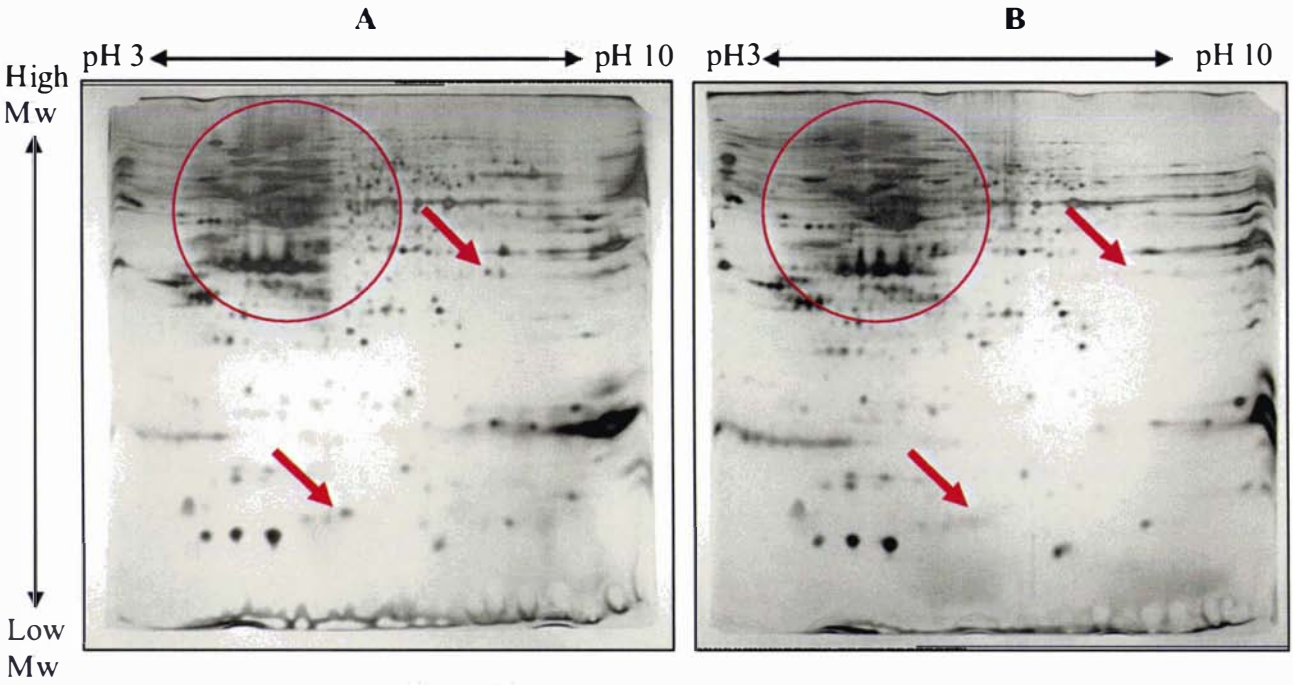

Fig. 4.1: 2DGE gels of MDA MB 231 cells using 60 µg of protein

Two representative results of 2DGE analyses using 13% polyacrylamide of MDA MB 231, unexposed (A) and 2 h after doxorubicin exposure (B) are shown. Arrows highlight potentially differentially regulated proteins. The circle displays an area of densely populated high Mw proteins and ionic impurities resulting in streaking and poor resolution.

Due to accumulation of high Mw proteins, ionic impurities, and faint protein staining of less abundant proteins, the results obtained were inconclusive and demanded further optimization, combining higher loading capabilities with better resolution.

4.4 Purification Strategies

Proteins are commonly alkylated before transfer of the IPG strip to the 2nd dimensional gel to eliminate any protein interactions due to disulphide bonding (section 2.2.3.3). Commonly, DTT is used to reduce disulphide bonds prior to IEF, and subsequently they are irreversibly alkylated using iodoacetamide (Berkelman and Stenstedt, 1998). This protocol has been followed by much of the scientific community, but recent reports have indicated that this may not be the best practice. Two problems arise when reducing and alkylating proteins using this standard protocol. Firstly, reduction of proteins is not permanent, and as they are not alkylated during IEF it is possible for disulphide interactions to occur, resulting in improper focusing. Secondly, it has been argued that iodoacetamide was not the best alkylating agent to use, and that reaction times for proteins captured in the gel matrix of the strip to be completely

alkylated were much too short (Galvani *et al.*, 2001; Galvani *et al.*, 2001; Herbert *et al.*, 2001). In fact, insufficient alkylation results in several alkylation states of proteins, depending on the number of possible thiol-containing residues. As a consequence, a protein spot can appear spurious and may be hard to identify using peptide mass fingerprinting methods. Near complete alkylation of thiol-groups is therefore essential when trying to identify minute amounts of protein, as is commonly the case in proteomic studies (Herbert *et al.*, 2001).

To overcome difficulties mentioned above, the substitution of iodoacetamide for acrylamide has been proposed. Because alkylation using acrylamide works best under slightly basic conditions, it was necessary to increase the pH of the sample buffer to ~ 9 (Herbert *et al.*, 2001). Furthermore, excess acrylamide had to be scavenged by the addition of free cysteine to prevent alkylation of lysine residues during electrophoresis. The increase in pH was another problem, as samples required filtering to remove residual nucleic acids and impurities prior to reversed-phase high performance liquid chromatography (RP-HPLC). The filtering membranes used were compatible only with solutions not exceeding pH 8. Adjusting the pH to acceptable values proved very difficult, as the sample volume was very small after filtration. A report published shortly after initial trials using acrylamide as an alkylating agent, identified 4-vinylpyridine as a more potent alkylating agent (Sebastiano *et al.*, 2003). Another important advantage of 4-vinylpyridine is its compatibility with Tris(2-carboxyethyl)phosphine (2-TCEP), which is a stronger reducing agent than DTT (Getz *et al.*, 1999). Replacing acrylamide with 4-vinylpyridine, and DTT with 2-TCEP provided several improvements to the current protocol. It was then possible to completely reduce and alkylate a protein sample simultaneously, prior to IEF, without the necessity of adjusting the pH and therefore, providing a robust protocol (section 2.2.3.3).

4.5 Protein Prefractionation

In addition to a very effective extraction protocol, a suitable strategy needed to be implemented to achieve improved resolution and loading capabilities. Using RP-HPLC as a prefractionation method prior to 2DGE has been reported to provide the necessary improvements. Individual fractions have been shown to yield better resolution, due to salt removal and simplified protein mixtures (Badock *et al.*, 2001; Van den Bergh *et al.*, 2003). In addition, the total amount of sample protein distributed over the individual fractions was far greater than could have been loaded onto a single gel (>1 mg rather than ~100 µg). This was

equivalent to a 10 fold increase in sensitivity, allowing less abundant proteins to be studied without interference from spots representing highly abundant proteins.

To further enhance resolution of high molecular weight proteins and to avoid clustering in upper gel areas, gradient gels were used. 10%-15% polyacrylamide gradient gels were found to allow good separation of high Mw proteins while at the same time preventing smaller proteins from running off the gel.

Nevertheless, the protein extraction and purification protocol still necessitated modifications to suit requirements dictated by the use of RP-HPLC. It was paramount to successfully remove cell debris from samples prior to analysis by RP-HPLC. One solution was the use of Benzonase®, a urea tolerant, highly active exonuclease which digests both DNA and RNA, significantly helping to reduce viscosity. After this treatment however, the sample was still not sufficiently pure, as different ultrafiltration devices used for pre-run purification still suffered from immediate clogging of the filter membrane. One possible method to eliminate this problem was to use TCA precipitation. As precipitation is not recommended when doing proteomic studies (Berkelman and Stenstedt, 1998), it was necessary to ensure that any protein loss, be it selective or unselective, was avoided. To ensure sample reproducibility a TCA precipitated whole sample, which was subsequently separated on a RP-HPLC column, was compared to an untreated standard whole sample (data not shown). Indeed, not only were there no apparent spot losses, but RP-HPLC also improved resolution and focusing of some proteins.

While the aim of using RP-HPLC to prefractionate protein samples was to improve protein loading and protein spot resolution, the number of fractions used had to be kept to a minimum to ensure the feasibility of this approach. Hence, the original protocol (Badock *et al.*, 2001) was modified to a two-step fractionation protocol which was found to be the most successful compromise (Fig. 4.2). In the first step, any interfering substances were eliminated from the samples, for example salts stemming from the buffer and sample. After collecting the first fraction using 45% acetonitrile (AcN), all remaining proteins were eluted using 100% AcN.

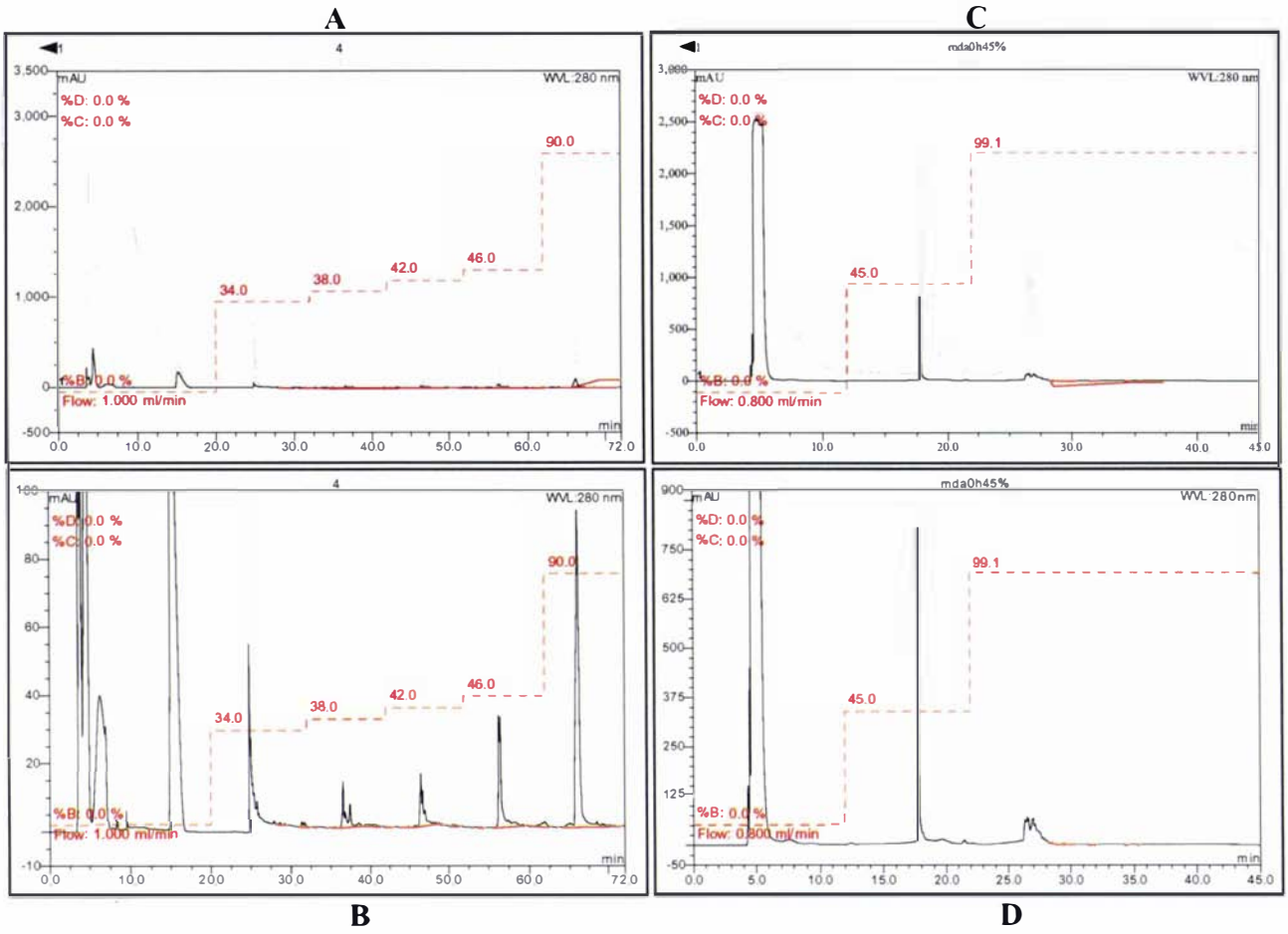

Fig. 4.2: RP-HPLC prefractionation elution profiles

The original protocol, comprising of a five-step protein fractionation using increasing amounts of acetonitrile, was initially used to estimate protein distribution and to determine the most feasible fractionation strategy (A and B (expanded y-scale)). Protein fractions eluted with 45% and 100% AcN (C and D (expanded y-scale)) resulted in the best spot distribution and resolution patterns on 2D gels. After an initial wash step, protein elution was monitored by measuring light absorption at 280 nm (Welcsh *et al.*, 2002) and 230 nm (gray).

The two fractions were subsequently concentrated using a speed vac and separated on a 2D gel. To evaluate any spot differences relating to the fractionation procedure, gels from the 45% and 100% acetonitrile fractions were compared to a gel using whole cell extract (Fig. 4.3).

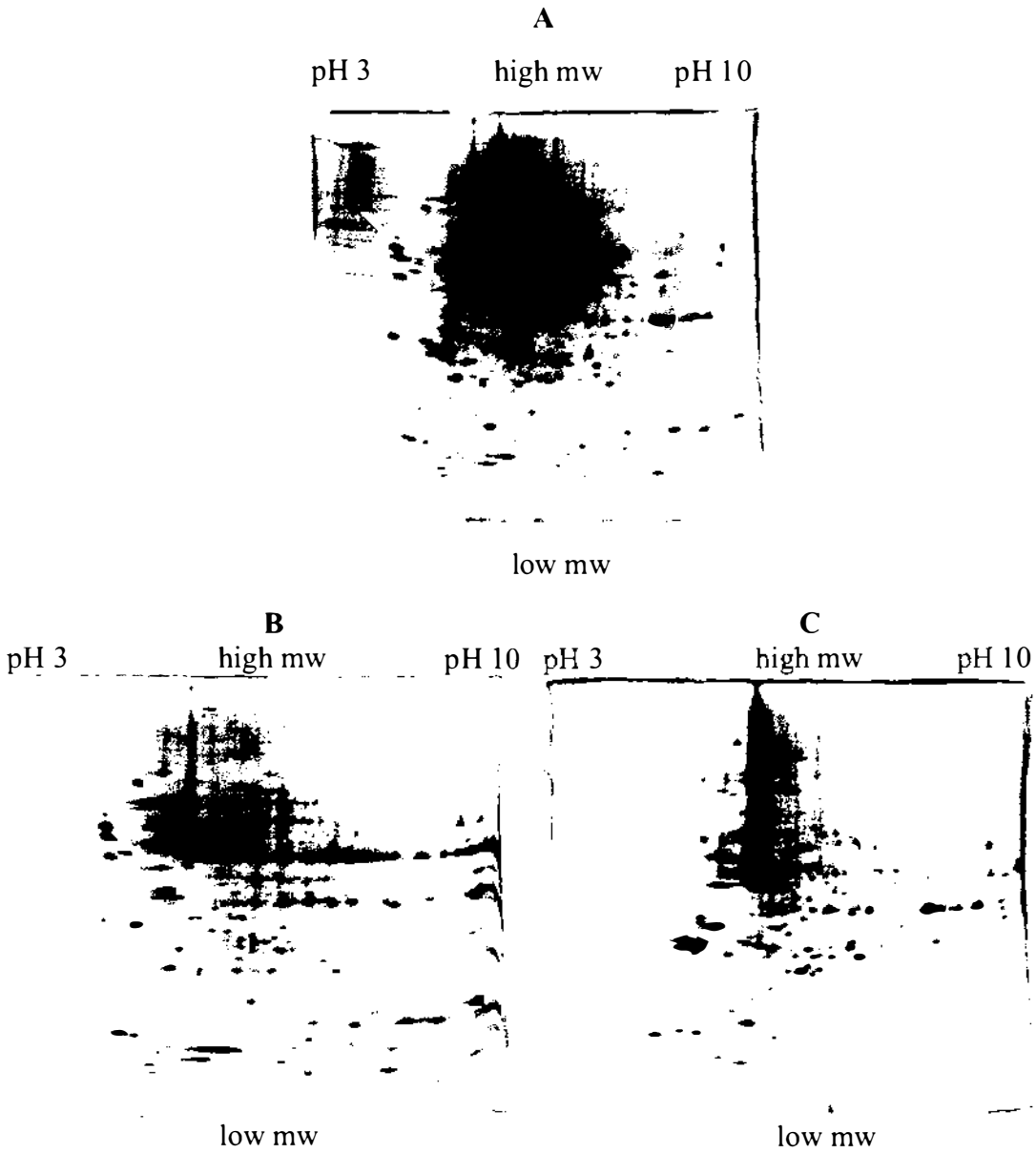

Fig. 4.3: 2D gels after sample prefractionation

2D gels of a prefractionated MDA MB 231 sample (gel A: whole sample; gel B: 100% acetonitrile fraction; gel C: 45% acetonitrile fraction). 75 ug of protein was loaded on each of the three 10-15% SDS-PAGE gradient gels. Some spot intensities were either increased (arrows) or decreased (rectangles) in gels of fractionated samples compared to the whole extracts, while others appeared in both fractions (circles). In general, fractionated samples exhibited lower background than did the whole extract.

4.6 Narrow Range Immobilized pH Gradient (IPG) Dry Strips

A further alternative for simplifying spot patterns was to use narrow pH range immobilized gradient strips. Indeed, this approach succeeded in improving spot resolution, while only a few proteins at the acidic and basic end were lost (Fig. 4.4 and Fig. 4.5).

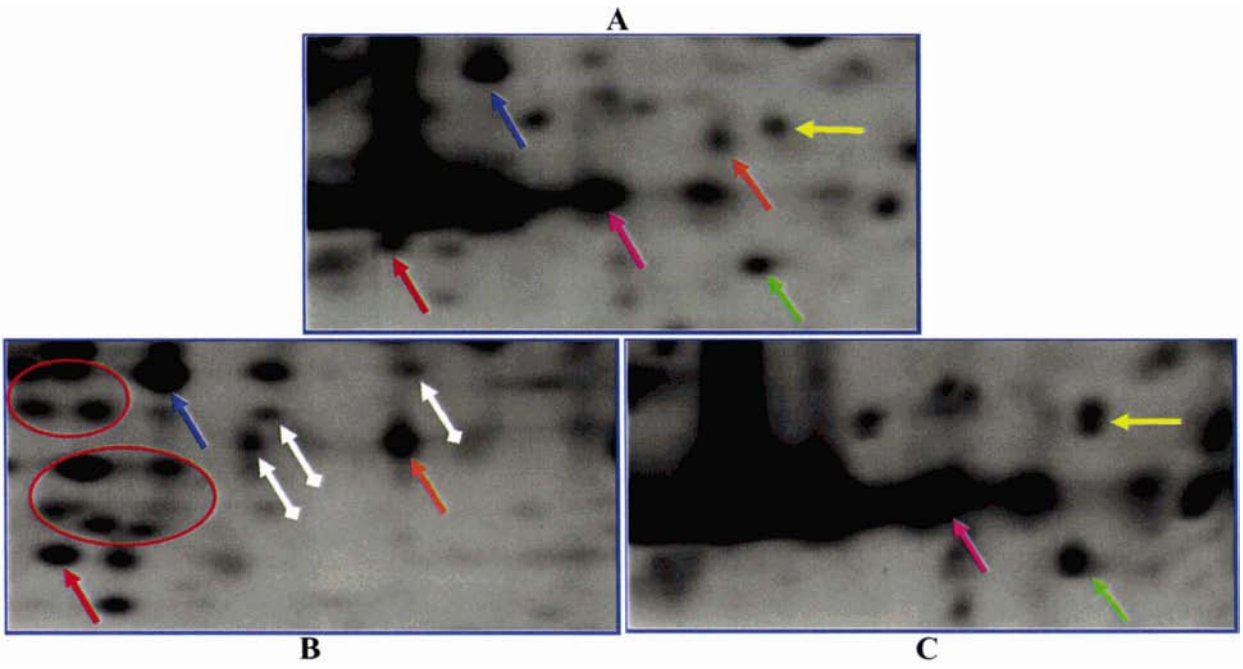

Fig. 4.5: Native and prefractionated samples on pH 4-7 strips

Close up of an area (blue boxes, Fig. 4.4) benefiting from sample prefractionation by increasing the resolution of obscured proteins. 300 µg of MDA MB 231 cell extract was fractionated using RP-HPLC and loaded onto pH 4-7 strips. 64 µg of the 45% (Gel C) and 44 µg of the 100% (Gel B) acetonitrile fractions were separated on 10-15% gradient gels and compared to native sample (Gel A), which contained 75 µg of protein. Coloured arrows show landmark proteins and their distribution in the prefractionated samples. Red circles illustrate proteins which were obscured in the unfractionated sample, but could be resolved in the 45% AcN fraction. Proteins only identifiable as individual spots after fractionation, are highlighted by white diamond arrows.

Although the employment of RP-HPLC and sample prefractionation allowed comparatively more protein to be loaded onto 2D gels, it also demanded higher initial amounts of protein. Therefore, the sample volume required reduction after RP-HPLC to achieve feasible gel loading quantities. Several methods were used including different types of concentrators, freeze-drying and precipitation in order to overcome this difficulty. None of these approaches however, were successful in generating reproducible and consistent protein yields, as they resulted in an average loss of 80-90%, and therefore this method was not feasible (Table 4.1). At one point, concentration of samples in a speed-vac appeared to be more useful, incurring

losses of only 20%, but proved inconsistent and the majority of samples eventually suffered from losses equivalent to those of the other methods tried.

Concentration Method	Starting Amount	Final Amount	Possible Cause
Vivaspin®	3.5 mg	0.6 mg	Membrane adsorption
Centricon® SR-3	1 mg	0.1 mg	"
Macrosep®	1 mg	0.2 mg	"
TCA precipitation	1.25 mg	0.11 mg	Organic solvent interference
Freeze-dry	1 mg	Total loss	Tube surface adsorption
Speed-vac	varying	varying	Tube surface adsorption

Table 4.1: Concentration methods

In general, approximately 80% of a sample was lost during sample concentration after RP-HPLC separation, irrespective of the technique and devices used.

Unfortunately, the problems posed by prefractionating protein samples using RP-HPLC proved to be insurmountable and therefore this approach was not feasible.

4.7 Peptide Mass Fingerprinting Using MALDI-MS

Matrix-assisted laser desorption mass spectrometry (MALDI-MS) is a commonly used procedure in peptide fingerprinting, in which a protein spot is excised from a gel and subsequently digested with a peptidase (e.g. trypsin). The resulting peptides are then extracted from the gel and loaded onto the mass spectrometer for analyses, during which the peptides are ionised by laser pulses. Each individual peptide should then be displayed as a mass/charge (m/z) peak. If a sufficient number of peptides are displayed a peptide fingerprint can be established. As each protein has a unique peptide finger print, unknown proteins can be identified by searching their peptide fingerprint profile against a protein database, for example

Mascot or Swissprot (Simpson, 2003). In this study MALDI-MS was employed to help identify possible candidate proteins determined by 2DGE.

The first requirement was a methodology that was sensitive enough to identify small amounts of protein and reproducible enough to discern peptide and background peaks, thereby increasing confidence in data. To establish such a method, different concentrations of BSA ranging from 100 pmol to 1 pmol were subjected to a standard SDS-PAGE. BSA was visualised by either Coomassie or silver staining, and the BSA band was excised from the gel. Silver stained BSA bands had to be destained prior to trypsin digestion (Sumner *et al.*, 2002). The resulting peptides were then extracted from the gel and dried in a speed-vac, before being resuspended in matrix solution in preparation for MS analysis (section 2.2.5). Only peaks significantly larger (>10%) than the background noise were used for peptide mass fingerprinting (Fig. 4.6).

Sample handling proved to be critical in obtaining useful MALDI-MS data. No sample peaks could be obtained when using standard Eppendorf-tubes, even when digesting a 100 pmol BSA-band. The use of lubricated (low protein binding) tubes proved to be essential in obtaining peptide peak spectra that succeeded in correctly identifying BSA as the protein in question. In addition, the use of Zip tips (Millipore®) allowed the sample to be concentrated, leading to improved spectra and significant noise reduction (data not shown).

Sample loading was another critical step in successfully obtaining MALDI-MS data. In general, there is no optimal protocol for sample preparation and the best conditions needed to be determined empirically, as the spectra obtained depend largely on the matrix, the matrix solvent ratio, and the sample composition used (Kussmann *et al.*, 1997). Sinnapinic acid, genetisic acid (DHB), and α-cyano-4-hydroxycinnamic acid (alpha-CHCA) are three matrices commonly used for MALDI-MS of peptide mixtures. Furthermore, there are a variety of different methods for loading a sample onto a MALDI-MS target plate prior to analysis. Of these techniques the dried-droplet and the fast evaporation method are the most common (Taylor, 2003).

Experiments revealed that the fast evaporation method using CHCA as matrix produced the best and most reliable data (section 2.2.5.6). Unlike other preparation methods, the sample could be washed on the target plate due to the addition of nitrocellulose to the matrix solution

(Landry *et al.*, 2000). Peptides bound to the nitrocellulose, therefore allowing interfering substances such as salts to be to be washed off, and thus reducing background noise.

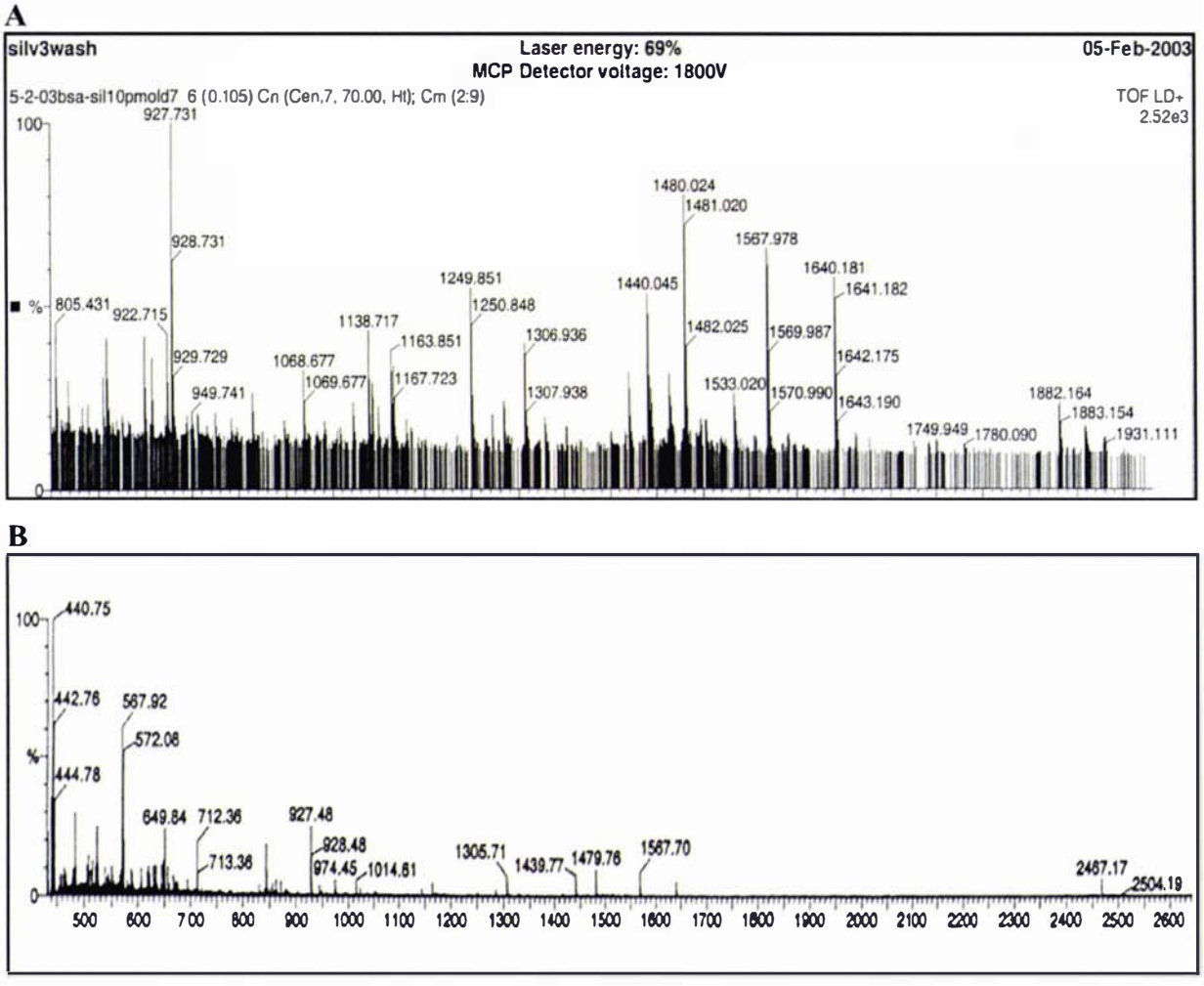

Fig. 4.6: MALDI-MS BSA peak spectrum using the fast evaporation method

Peak spectrum for 10 pmol silver stained BSA protein which had been concentrated using Zip-tips (A). 10 pmol of Coomassie blue stained BSA was digested with trypsin and extracted from the gel. 1/10 of the extracted digest was loaded for analysis. Results show the corresponding peak spectrum after background subtraction (B).

A list of significant peaks was compiled and searched against the Mascot protein data base for protein identification. Results obtained included a score indicating the likelihood of having correctly identified the protein in question, as well as protein mass and pI, which were used for additional verification of the protein. The results also included a sequence coverage score (as a percentage), depicting identified peptides. Using this procedure, a methodology was established that successfully identified BSA, while using as little as 1/10 of 10 pmol (67 ng)

starting material when using Coomassie blue stain and 10 pmol when using silver stained gel spots (Fig. 4.7 and Fig. 4.8).

Match to: **AAA51411**; Score: **152**
BOVALBUMIN NID: - Bos taurus

Nominal mass (M_r): **69248**; Calculated pI value: **5.82**
NCBI BLAST search of AAA51411 against nr
Unformatted sequence string for pasting into other applications

Taxonomy: Bos taurus
Links to retrieve other entries containing this sequence from NCBI Entrez:
ALBU_BOVIN from Bos taurus

Cleavage by Trypsin: cuts C-term side of KR unless next residue is P
Number of mass values searched: **25**
Number of mass values matched: **22**
Sequence Coverage: **36%**

Matched peptides shown in **Bold Red**

```
     1 MKWVTFISLL LLFSSAYSRG VFRRDTHKSE IAHRFKDLGE EHFKGLVLIA
    51 FSQYLQQCPF DEHVKLVNEL TEFAKTCVAD ESHAGCEKSL HTLFGDELCK
   101 VASLRETYGD MADCCEKQEP ERNECFLSHK DDSPDLPKLK PDPNTLCDEF
   151 KADEKKFWGK YLYEIARRHP YFYAPELLYY ANKYNGVFQE CCQAEDKGAC
   201 LLPKIETMRE KVLASSARQR LRCASIQKFG ERALKAWSVA RLSQKFPKAE
   251 FVEVTKLVTD LTKVHKECCH GDLLECADDR ADLAKYICDN QDTISSKLKE
   301 CCDKPLLEKS HCIAEVEKDA IPENLPPLTA DFAEDKDVCK NYQEAKDAFL
   351 GSFLYEYSRR HPEYAVSVLL RLAKEYEATL EECCAKDDPH ACYSTVFDKL
   401 KHLVDEPQNL IKQNCDQFEK LGEYGFQNAL IVRYTRKVPQ VSTPTLVEVS
   451 RSLGKVGTRC CTKPESERMP CTEDYLSLIL NRLCVLHEKT PVSEKVTKCC
   501 TESLVNRRPC FSALTPDETY VPKAFDEKLF TFHADICTLP DTEKQIKKQT
   551 ALVELLKHKP KATEEQLKTV MENFVAFVDK CCAADDKEAC FAVEGPKLVV
   601 STQTALA
```

Fig. 4.7: Peptide mass fingerprint

Pooled Mascot search result for trypsin digested 10 pmol silver stained BSA sample, positively identifying BSA, with a sequence coverage of 36% and a total score of 152. Experimental data of several samples was pooled to eliminate "false" positive peaks and include reproducible peaks close to the threshold.

Match to: **AAA51411**; Score: **77**
BOVALBUMIN NID: - Bos taurus

Nominal mass (M_r): **69248**; Calculated pI value: **5.82**
NCBI BLAST search of AAA51411 against nr
Unformatted sequence string for pasting into other applications

Taxonomy: Bos taurus
Links to retrieve other entries containing this sequence from NCBI Entrez:
ALBU_BOVIN from Bos taurus

Cleavage by Trypsin: cuts C-term side of KR unless next residue is P
Number of mass values searched: **12**
Number of mass values matched: **10**
Sequence Coverage: **17%**

Fig. 4.8: Protein identification

Mascot search result for 1/10 of a trypsin digested 10 pmol Coomassie blue stained BSA sample, positively identifying BSA, with a sequence coverage of 17% and a total score of 77 (matched peptides not shown). (Note: Scores greater than 73 are significant)

4.8 Discussion

Initially, a protocol needed to be developed that allowed the reproducible 2DGE analysis of proteins differentially regulated in human breast and breast cancer cell lines in response to doxorubicin. A time-consuming process of trial and error was necessary to produce good quality 2D gels sufficient to obtain a significant amount of meaningful data.

One strategy devised to improve overall sensitivity and increase the chance of detecting any protein candidates was the use of RP-HPLC as a prefractionation method. This strategy had previously been used successfully in 2DGE, studying proteins of the brain using a buffer composition similar to that used in this research (Badock *et al.*, 2001; Van den Bergh *et al.*, 2003). Unfortunately, the use of the column recommended by the authors had to be discontinued, after two faulty columns were trialled and failed quality testing. The faulty pieces had to be substituted for a RP-HPLC column from a different supplier, possibly compromising the original protocol, due to different packaging materials.

Clogging of the guard columns was a major problem when loading the sample onto the column. Since water (+ 0.1% TFA) is used for this process the sample buffer was inevitably diluted out causing hydrophobic proteins to come out of solution and block the column pores.

Consequently, only 50-100 μg of protein could be fractionated per run, resulting in very dilute large post-separation sample volumes of typically 4-5 mL. As a result, sample volumes had to be reduced dramatically since only 350 μL of protein sample could be loaded onto an IPG strip. Unfortunately, none of the various concentrating methods tested could consistently recover sufficient amounts of protein, therefore this approach was not feasible.

Since sample prefractionation can significantly enhance the performance of a 2DGE protocol, a growing number of such strategies are being described in the literature, for example: size exclusion ultrafiltration, sepharose assisted separation, sub-cellular fractionation, differential solubilization, chromatographic separation techniques, to name a few. Chromatography based protocols are likely to be the most potent techniques available, provided they are compatible with sample buffers. As the solvent concentration determines which proteins are eluted off the column, these techniques allow the user to "customize" fractions for the specific purpose in mind. In this study, the potential use and power of such an approach was highlighted using RP-HPLC. In retrospect, anion exchange/cation exchange chromatography or gel filtration chromatography may have been more suitable with regard to the sample buffer.

A robust MALDI-MS sample preparation and purification protocol is paramount for successful peptide fingerprinting. There has been much debate in the literature, as to whether the use of Coomassie blue or silver for protein staining is preferable for proteomic studies. This study, like many others, employed silver staining because it is about 10 fold more sensitive than Coomassie blue staining. Many scientists argue that destaining is essential if any peaks are to be detected after silver staining while others refute this claim (Gharahdaghi *et al.*, 1999; Mortz *et al.*, 2001). During the experimental setup stage it was not possible to detect BSA peaks from silver stained gels without prior destaining. In general, it was more difficult to obtain peak spectra from silver stained than from Coomassie blue stained protein bands. The destaining protocol used here (Sumner *et al.*, 2002) was preferred over that most widely used (Gharahdaghi *et al.*, 1999) as it delivered more consistent results and omitted toxic substances.

The use of Zip-tips for sample purification and concentration has previously been reported to result in improved MALDI-MS data (Jin *et al.*, 1999), and proved to be crucial in this work for obtaining adequate MALDI-MS data from silver stained gels. The enhancement of data quality is mainly due to the combination of two factors. Firstly, silver ions and other

interfering substances e.g. salts are removed from the sample, significantly reducing background noise. Secondly, sample concentration allows the entire peptide mixture to be loaded onto one target, radically improving the signal to noise ratio.

Overcoming the loss of proteins during sample preparation and purification was one of the most difficult tasks in establishing a sound proteomics protocol. Peptide preparation after in-gel digestion for MALDI-MS, and concentrating of protein fractions after RP-HPLC, resulted in the most severe losses probably due to adhesion of protein to tube surfaces and filter membranes. One remedy was the use of lubricated tubes which dramatically reduced protein adhesion to the plastic surface and proved to be essential for successful MALDI-MS analysis. Although low-protein binding filter membranes were used with all centrifugal devices to concentrate RP-HPLC separated protein, losses remained unacceptable. Some researchers propose pre-treatment of such devices with "sticky" proteins such as BSA, to block potential binding sites. This approach however, was unsuccessful in preventing those losses. As a result the use of membrane based protein concentration devices was not feasible. An effort to use lubricated tubes for drying proteins in a speed-vacuum was likewise unsuccessful.

Spot resolution achieved on 2D gels however, was successfully improved by replacing pH 3-10 IPG strips with pH 4-7 strips. Not only were spot patterns simplified, but previously undetectable proteins were also visible, while only a few proteins were lost at both the acidic and basic ends of the strip. The use of gradient gels further increased spot resolution, and high quality spot patterns were obtained. As a result, a protocol with the potential to identify differentially expressed proteins using 2D gels was successfully established.

Chapter Five

2D gel electrophoresis

5.1 Introduction and Strategy

The aim of this study was to investigate the immediate (2 h) and prolonged (24 and 48 h) response of drug sensitive breast cancer cells to doxorubicin using two dimensional gel electrophoresis (2DGE). In addition, drug tolerant ("resistant") cells, which were harvested 24 h after a third doxorubicin exposure, were also analysed.

To obtain drug tolerant ("resistant") breast cancer cells, MDA MB 231 cells were exposed to 1, 2, 3, 4, or 5 μM doxorubicin for 1 h, before being returned to conditioned media. After cells had recovered and re-grown to about 80% confluence they were exposed again. This procedure was repeated once more and cells were harvested 24 h after the third exposure. Analysis of cell survival and re-growth indicated that the use of 3 μM doxorubicin was the most feasible for this analysis, as higher concentrations led to almost complete culture annihilation. Consequently, all experiments presented in this chapter, including the generation of resistant cells (R sample), were performed by treating cells with 3 μM doxorubicin.

Growth of large numbers of cells was required to achieve sufficient protein yield for analysis. To eliminate proteins responding to confluence-related differential regulation an "over-confluent" sample, which was purposely grown to confluence, was included in the analysis.

5.2 Results

Differential protein regulation was compared in six samples from two different batches of cells in the first experiment. The 0 h (untreated control) and RI (resistant) samples were from batch 1, while the 2 h, 24 h, 48 h, and OC (over-confluent) samples were from batch 2 (Fig. 5.1). As the 0 h sample of batch 2 had been lost during RP-HPLC fractionation (which was discontinued after this incident), it was replaced by the control sample of batch 1. This approach did not compromise data validity because the aim of this experiment was to look at genuine batch-independent changes in protein expression after drug treatment. Hence the origin of the control sample should have been irrelevant for verifying drug-induced changes in protein expression. The RI (resistant) sample of batch 1 was chosen, as that of batch 2 was still in preparation at the time of analysis.

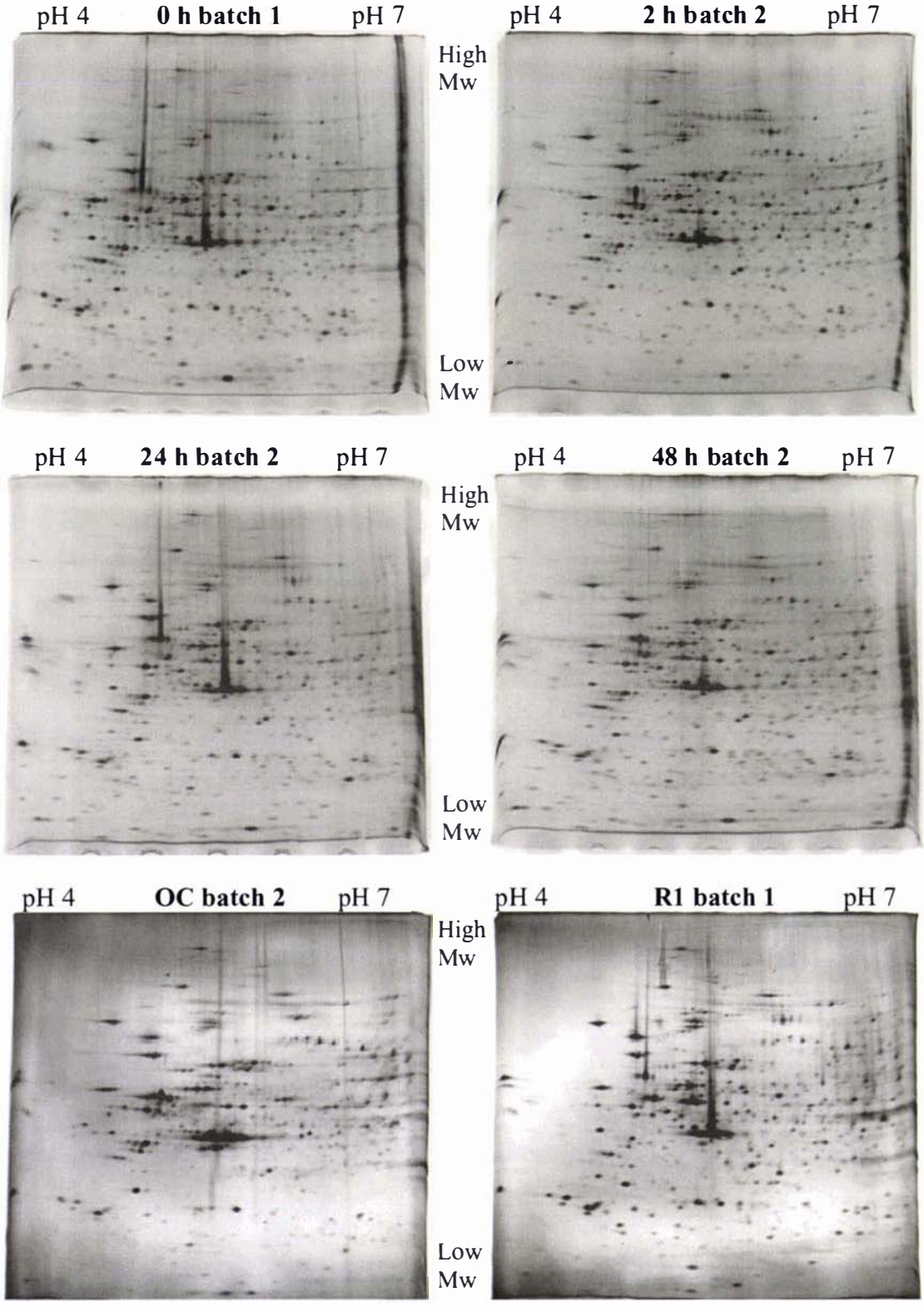

Fig. 5.1: First set of 2D gels for MDA MB 231 cells

75 µg of protein extracted from 0 h, 2 h, 24 h, 48 h, overconfluent (OC) and resistant (R) sample were run on a pH 4-7, 10-15% SDS-PAGE gradient gel and silver stained. The control (0 h) and resistant samples were from batch 1, while the remaining samples were from batch 2. Samples OC and R1 exhibited higher background, however, this did not have any significant detrimental effects on gel analysis.

The results indicated a few striking differences in spot intensities between the control and drug treated samples, as well as within the group of treated samples. The most apparent differences are highlighted in figure 5.2.

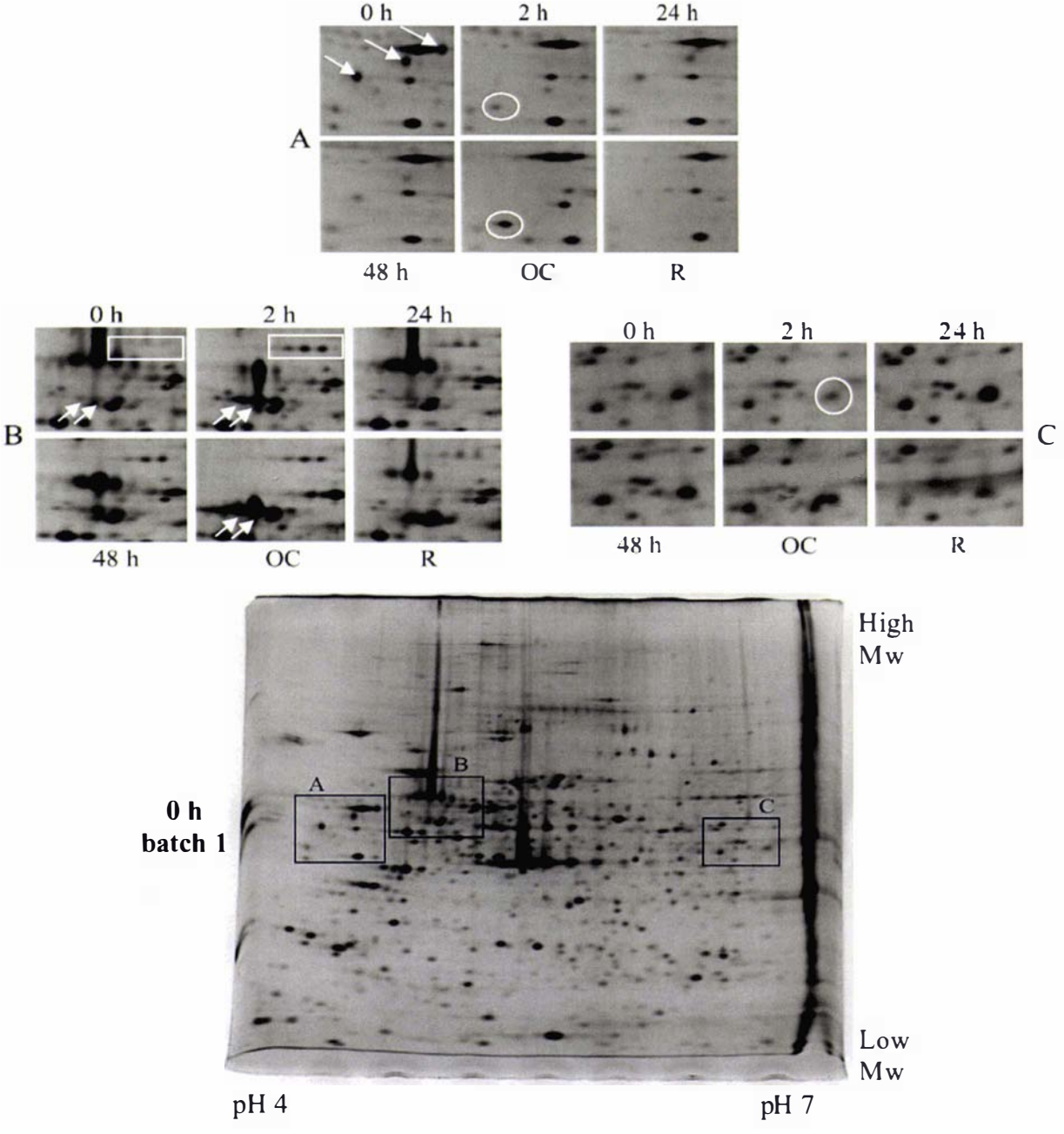

Fig. 5.2: Potential candidates in MDA MB 231 cells

Three gel areas in the first set of experiments (75 µg of protein separated on a pH 4-7, 10-15% SDS-PAGE gradient gel) featuring potential candidate proteins (boxes A, B, C), were analysed and are shown using the control sample from batch 1 (0 h) as a reference gel. These areas were evaluated for differential protein regulation and are shown as close-ups for all samples (A, B, C). In area A, down-regulation of three spots (arrows) was observed in all samples compared to the native sample (0 h), as well as a spot unique to the 2 h and OC sample (circle), indicating confluence-related expression. A set of spots very weakly expressed in the control sample, but up-regulated in all others (rectangle), and proteins up-regulated in 2 h, and OC samples (arrows), were seen in area B. A protein spot was down-regulated in the 2 h samples compared to the remaining samples in area C (white circle).

To confirm that the differences observed in this first experiment were reproducible and batch-independent, new cells were grown from frozen stocks (batch 3) in order to obtain a new control sample (0 h). In addition, cells from batch 1, harvested soon after doxorubicin exposure (2 h), were also analysed (Fig. 5.3). Samples harvested at these time points had exhibited the most significant differences (see Fig. 5.2), therefore this new set was used for comparison.

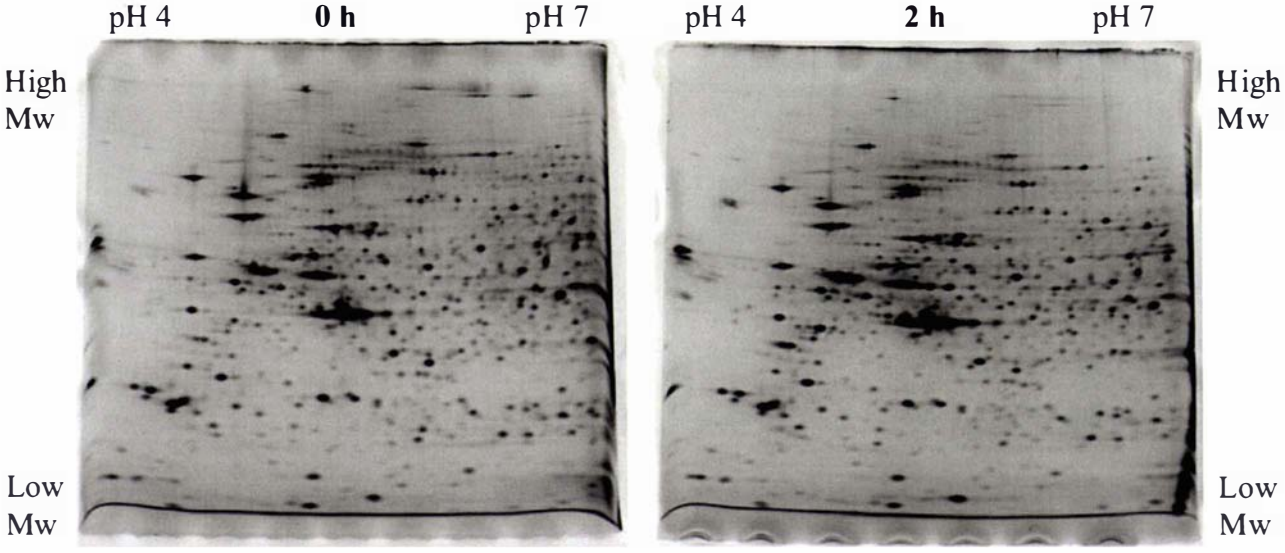

Fig. 5.3: 2D gels of 0 h batch 3 and 2 h batch 1

An additional control sample (0 h), as well as a different 2 h sample were analysed to confirm potential candidate proteins observed in the first experiment. 75 µg of protein were separated on a pH 4-7, 10-15% SDS-PAGE gradient gel.

Data obtained from these two samples revealed that spots, which had been regarded as potential candidates for differential regulation due to drug exposure in the first set of experiments, could not be confirmed. Indeed, the two controls (0 h) of batches 1 (Fig. 5.1) and batch 3 (Fig. 5.3) showed marked differences in expression of the candidate proteins. To illustrate these findings, the spot areas containing potential candidate proteins from experiment one (Fig. 5.2) were compared to corresponding areas of the two new samples (Fig. 5.4).

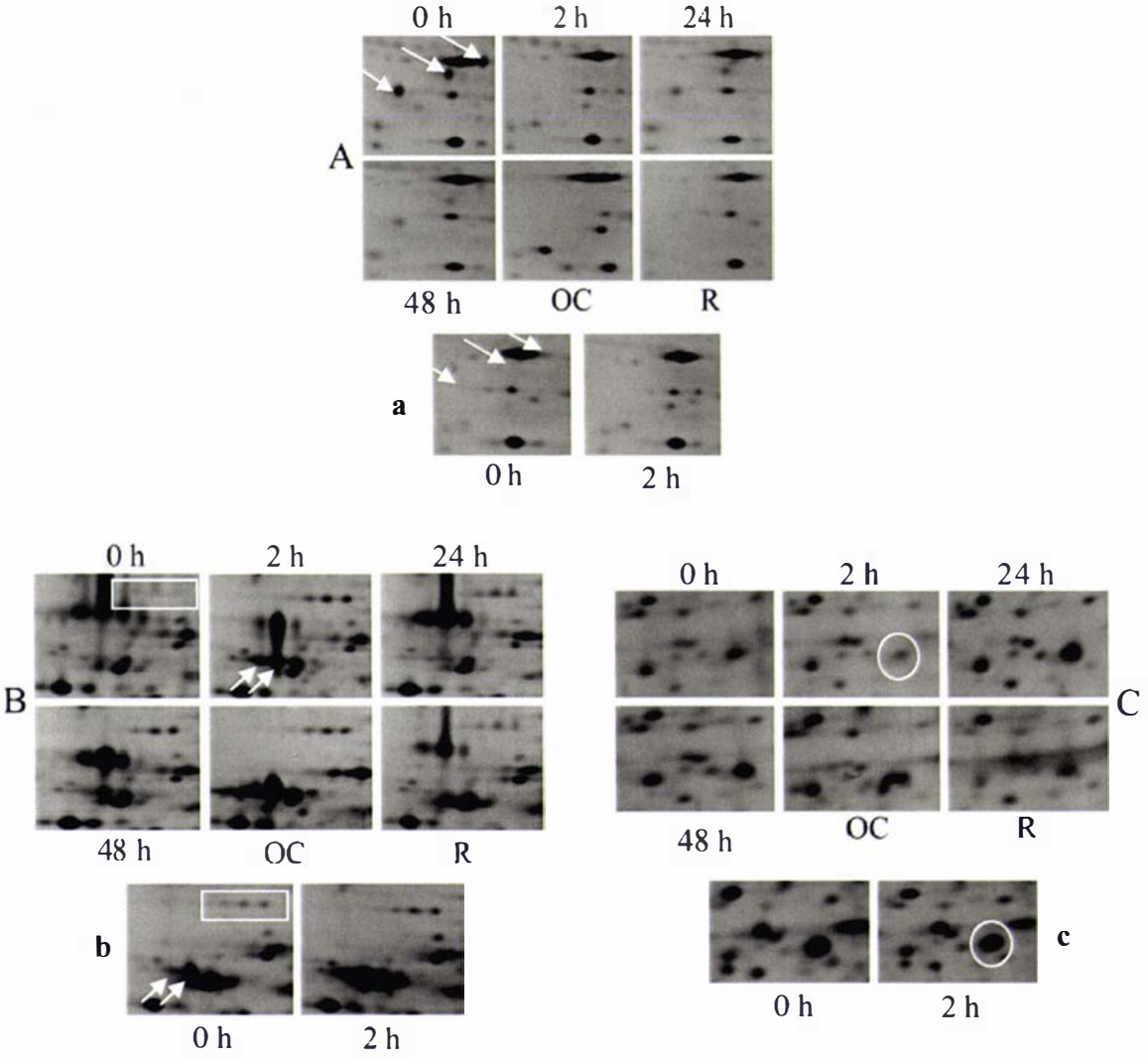

Fig. 5.4: Candidate confirmation using samples 0 h batch 3 and 2 h batch 1

Gel areas exhibiting potential candidate proteins from the first set of experiments (75 µg of protein separated on a pH 4-7, 10-15% SDS-PAGE gradient gel) (Fig. 5.2) are indicated as A, B, and C. To confirm these findings, a comparison was made to gels obtained from 0 h batch 3 and 2 h batch 1, for each of these areas, labelled a, b, and c.

Proteins thought to be down-regulated in area A (arrows) after drug treatment were not expressed in the control sample (0 h) of batch 3 (a) at all. Moreover, proteins which appeared absent from the control sample of batch 1 (0 h, B) were present in the control of batch 3 (0 h, b), as indicated by the white box. Candidate proteins which seemed to be up-regulated 2 h after drug exposure in the first experiment (arrows, B), were also strongly expressed in the native sample of batch 3 (arrows, b). Furthermore, a spot which appeared to be down-regulated 2 h after exposure (batch 2) in area C (circle) was present at a much higher concentration in the 2 h sample of batch 1 (circle, c). Unfortunately, none of the initial candidates (Fig. 5.2) could be confirmed as being differentially regulated.

As the two control samples (0 h) of batches 1 and 3 had exhibited striking differences in expression of the candidate proteins, a fresh batch (4) of cells was grown from frozen stocks in an attempt to validate the result obtained for either one of the controls, and to determine if any of the observed differences were batch specific (Fig. 5.5). This new batch was also going to be used to investigate any drug dosage-dependent changes in protein expression 24 h after doxorubicin treatment.

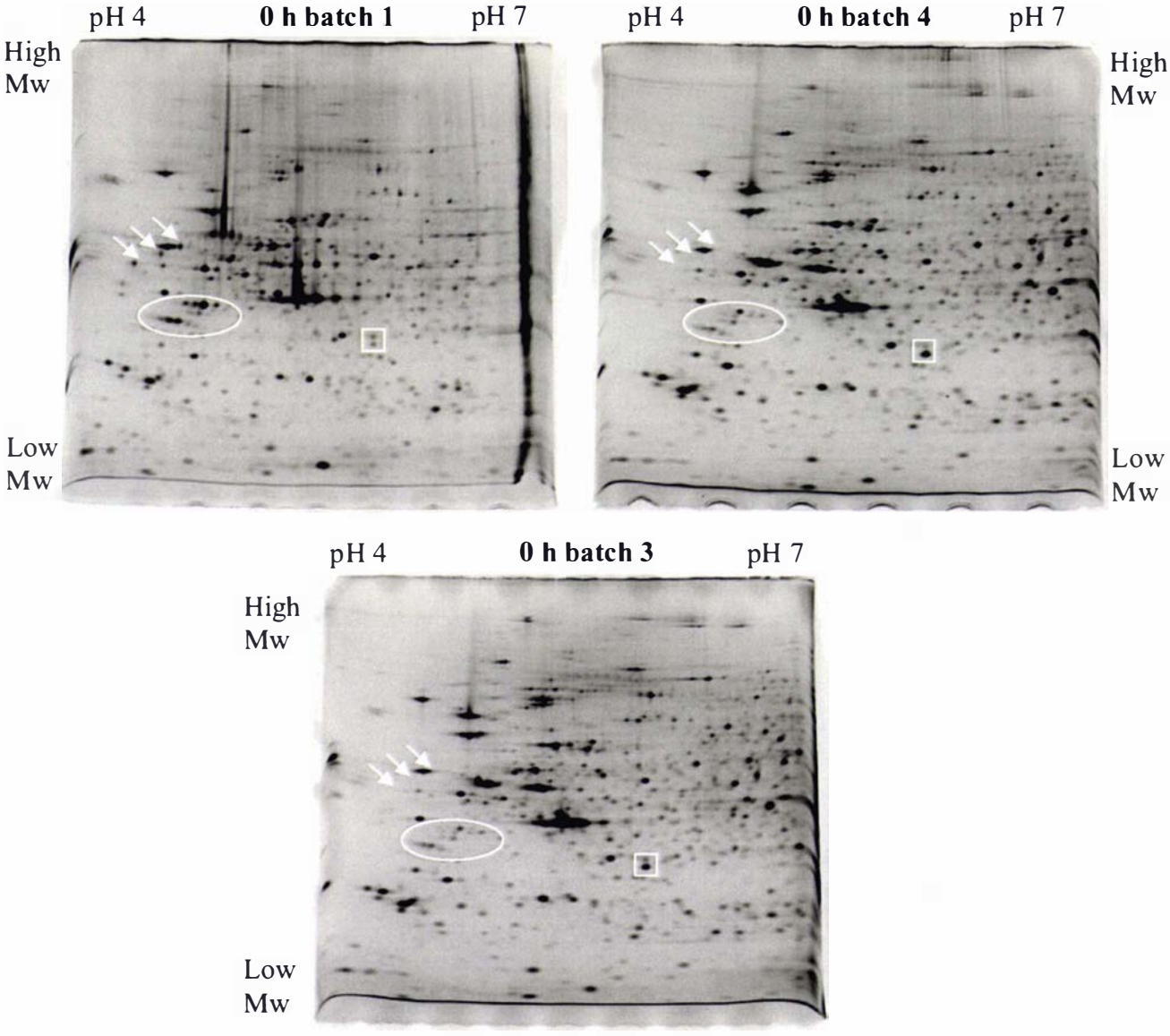

Fig. 5.5: Reproducibility of control (0 h) samples from batches 1, 3, and 4

75 µg of protein were separated on a pH 4-7, 10-15% SDS-PAGE gradient gel. The overall level of reproducibility was high, but a few marked differences could be observed between the different batches. Proteins which appeared up-regulated or down-regulated in batch 1 are indicated by an ellipse or box, respectively. Arrows point to proteins exclusive to the control of batch 1. In general, batches 3 and 4 displayed the most similarities. Gels of 0 h batch 1 and 0 h batch 3 are the same as in figure 5.1 and 5.3, respectively.

In a parallel experiment three equivalent samples obtained 24 h after drug exposure from batches 1, 2, and 4 were analysed for reproducibility. The 24 h sample of batch 1 was run on a 12.5-17% SDS-PAGE during gradient optimization experiments. Hence, spots identical with those on the other gels are observed at a higher position on this gel, in comparison. Nevertheless, the data obtained allowed for spot comparison and evaluation of sample reproducibility. The results were similar to those obtained from the analysis of control samples of different batches, with a high overall reproducibility and only a few marked differences (Fig. 5.6).

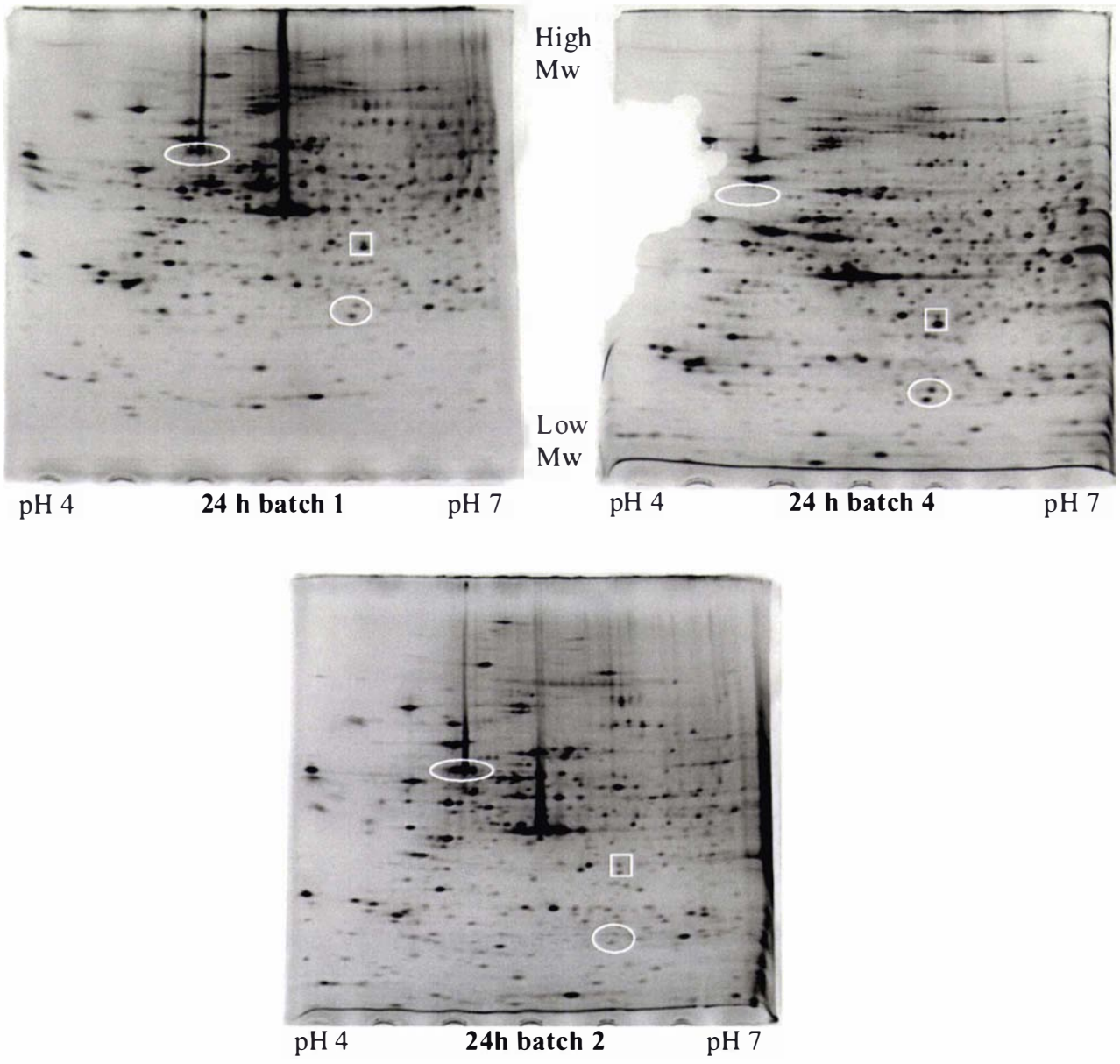

Fig. 5.6: Samples taken 24 h after treatment of batches 1, 2, and 4

75 µg of protein separated on a pH 4-7, 10-15% (24 h batch 2 and 4) or 12.5-17% (24 h batch 1) SDS-PAGE gradient gel. Ellipses and squares mark differences between the three 24 h samples of batches 1, 2 and 4. The gels of the 24 h samples of batches 1 and 2 are the same as in figures 5.3 and 5.1, respectively.

As the previous experiments did not indicate any genuinely differentially regulated proteins, an additional experiment was designed to investigate the possibility of drug-dosage-related changes in protein levels. For this purpose cells of batch 4 were exposed to the standard concentration of 3 µM doxorubicin, as well as 25 µM and 50 µM, respectively and harvested 24 h after treatment (Fig. 5.7).

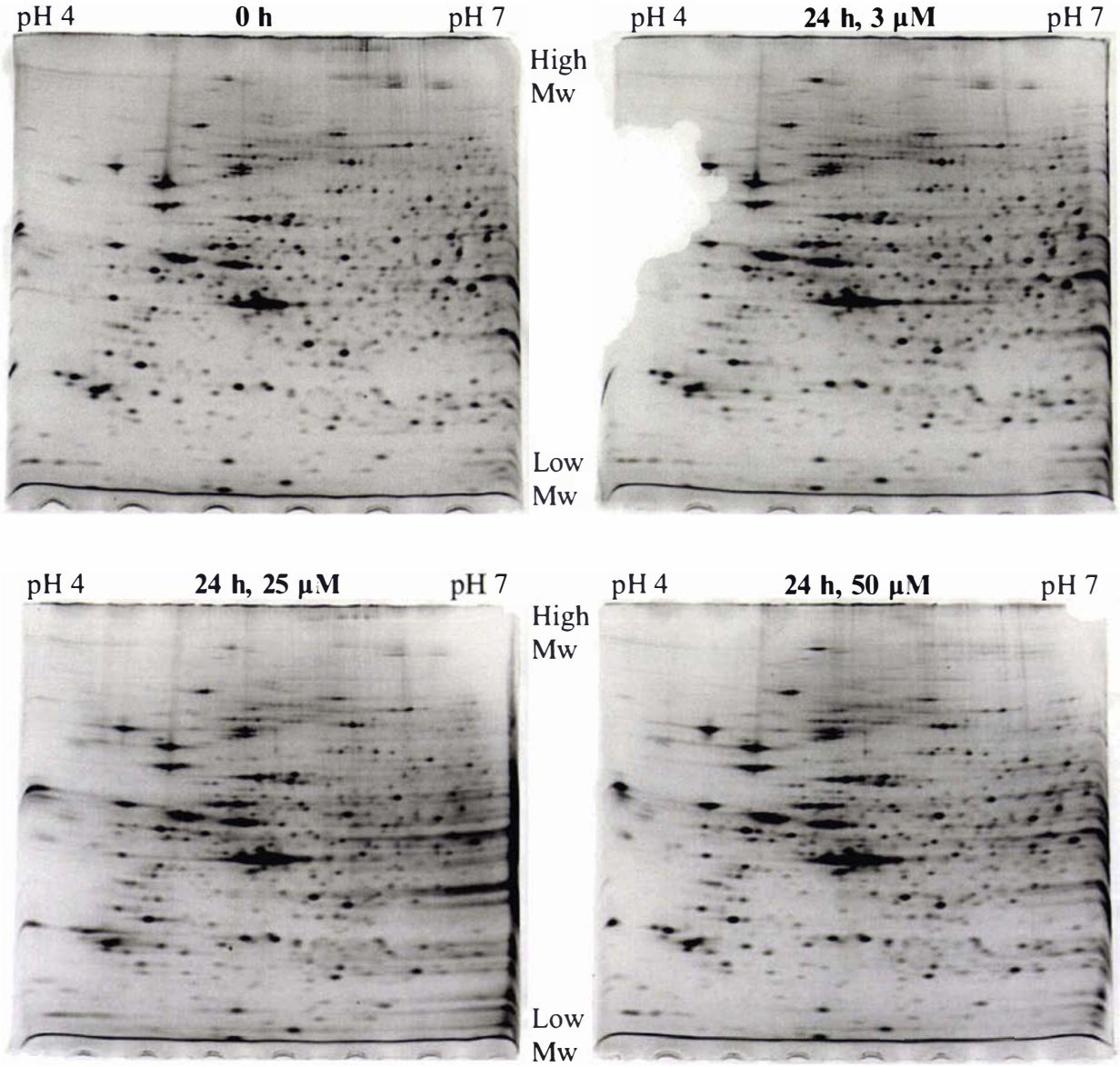

Fig. 5.7: Drug-dosage-effect 24 h after 3, 25, and 50 µM doxorubicin treatment
75 µg of protein separated on a pH 4-7, 10-15% SDS-PAGE gradient gel. Three of the four samples (all batch 4) were exposed to different amounts of doxorubicin and analysed 24 h post treatment. Parts of the gel showing the expression profile 24 h after 3 µM doxorubicin treatment were destroyed, but no vital information was lost. Streaking was observed in the 24 h 25 µM sample slightly reducing gel quality. Gels of the control (0 h) and the sample obtained 24 h after treatment with 3 µM, are the same as in figure 5.5 and 5.4, respectively.

While reproducibility between gels was very high, a drug-dosage-dependent response could not be detected, as no significant differences were observed between any of the samples tested.

Since some of the protein extracts used had been stored for about 2 months prior to analysis, an investigation into the detrimental effects of prolonged storage as well as repeated freezing and thawing, was carried out using the "R" sample of batch 1. Repeated analysis of this sample also allowed an assessment of any perturbation caused by high background during the first analysis (Fig. 5.8).

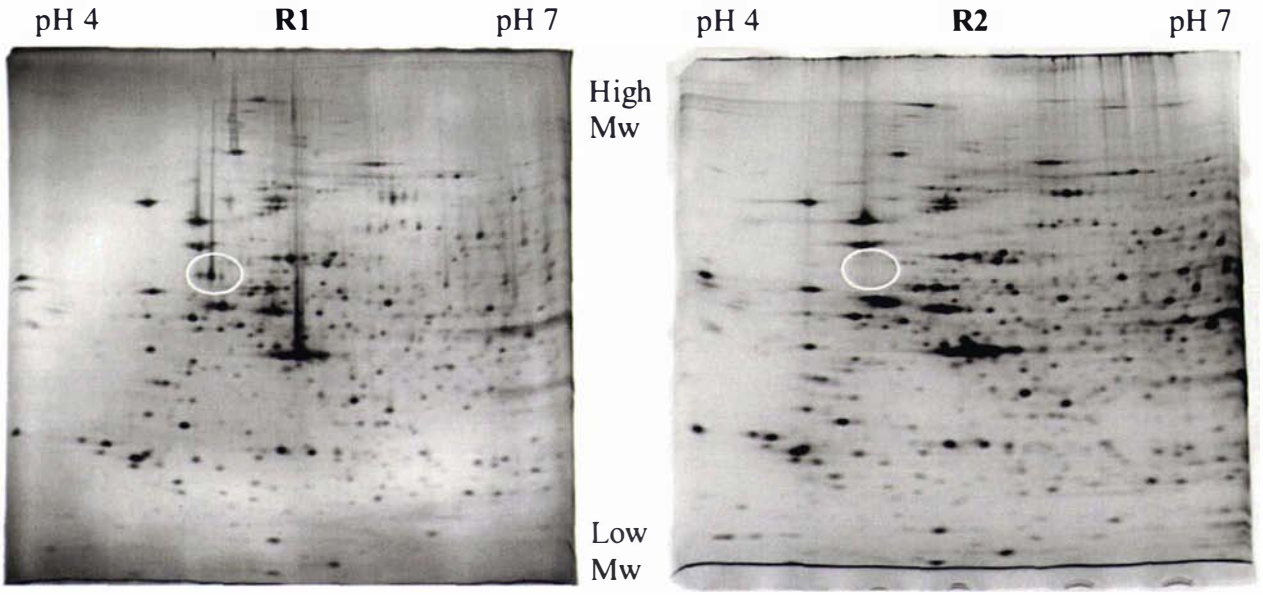

Fig. 5.8: Gel-to-gel reproducibility of sample "R"

75 µg of protein separated on a pH 4-7, 10-15% SDS-PAGE gradient gel. Although gel R1 (fresh sample) which is the same gel as in figure 5.1, exhibited a higher background, spots were almost identical with the stored sample (R2). The only apparent difference between the two samples is circled.

Apart from one protein cluster, which is likely to be a buffer contaminant, which was also observed in other gels (Fig. 5.6), no qualitative or quantitative changes in protein spots were observed between samples R1 and R2, strongly suggesting that the actual differences observed between samples in the earlier experiments were sample specific and not procedure related.

5.3 Summary

The immediate (2 h) and delayed (24 h and 48 h) drug-induced cellular response of breast cancer cells after exposure to doxorubicin was analysed using 2DGE. A total of 14 gels from 4 different MDA MB 231 batches were used to evaluate both the validity of observed differences, and batch-independent reproducibility. Although significant differences between drug exposed and control samples were observed initially, these were not reproducible and therefore had to be attributed to sample and batch variability. Moreover, a drug-dosage effect could not be established, although a higher incidence of dead cells was observed in the flasks (data not shown) administered with a higher drug concentration (24 h, 25 μM, and 50 μM). The only major differences observed were from a sample of confluent cells. The general reproducibility of gels was good. Marked differences could be observed however, between samples which had been treated in the same manner, but originated from different batches. A general variation in spot intensities could also be detected. Collectively, unequivocal evidence for drug-induced changes in protein expression could not be detected using these methods.

5.4 Discussion

For 2DGE analysis of changes in protein levels in response to doxorubicin treatment of breast cancer cells, samples were collected at different time points (0, 2, 24, 48 h). Since any data obtained required verification, it was necessary to use additional samples. Because 2DGE is a time consuming process it was not feasible to use all three cell lines (MDA MB 231, MCF12A and MCF7) which were used for SELDI-MS. The decision to use MDA MB 231 was based on the fact that more proteins exhibited differential regulation after drug treatment in this cell line, according to SELDI-MS data. The MDA MB 231 cell line was also much easier to grow and maintain in culture than MCF7, which was the only other cancerous cell line used in this study. Furthermore, during initial setup when protein extracts of each of the three cell lines were run on 2D gels, MDA MB 231 cells showed the highest number of potential changes in protein levels in response to drug exposure (Chapter 4, Fig. 4.1).

Unfortunately, none of the potential candidate proteins could be confirmed as genuinely differentially regulated in response to doxorubicin treatment. A comparison of different control samples showed unique differences between these samples. These differences could either be inherent differences acquired over time as cell stocks deviate from the parental cell stock or procedure related variations. In general, reproducibility between gels of the same sample has been reported to be less than 100%, and is in fact usually 80-90% when using

silver staining (Terry and Desiderio, 2003; Chevalier *et al.*, 2004). Taking this into account, the gels produced in this study were of very high quality.

The protocol used in this study was the result of extensive optimization of the original protocol, to ensure gel reproducibility and data quality. The inability to detect differentially regulated proteins was due to a combination of insufficient sensitivity and visualization methodology. For time course analysis, as used in this study, sample prefractionation would have significantly enhanced the scope and detection sensitivity. RP-HPLC was intended to be employed for this purpose, but proved unreliable as discussed in sections 4.5, 4.6, and 4.8.

Silver staining was used for visualising proteins on 2D gels as it has a much greater sensitivity than Coomassie brilliant blue staining. Unfortunately, silver staining is not an end-point stain like Coomassie brilliant blue and the results are consequently likely to be more variable. Hence, close monitoring of the developing process was required to ensure comparable spot intensities and background levels. Moreover, this procedure was very susceptible to the use of different chemical reagents, producing different outcomes when these were changed. An obvious example was seen with samples OC and R of the first experiment (Fig. 5.1), which displayed higher background than normal due to the use of a different type of sodium bicarbonate during staining. Although this did not notably alter the results obtained, it did underscore the impact slight variations in procedure could have on the reproducibility of the staining protocol.

The results of this study have demonstrated that silver staining is not ideal for the analysis of differentially regulated low abundance proteins. At the time of analysis however, silver staining was the only viable visualization methodology available. Since then, new technologies have emerged with a goal of improving MALDI-MS compatibility and staining sensitivity e.g.: Deep Purple, Sypro Ruby, and Cy-Dye stains (Knowles *et al.*, 2003; Chevalier *et al.*, 2004; Friedman *et al.*, 2004). In particular, the latter has gained much attention and use in work studying temporal changes in protein expression. In addition to an internal standard, up to two different samples can be run simultaneously, increasing throughput and decreasing sample variability, thereby making this a much more sophisticated approach than classical silver staining. In fact, current studies still relying upon silver staining usually investigate expression profiles of different disease states or differences between normal and malignant tissues. Changes observed in these studies are usually due to permanent

alterations in protein expression and can be quite dramatic. Hence these studies do not require the level of sensitivity and reproducibility necessary for investigating changes of a temporal nature, as in this research project, and silver staining may therefore be sufficient.

5.5 Analysis of 2D Gels Using Phoretix® 2D Evolution Software

Manual assessment of 2D gel profiles did not result in the detection of reproducible changes in protein expression as a result of drug exposure. Greater objectivity may be obtained in silico using software developed specifically for this purpose. Hence Phoretix® software (Nonlinear) was obtained on a "free trial" basis and used to analyse the 2D gels described in section 5.2. The results are summarized in table 5.1 (section 5.5.6). To attribute differential regulation of proteins as a genuine response to drug treatment, protein spots were required to exhibit at least a two fold up- or down-regulation in comparison to other samples. In addition, results had to be reproducible when different batches of cells were tested. Phoretix® 2D Evolution software was used for computerized spot detection and spot volume calculation (spot concentration) while manual editing was performed to optimize spot matching and spot area comparison where necessary.

5.5.1 Reference Gel and Spot Comparison Analysis

For spot identification and volume determination all gels were compared to a reference gel. From the three unexposed MDA MB 231 samples (0 h) of batches 1, 3, and 4, the software automatically selected the gel of batch 4 as the base for the reference gel. Consequently, prior to sample analysis all spots were matched to the corresponding spot on the reference gel. Volumes of the reference spots were the averages of this spot from all three control (0 h) gels. Spot matching was performed after background subtraction was completed. Because many different spots and gel areas were analysed, a reference map was constructed to assist in the identification of these regions on the gels (Fig. 5.9).

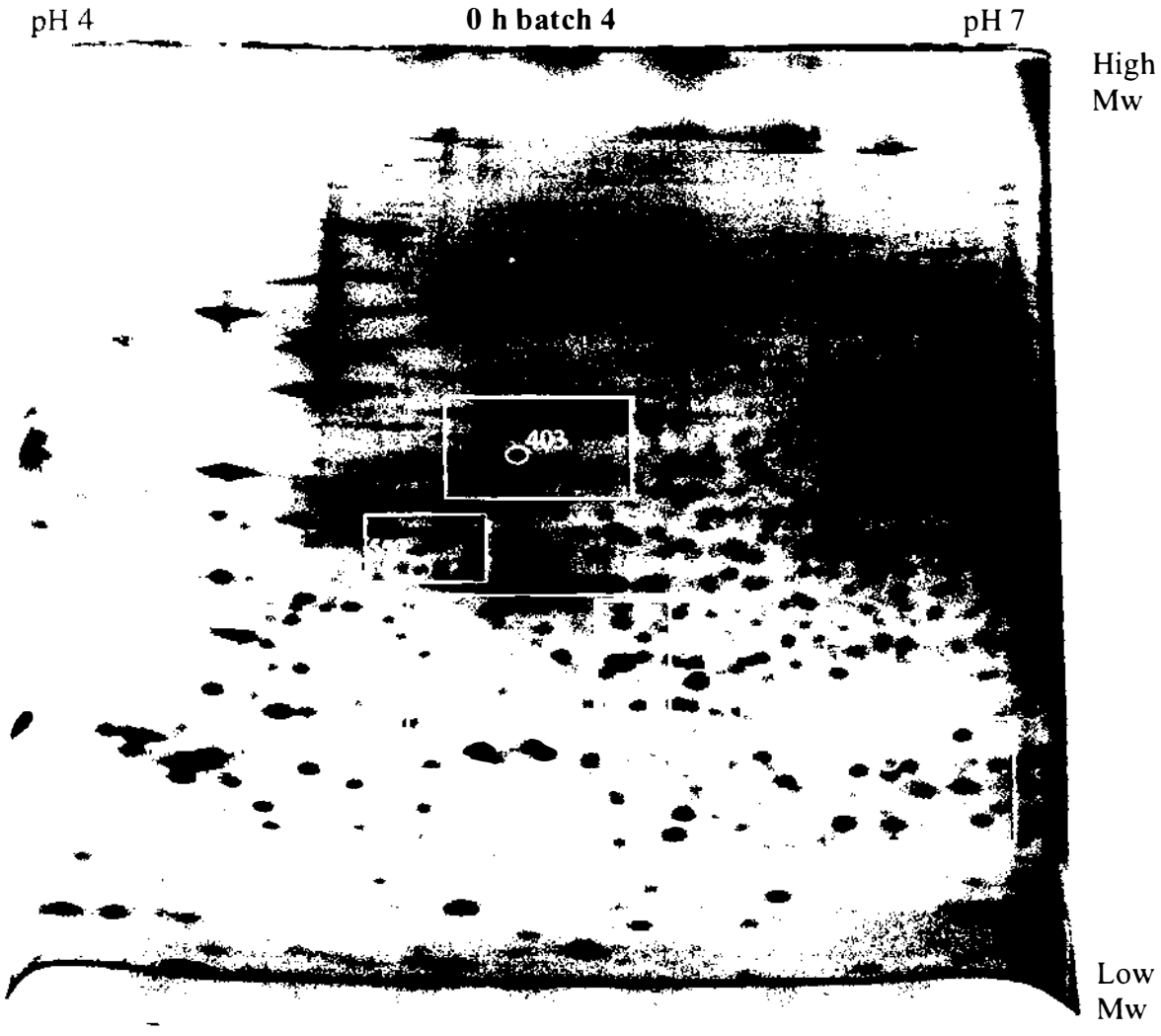

Fig. 5.9: Candidate spots as determined by Phoretix 2D software analysis

The reference gel (75 μg of protein of the control sample (0 h) of batch 4 separated on a pH 4-7, 5-10% SDS-PAGE gradient gel) was chosen to represent the gel areas containing the candidate spots discussed in this chapter. The areas of candidate proteins are shown with the boxed area, and the relevant spots are circled and numbered in accordance with the software analysis data. The surrounding spot areas are displayed to confirm that the alterations in spot intensity observed between gels were not due to differences in gel loading. The area labelled as 3D was chosen to investigate the reproducibility of the 2D gels.

5.5.2 Reproducibility Between Batches

Unexposed samples (0 h) of batches 1, 3, and 4 were analysed for variations in protein levels unrelated to drug treatment, and to estimate overall gel reproducibility. For this purpose, a central area of the gels, designated as "3D" in figure 5.9, was chosen featuring different spot intensities and low background interference (Fig. 5.10).

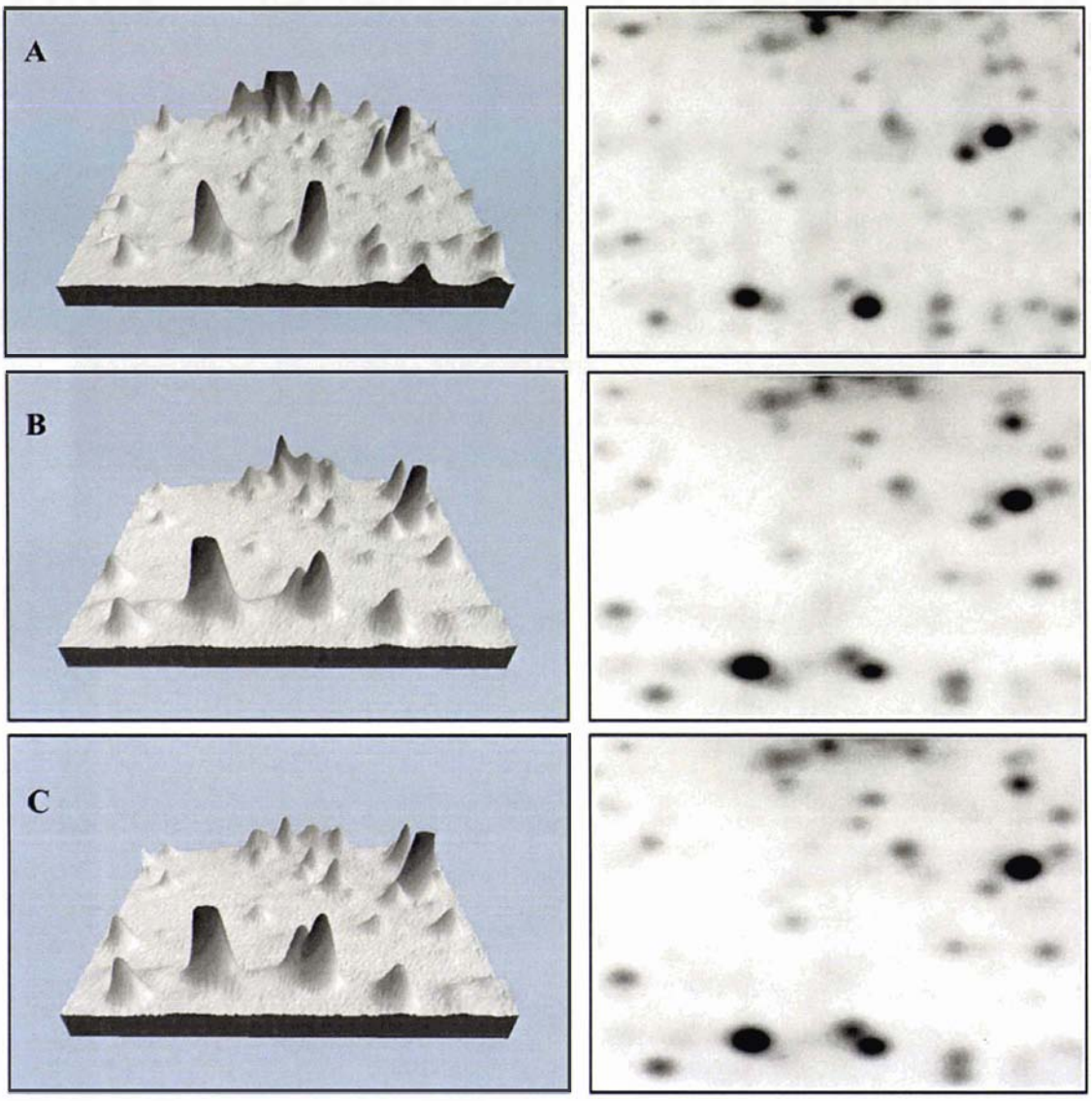

Fig. 5.10: Inter-batch reproducibility

Phoretix 2D Evolution software allowed visualising differences in spot intensities by selecting an area of interest on the gel and choosing the 3D map option from the menu. The height and width of peaks in the 3D diagram (left column) are representative of the circumference and concentration of the corresponding gel spot (right column). Spots featuring a dark flat peak exceeded the detection range limit. This was usually only the case with very intense spots. Sample and batch reproducibility is demonstrated using the untreated (0 h) cell extracts of batch I (A), batch 3 (B), and batch 4 (C).

While a certain degree of variability was present in the untreated sample of batch I, compared to the control samples of batches 3 and 4, the latter two exhibited almost identical spot patterns and spot intensities.

5.5.3 Gel Analysis

To determine differential protein expression, gels from the same batches were compared to each other as well as to the reference gel, as some sample spots may differ more strongly between different samples of the same batch, than between spots of the reference gel. Any candidate spots showing differential regulation were then compared to the same spot of an identically treated sample from a different batch to determine whether or not the observed difference was genuinely due to drug exposure. All expression data were verified visually to ensure that candidate spots did represent differentially regulated proteins, rather than being attributed to strong background differences, smears or position on gels (e.g.: edge of gel) (Fig. 5.11).

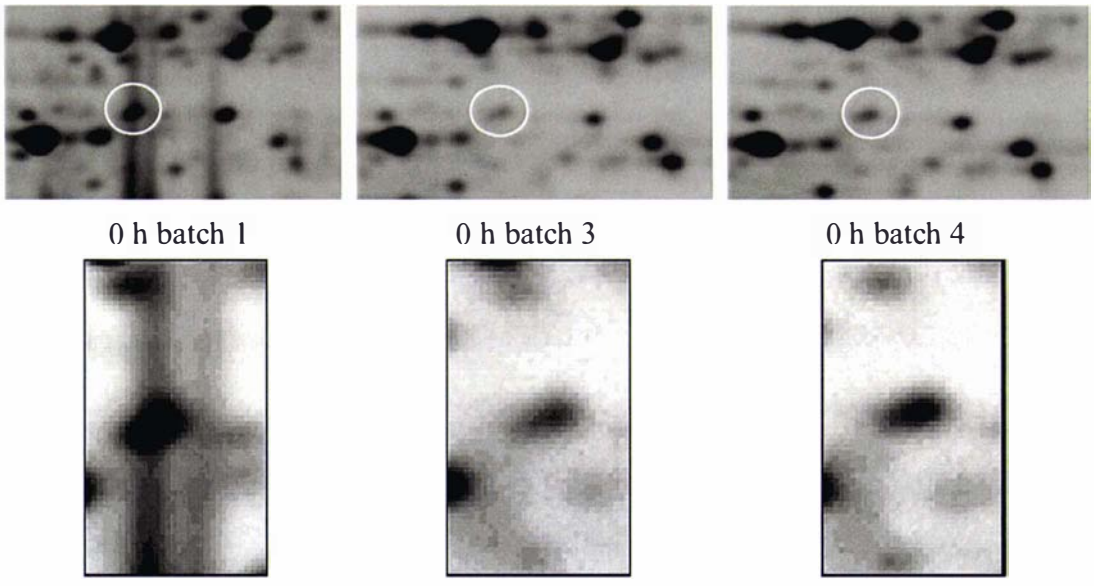

Fig. 5.11: Influence of background on spot 403

High background or smearing had a major impact on some spot values as demonstrated with spot 403 (circled) which is displayed as an area view (top), as shown in figure 5.9, and a close up view (bottom). According to the expression data, spot 403 was down-regulated 4.9 fold in the control sample of batch 3 and 4.5 fold in batch 4 compared to batch 1. Visual verification however, did not support this observation and indeed suggested that the differences in the expression data were due to the intense background in batch 1.

In the analysis of the first set of 2D gels, all of which were obtained from samples of batch 1, the spots from the reference gel as well as the unexposed sample (0 h) of batch 1 were used as controls. The remaining samples (2 h, 24 h, resistant (R1), and R2 (repeat R1) were compared

to the controls, as well as to each other. Data that suggested differences in expression levels of samples 2 h, 24 h, R1, and R2 in comparison to the control (0 h, batch 1) were verified against the reference gel. The importance of this was demonstrated in the case of spot 673 which was up-regulated 2.4 fold 2 h after doxorubicin treatment when compared to the control (0 h, batch 1), but decreased 2.8 fold in comparison to the reference gel. As a result, the observed increase in protein levels of spot 673 2 h after treatment in batch1, was attributed to sample variation rather than a genuine response to drug treatment. Hence spot 673 was not considered as a candidate (Fig. 5.12).

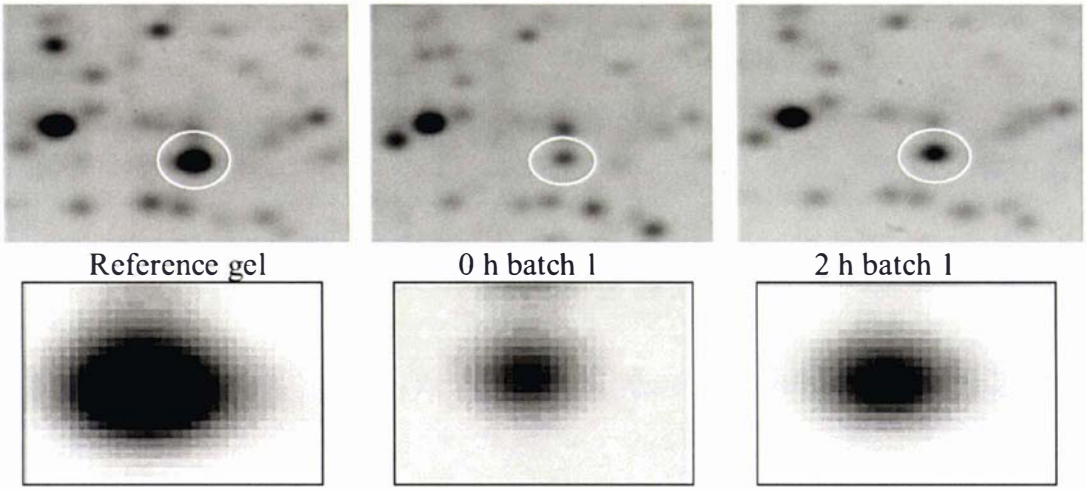

Fig. 5.12: Verification of genuine protein expression in spot 673

The gel area of spot 673 (top) is shown as indicated in figure 5.9. Differential expression of spot 673 (circled) in samples 0 h and 2 h of batch 1 was a typical example of sample variation which was not due to drug treatment, as the protein is present at higher levels in the reference gel (0 h, batch 4) than in the 2 h sample of batch 1.

Samples R1 and R2 made excellent markers for reproducibility between gels as the same protein extract was used to produce both gels (Fig. 5.8). The results show that overall reproducibility between gels was retained, with only a few marked differences in particular areas on the gels (data not shown).

5.5.4 Candidate Verification

Since batch 2 lacks a sample of unexposed cells that could be used as a control in addition to the reference gel, differences in protein expression were verified by comparing the 2 h sample

to the equivalent sample of batch 1, and the 24 h sample to those of batches 1 and 4. For example, if a spot was strongly down regulated in the 2 h sample of batch 2 in comparison to the reference gel, then the next step was to look for changes in expression levels of the 2 h sample of batch 1. This ensured the reproducibility of the observation (Fig. 5.13).

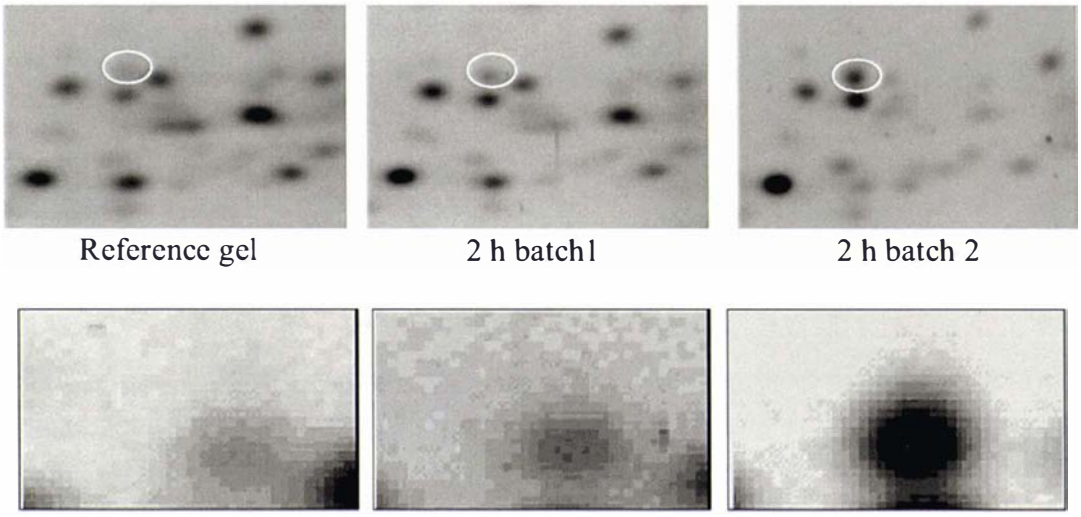

Fig. 5.13: Expression analysis of spot 723

The gel area of spot 723 (circled) is shown on top, as indicated in figure 5.9, while a close-up of spot 723 is displayed in the bottom row.

Data for the 2 h sample of batch 2 shows spot 723 (circled) to be up-regulated 2 fold compared to the reference spot. However, in the 2 h sample of batch 1 the equivalent spot is not differentially regulated. Hence, the up-regulation in the 2 h sample of batch 2 was not a genuine response to drug treatment, and therefore spot 723 did not qualify as a candidate.

5.5.5 Drug-Dosage Effect

To investigate the presence of any dosage-dependent changes in protein expression, samples of batch 4 were treated with 3, 25, or 50 μM of doxorubicin, and harvested 24 h later. Potential candidate spots were then compared to equivalent spots in identical samples of other batches for verification (Fig. 5.14). No genuine dosage-dependent effects were observed.

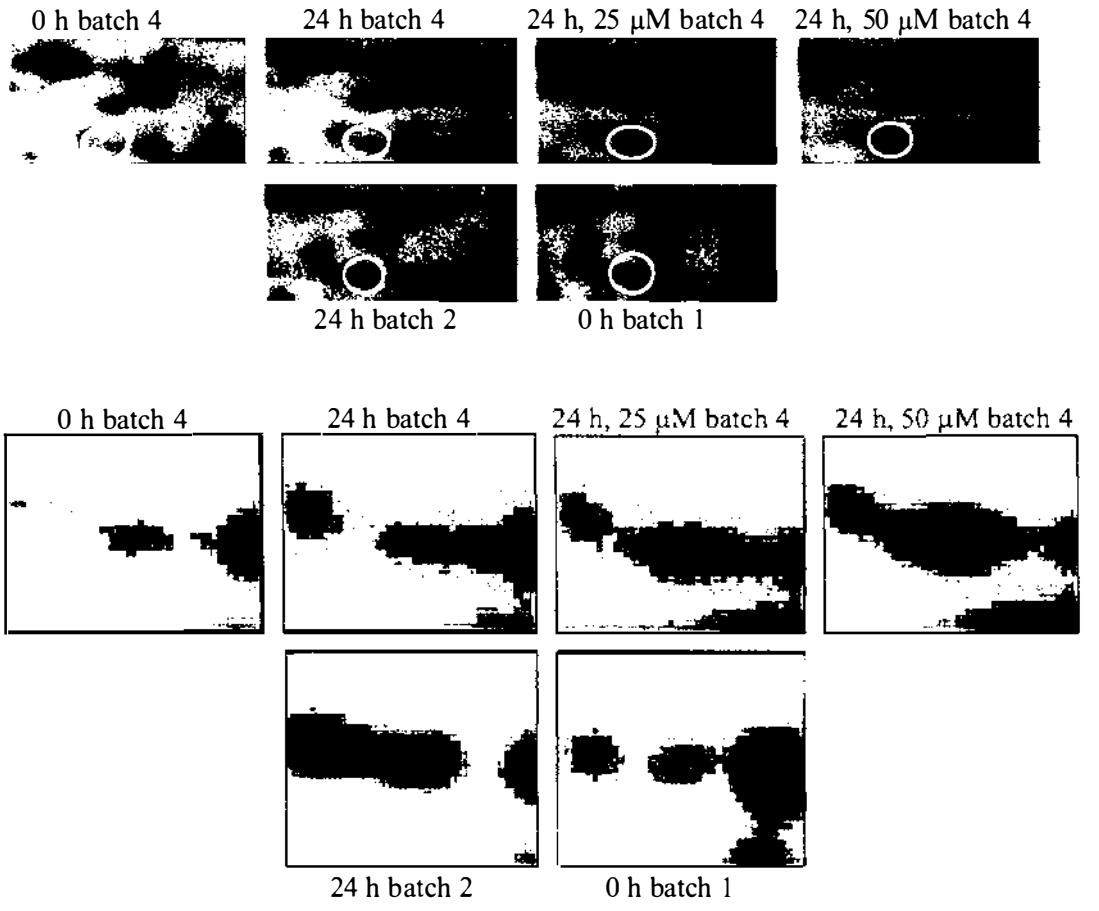

Fig. 5.14: Expression analysis of spot 552

The gel areas of spot 552 (top) are displayed in the top two rows, as indicated in figure 5.9, while the bottom two rows show a close-up of spot 552 for each sample. Expression levels of spot 552 (circled) increased 1.6 and 3.5 fold, after treatment with 25 µM and 50 µM doxorubicin, respectively (top row). In comparison, the 24 h sample of batch 2 featured higher concentrations of spot 552 than the corresponding sample of batch 4. Furthermore, expression levels of the reference spot and of the control sample (0 h) of batch 1, indicated approximately 3 fold higher protein levels compared to the control sample of batch 4. This suggested sample variability was responsible for changes in protein levels of spot 552 rather than a genuine dosage-dependent effect.

5.5.6 Summary

Analysis of 2D gels using the 2D Phoretix Evolution analysis program did not result in the identification of differentially regulated proteins, and results were consistent with those obtained during manual analysis. Although a variety of changes were observed within each

batch tested, all of these were most likely to be the consequence of sample variability. Two-fold up- or down-regulation of a protein was required to be considered a candidate. In order to ensure that all candidates close to the threshold were considered, proteins showing at least 1.7 fold up- or down-regulation were included in the analysis (Table 5.1).

SAMPLE	Treat-ment	B1 0 h	B1 2 h	B1 24 h	B1 R 1	B1 R 2	B2 2 h	B2 24 h	B2 48 h	B3 0 h	B4 0 h	B4 24 h	B4 24 h, 25 µM,	B4 24 h, 50 µM,
	# of spots analysed	446	460	423	423	465	476	431	442	576	576	570	477	517
	# of spots unmatched	12	2	7	6	0	5	11	8	1	0	0	2	0
Ref		41 40	0 31	40 42	34 26	9 33	39 56	24 63	36 33	2 94	2 74	7 67	25 36	6 50
B1 0 h			37 67	60 48	71 61	63 83								
B1 2 h				59 37	58 28	41 26								
B1 24 h					49 49	48 63								
B1 R 1						25 42								
B2 2h								23 28	35 17					
B2 24 h									24 10					
B4 0 h												22 15	67 26	55 24
B4 24 h													40 24	36 31
B4 24 h 25 µM														15 25

Table 5.1: Differentially regulated protein spots

The total number of potentially differentially regulated spots of each sample compared to the reference gel and gels of the same batch is summarized in this table. The batch number and sample treatment, as well as the total number of analyzed spots of each sample, including those unmatched to the reference gel, are indicated. The top numbers in each cell indicated the number of spots up-regulated, the bottom number indicated spots down-regulated by at least 1.7 fold, when comparing a sample in the top row to a sample in the left side column of the table. For example, the control (0 h) of batch 1 (which is abbreviated B1 0 h) displayed 446 spots of which 12 could not be matched, and shows 41 spots up-regulated and 40 spots down-regulated, when compared to the reference gel.

5.5.7 Discussion

Although significant differences between gels were observed, each spot was subsequently eliminated when compared to spots in other samples. Generally, the overall reproducibility of spots was very high. There was a general variability between gels however, which was mainly due to differences in background intensities and a different quality of resolution in areas close to the gel edges.

Phoretix 2D software automatically generated P-values intended to assist in determining the significance of any expression differences between identical spots on different gels. The use of these statistical tools however, is ineffective when analysing silver stained gels. This is mainly due to the narrow dynamic range of silver staining and the variability in overall staining intensity encountered between different gels. For this reason other methods such as immunoblotting are generally used to verify any differences in protein regulation and to perform statistical analysis of differential protein (Chen *et al.*, 2002).

Although the software succeeded in comparing spot values, extensive manual gel warping[1], spot matching, and background analysis was required. In particular, areas suffering from high or low background values and spot intensities close to the cut-off value compromised the interpretation of results.

To collect valid data and to avoid the detection of "false" spots, a sensitivity limit was utilized. As a consequence, very weak spots below the cut-off value were excluded from analysis unless they could clearly be matched to spots on other gels. Since slight differences in spot migration between individual gels are common, and because very weak spots in particular could not always be clearly distinguished from the background, some spots could not be matched between certain samples (Table 5.1).

Taken together, the results of manual and computer-assisted analysis of 2D gels suggest that silver staining is insufficiently sensitive to detect changes in protein expression due to doxorubicin treatment of breast cancer cells under any of the conditions used.

[1] The superimposing of two gel images which uses identical proteins on these gels as anchor-points for gel alignment, with the aim of producing matching protein spot patterns between the two gels.

Chapter Six

DNA Double-Strand (DSB) Repair

6.1 Introduction

In humans and other eukaryotes the breaking of both strands of DNA can be caused by endogenous factors e.g. reactive oxygen species, V(D)J recombination[2], replication associated damage, and exogenous factors such as mechanical stress, chemicals, chemotherapeutic agents and ionizing radiation. If left unrepaired these DNA double-strand breaks (DSBs) can lead to chromosome aberrations, higher radiation sensitivity, and cell death (Lees-Miller and Meek, 2003). There are two main DSB repair mechanisms in place: homologous recombination repair (HRR) and non homologous end-joining (NHEJ). Cell cycle state is critical in determining which of these pathways is utilized for the repair process. NHEJ is predominantly responsible for DNA DSB repair during G1- and early S-phase, while in late S and G2 both HRR and NHEJ seem to be of equal importance (Rothkamm *et al.*, 2003) (Fig. 6.1).

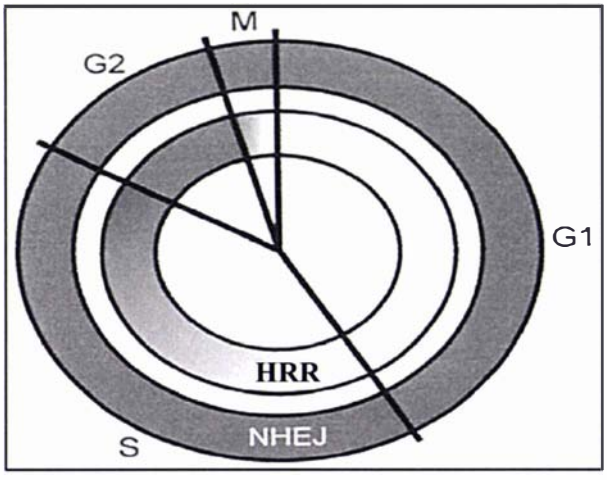

Fig. 6.1: Cell cycle-dependent DNA DSB repair pathways

Dark coloured parts of the circle indicate activity, while white coloured parts indicate inactivity of the pathway. NHEJ is predominantly responsible for DNA DSB repairs during G1 and early S, while in late S and G2 both HRR and NHEJ seem to be of equal importance.

NHEJ is an inherently more error prone repair process than HRR, potentially causing loss of nucleotides from the site of breakage. However, since only a small percentage of genomic

[2] Process whereby segments of the immunoglobulin genes and the T-cell receptor are rearranged during development of the vertebrate immune system

DNA encodes proteins, entering replication and mitosis with an incorrectly repaired DSB may well constitute a lower risk to the organism than doing so with an unrepaired DSB.

HRR is the most precise form of repair, but it is comparatively slow, and may not always be feasible as a homologous chromosome template is required for repair. One of the pitfalls of HRR is the possible loss of heterozygosity due to crossing over events of sister chromatids. Furthermore, apart from during and directly after replication, the two homologous chromosomes are not paired and the distance between them makes HRR virtually impossible. This may also be the reason why HRR seems to be restricted to the late S- and G2-phase and is indeed championed by some researchers as being more important during these phases than NHEJ (Henning and Sturzbecher, 2003).

6.2 Non-Homologous End Joining

During NHEJ, the Ku heterodimer binds to DNA at the ends of DSBs and subsequently recruits Xrcc4 (X-ray repair cross-complementing protein 4) and ligase IV, to form a complex which aligns and ligates the DNA ends (Fig. 6.2). Ku also facilitates the recruitment and binding of the 465 kDa DNA-dependent protein kinase catalytic subunit (DNA-PKcs) to the site, forming an activated DNA-PK complex which requires auto-phosphorylation in the process of repair (Burma and Chen, 2004) and potentially phosphorylates (serine/threonine) other DNA binding proteins involved in cellular response mechanisms. The importance of these proteins is underscored by the increased sensitivity toward IR and severe deficiencies of cells defective in any of these genes (Ramsden and Gellert, 1998; Pastink *et al.*, 2001; Hopfner *et al.*, 2002).

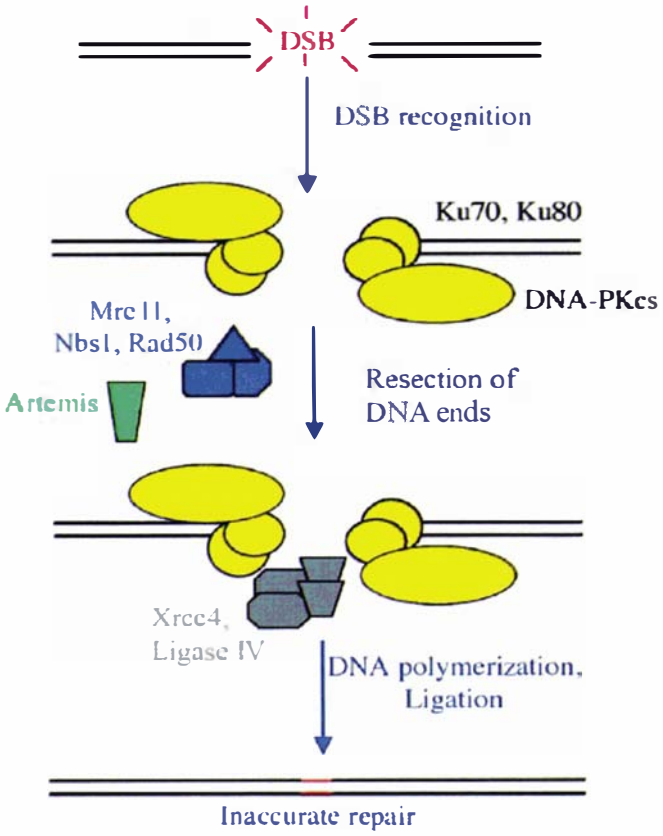

Fig. 6.2: Schematic representation of NHEJ

Drugs or ionizing radiation-induced DNA DSBs are first recognized by Ku70 and Ku80, which bind to the DNA ends and recruit the DNA-dependent catalytic subunit DNA-PKcs to form an active DNA-PK complex. The Artemis protein, which opens hairpin structures, and the Mre11 protein complex, consisting of Rad50, Nbs1 and Mre11, and possessing endo- and exo-nuclease activity, may both play a role in NHEJ if resecting of the ends is necessary. A DNA polymerase then synthesises new DNA ends which are joined by the Xrcc4 and ligase IV protein complex. As a result, the repaired DNA region is likely to deviate from the original sequence. (Modified from Jackson, 2002)

6.3 Homologous Recombination Repair

HRR involves many proteins e.g. Rad51, Rad52, Rad54, and the Mre11-Rad50-Nbs1 complex (Fig. 6.3).

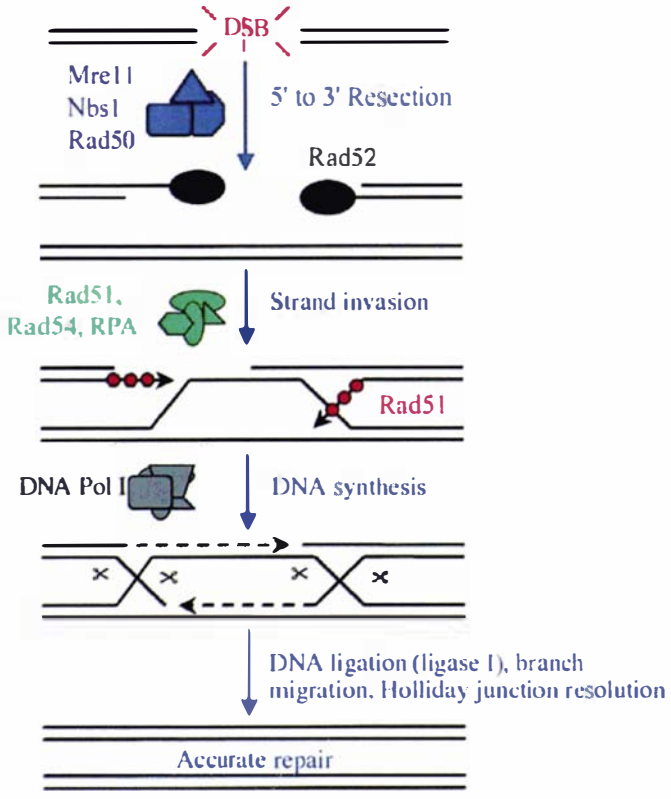

Fig. 6.3: Schematic representation of HRR

The repair procedure is believed to be initiated by resection of the break by the Mre11 complex (Mre11, Rad50, Nbs1), creating single-strand overhangs. Rad52 binds to these overhangs while Rad51, which is critical for catalysing homologous strand pairing and exchange, forms filaments along the unwound DNA strand, facilitating strand invasion in conjunction with other proteins, such as Rad54 and RPA (replication protein A) (Khanna and Jackson, 2001; Jackson, 2002; Henning and Sturzbecher, 2003; Valerie and Povirk, 2003). The resected 3' end invades a homologous DNA duplex and is extended by DNA polymerase. The ends are ligated by DNA ligase I and the interwound DNA strands (Holliday junctions) are resolved resulting in either crossover or non-crossover gene conversion products. (Modified from Jackson, 2002)

Increasing evidence has been obtained linking increased rates of DNA damage repair to elevated levels of DNA-PK and Rad51, which contribute to cell resistance against IR and chemotherapy (Vispe *et al.*, 1998; Hansen *et al.*, 2003). Alteration in expression or activity of proteins involved in either the NHEJ or HRR pathway have been implicated as causing tumourigenesis and IR/chemo resistance mechanisms. Ku 70 and Ku 80 have been found to exhibit both higher and lower DNA-binding activity in advanced tumours compared to normal tissue, independent of tissue origin (breast/bladder). The differential activity may reflect different stages of disease progression, as more advanced tumours collectively displayed

much lower DNA-binding activity towards the heterodimer (Pucci *et al.*, 2001). Overexpression of Rad51 has been implicated in a variety of cancers, including breast cancer and contributes to resistance mechanisms and tumour progression in these cells (Raderschall *et al.*, 2002; Henning and Sturzbecher, 2003; Richardson *et al.*, 2004).

6.4 DNA Damage Repair or Apoptosis?

Although little is known about DNA damage-induced signal transduction, it seems that ATM, ATR, and DNA-PK, which are all phosphatidylinositol 3-kinase-like kinases (PIKKs), play an important role in phosphorylating (serine/threonine) p53 and other sensory proteins. PIKKs are known to modulate DNA-damage responses using different cell cycle checkpoints, apoptosis, and DNA repair (Norbury and Zhivotovsky, 2004). Apoptosis and DNA repair are likely to be counteracting pathways, predictably utilizing proteins involved in both pathways, such as ATM, ATR, DNA-PK, and BRCA1. Silencing of genes like ATM, ATR and DNA-PKcs using siRNA has resulted in sensitizing cancer cells to ionizing radiation and chemotherapeutic agents, providing new insights for future treatment options (Collis *et al.*, 2003; Yang *et al.*, 2004).

Another important protein mediating apoptosis after DNA damage is c-Abl. In the event of a DNA lesion, ATM phosphorylates c-Abl which, in turn can phosphorylate two different tyrosine residues, the tyrosine (T) 54 and/or T315 site of Rad51. Phosphorylation of T54 results in the loss of Rad51's DNA-binding ability and promotes DNA strand exchange, while phosphorylation of T315 enhances interaction with Rad52 increasing HRR activity. Depending on the cell cycle and the extent of DNA damage, it appears that the phosphorylation of T54 may inhibit HRR and initiate apoptosis. The phosphorylation of T315 however, may augment HRR while suppressing apoptosis at the same time. Because of Rad51's crucial role in HRR it has been proposed that the c-Abl-Rad51 complex may act as a gatekeeper between DNA repair and apoptosis (Henning and Sturzbecher, 2003; Valerie and Povirk, 2003).

6.5 Rad51 and DNA-PK Initiated Repair of Topoisomerase II Alpha Mediated DNA DSB

In contrast to Rad51, which is expressed in a cell cycle-dependent manner, peaking in late S/G2, DNA-PKcs and Ku70/80 levels remain constant throughout the cell cycle. However, nuclear relocalisation and an increase in DNA-PK activity, occur after the G1/S transition

(Flygare *et al.*, 1996; Nilsson *et al.*, 1999). As mentioned earlier, the topoisomerase II alpha enzyme is involved in DNA replication and chromosome segregation with low levels of enzyme in G0/G1, which increase during late G1/S and peak during G2/M. Moreover, it has been shown that low concentrations of doxorubicin can halt the cell cycle at G2/M, while high drug concentrations can lead to arrest at early S-phase. The cell cycle state of a cell exposed to doxorubicin is one of the determining factors for subsequent steps. This is because the extent of DNA damage is correlated with the topo II alpha concentration, which depends on the cell cycle state, which in turn determines the preferred mechanism of repair (or apoptosis).

Interestingly, recent studies revealed that in the case of NHEJ, in order to repair topo II poison-mediated DNA-DSB it was essential that the enzyme was removed from the DNA to allow binding of the Ku heterodimer (Martensson *et al.*, 2003). Studies in chicken cells (DT 40) have indicated that NHEJ is the predominant repair pathway for topo II poison-induced DNA lesions (Adachi *et al.*, 2003), and that cells deficient in NHEJ are much more sensitive to chemotherapeutic agents than an HRR deficient variant. Furthermore, this group also speculated that at high drug dosage, an unknown type of DNA-damage may be produced, in addition to the common lesions, which may require HRR and/or NHEJ. On the contrary, Hansen (Hansen *et al.*, 2003), suggested that both Rad51-dependent homologous recombination and DNA-PK-dependent NHEJ play a role in DNA-DSB repair. These authors further suggested that NHEJ may be more focused on DNA repair upon G1 arrest, whereas HRR may be more important in terms of cell survival after DNA damage-induced G2 arrest. NHEJ is claimed to repair up to 80% of the DNA lesions very quickly and within 3 h of occurrence, while HRR is more tedious, but error-free (DiBiase *et al.*, 2000).

It has also been shown that DNA-PK specific inhibitors, such as NU7026 (2-(morpholin-4-yl)-benzo[h]chomen-4-one) and SU11752, significantly enhance the efficacy of topo II poisons, leading to increased DNA-DSB levels and G2/M checkpoint arrest (Veuger *et al.*, 2003; Ismail *et al.*, 2004; Willmore *et al.*, 2004). Inhibition of DNA-PK using target-peptides also succeeded in sensitizing human breast cancer cells to IR (Kim *et al.*, 2002). Moreover, another study suggests a correlation of DNA-PK levels and doxorubicin resistance in relapsed leukaemia patients (Eriksson *et al.*, 2002). This notion was further underscored as HL60 cells, which were selected for doxorubicin resistance, were found to have a 15 fold increase in DNA-PK levels (Shen *et al.*, 1998).

6.6 Aim

Doxorubicin and other topoisomerase II alpha (topo II) poisons are commonly used in chemotherapy of breast cancer patients, primarily causing cell death by producing DNA-DSB, but also forming reactive oxygen radicals. Although many studies have investigated the effects of doxorubicin on cell cycle and cell viability, little is known about the response of proteins involved in the repair of doxorubicin-generated DNA damage, which represent major factors in the cells struggle for survival and drug resistance. A better understanding of the cells response to overcome this cellular assault is essential for the development of targeted and more effective approaches to killing cancer cells. To investigate the DNA damage repair response to doxorubicin the expression of two key proteins, Rad51 and DNA-PKcs, were monitored in estrogen receptor (ER) negative MDA MB 231, ER positive MCF7 breast cancer cells, and normal human breast cells MCF12A. Additionally, 10 clinical samples were analysed for overexpression as well as any potential correlations in expression of these two repair proteins in tumour compared to normal tissue.

6.7 Experimental Design

Before analysing actual proteins, samples of antibodies for DNA-PKcs and Rad51 were tested for their specificity and functionality. A dilution series of 1:100, 1:500 and 1:1000, of both antibodies in 0.5% blocking reagent (POD substrate, Roche®) in TBST were directly spotted onto nylon membrane and treated according to the standard protocol. Both antibodies produced positive signals after treatment with anti-rabbit secondary antibody confirming primary and secondary antibody interaction. In order to verify protein detection limits and specificity, extracts containing 1 µg, 5 µg and 20 µg of total protein, were spotted onto a piece of membrane and treated according to the standard protocol. Using dilutions of 1:500 primary antibody and 1:2500 secondary antibody, all of the spotted protein dots could be detected without background reactivity. To ensure protein specificity, identical quantities of protein extract were loaded onto an 8% and a 5% gel. The low percentage gel was used to allow the large DNA-PKcs (465 kDa) to migrate into the gel more easily. Both antibodies specifically detected gel bands corresponding to the expected molecular weights of DNA-PKcs and Rad51 (39 kDa). After assessing the signal intensities and signal to noise ratio, the optimal protein loads were determined to be 5 µg and 25 µg, for DNA-PKcs and Rad51, respectively.

To investigate whether DNA-PKcs and Rad51 protein levels change in response to 3 µM doxorubicin treatment, an unexposed control sample and samples harvested 2 h and 24 h after

exposure, were analysed. Alpha tubulin was used as a loading control and gave strong signals with the 25 μg samples, but failed to produce any signals when 5 μg of protein was used, therefore demanding further optimization.

In order to ensure reproducibility and consistency, both Rad51 and DNA-PKcs needed to be assayed on the same gel. Conditions for the detection of topo II alpha also required optimization. A primary antibody dilution of 1:4000 for DNA-PKcs and 1:250 for Rad51, was used with a 1:2500 anti-rabbit secondary dilution and gave optimal signals when analysing 20 μg of protein. Clear and consistent detection of topo II alpha was obtained when using a primary antibody dilution of 1:200 and 1:5000 for anti-goat secondary antibody.

Since these four proteins were very different in size, ranging from 465 kDa to 39 kDa, gradient gels were utilised to allow proper separation prior to western analysis. The best separation pattern was achieved when pouring 5-10% SDS-PAGE gels (2.7 ml 10%, 1.2 ml 5%, 3% stacking gel). After electrotransfer the blotted nylon membranes were cut into four pieces, each containing a protein of interest, which were subsequently subjected to standard immunodetection.

6.8 Results

MDA MB 231, MCF12A, and MCF7 cells were exposed to 3 μM doxorubicin and the subsequent immunoblots analysed for expression of DNA-PKcs, Rad51, topo II alpha and alpha tubulin 0, 2, 24, and 48 hours after exposure, as previously described for the 2D gel electrophoresis studies. Images of the immunoblots were taken in a Fuji Dark Box and subsequently analyzed using Image J software for semi-quantitative comparisons (Fig. 6.4) (section 2.2.4.3).

In both MDA MB 231 and MCF12A cell lines, an increase in Rad51 and topo II alpha levels was observed 24 h and 48 h after drug exposure (Fig. 6.5 and 6.6). In MCF7 cells topo II alpha levels remained largely unchanged 24 h post-treatment, but decreased 48 h after initial drug exposure. In contrast to the results obtained for MDA MB 231 and MCF12A cells, post-treatment Rad51 levels were decreased at all time points in MCF7 cells. DNA-PKcs signals showed some degree of variation between experiments, but essentially remained unaltered. Samples taken from cells 2 h after first contact with doxorubicin did not always yield reproducible results.

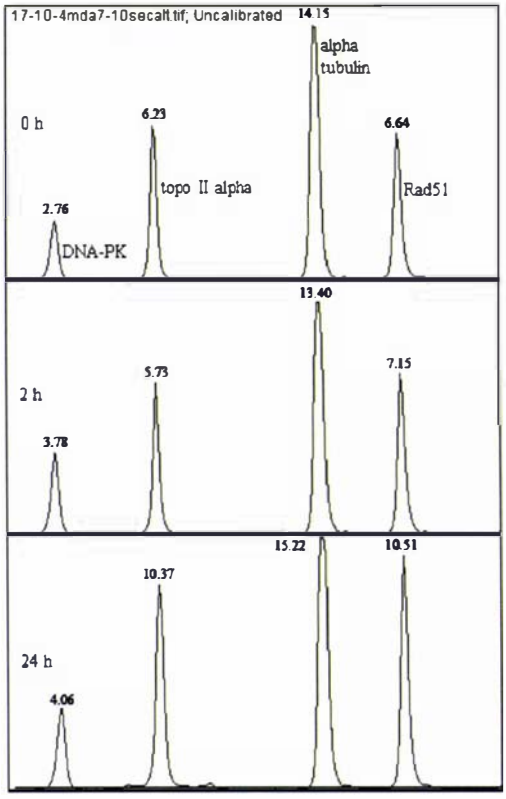

Fig. 6.4: Densitometric analysis of MDA MB 231 extracts separated by SDS-PAGE

The graph shows the representative densitometric results of MDA MB 231 cells 0, 2, and 24 h after exposure to doxorubicin using Image J software. Peak areas of DNA-PK, topo II alpha, and Rad51 were compared to the corresponding alpha tubulin value, which was set to 100%. Protein concentration levels, relative to alpha tubulin, were then compared between samples for semi-quantitative analysis.

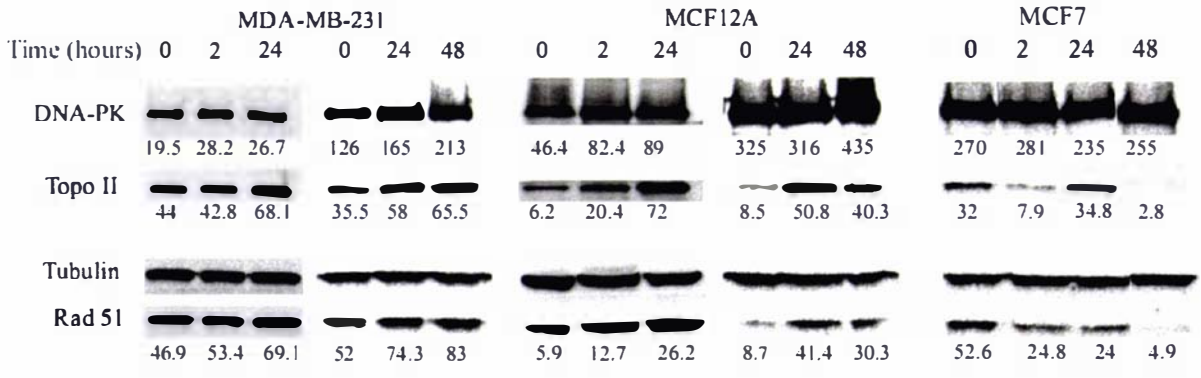

Fig. 6.5: Immunoblot of MDA MB 231, MCF12A, and MCF7 cell protein extracts

20 μg of total protein were separated on a 5-10% polyacrylamide gel to compare temporal changes in topo II alpha and DNA repair proteins Rad51 and DNA-PK relative to alpha tubulin 0, 2, 24 and 48 hours after 3 μM doxorubicin treatment. Numbers indicate signal intensity as a percentage, relative to tubulin (100%). The results are representative of three experiments.

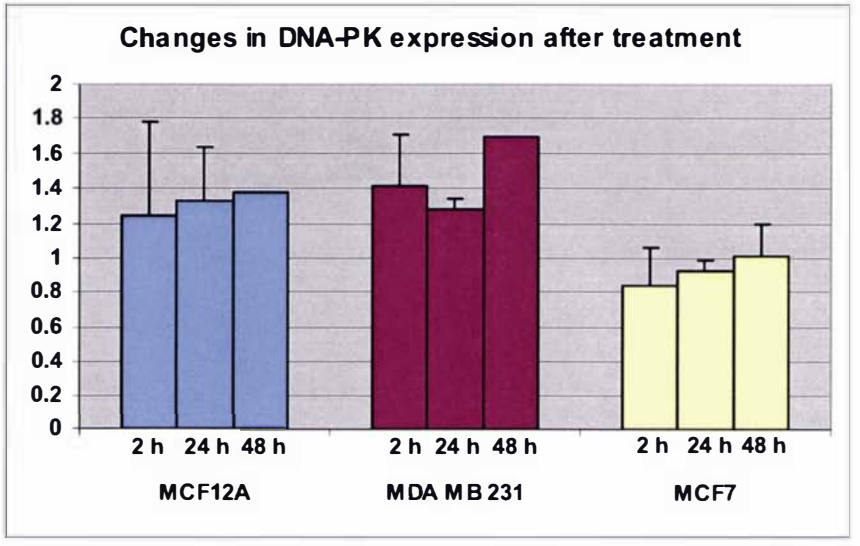

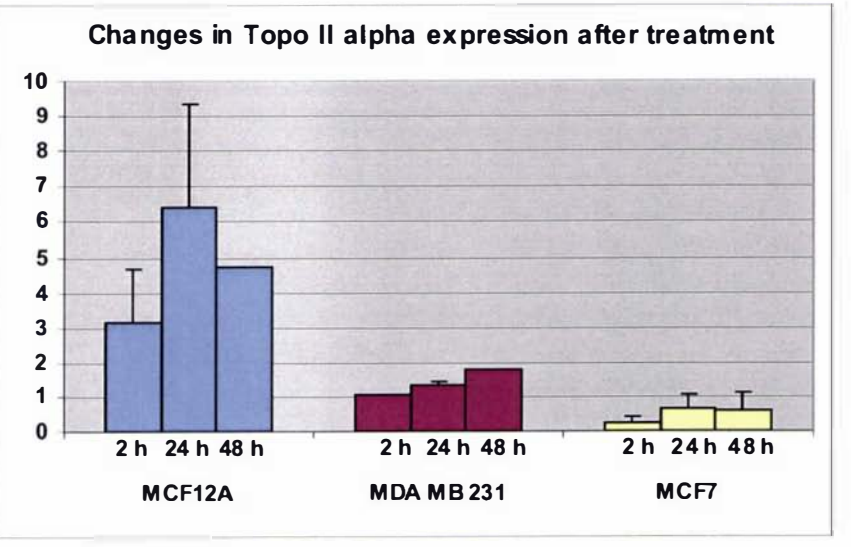

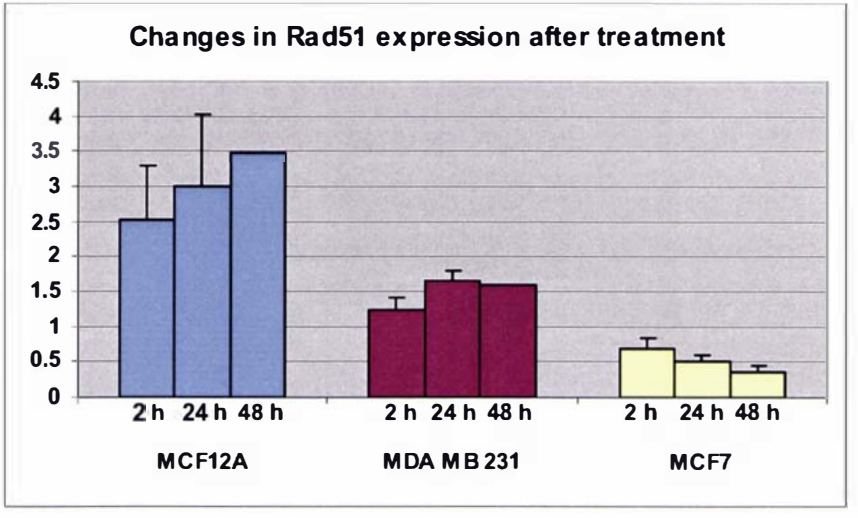

Fig. 6.6: Statistical analysis of temporal changes in protein expression

Graphs show mean levels of DNA-PKcs, Topo II alpha, and Rad51 levels 2, 24, and 48 hours after doxorubicin treatment compared to the mean of the control (0 h) which was set to a value of 1. Error bars indicate standard error of means of 2 experiments for the 2 h samples and 3 experiments for the 24 h sample. Additional experiments were conducted for all time points and all cell types, confirming trends of the other replicates. These were captured on x-ray film only and hence could not be used for statistical analysis. Changes in expression of DNA-PK ($p=0.01$), Topo II alpha (0.04), and Rad51 (0.01) in MDA MB 231 celss 24 h after drug treatment were statistically significant when compared to the control. All other changes did not reach statistical significance ($p>0.05$).

6.8.1 FACS Analysis

Rad51 and topo II alpha expression is known to be increased in late S- and G2/M-phases of the cell cycle (Woessner *et al.*, 1991; Flygare *et al.*, 1996). FACS analyses were employed to establish whether the observed changes in protein levels were due simply to a change in cell cycle distribution, or were a genuine response to drug exposure. FACS analysis revealed that only MDA MB 231 cells showed a strong increase of S and G2/M cells, with a concomitant decrease of cells in G1 compared to the control, 24 h and 48 h after drug exposure. MCF7 cells showed a marginal decrease of cells in S-phase, causing an increase in the number of G2/M cells. FACS profiles of MCF12A samples remained almost identical (Fig. 6.7). No changes in cell cycle distribution were detected in any of the cell lines tested 2 h after drug treatment, compared to the control (data not shown). Consequently, the increase in Rad51 expression observed in MCF12A and MCF7 cells 24h and 48h after drug treatment, must be due to drug exposure, and is independent of cell cycle state. Unexpectedly, the same must be true for topo II alpha levels which were also elevated. Indeed, up-regulated topo II alpha and Rad51 levels show a strong correlation in MDA MB 231 and MCF12A cells. As the cell distribution profile of MDA MB 231 cells changes dramatically as a result of drug treatment further investigations were necessary to determine if the exhibited alterations in Rad51 and topo II alpha protein content were independent of cell cycle state in this cell line.

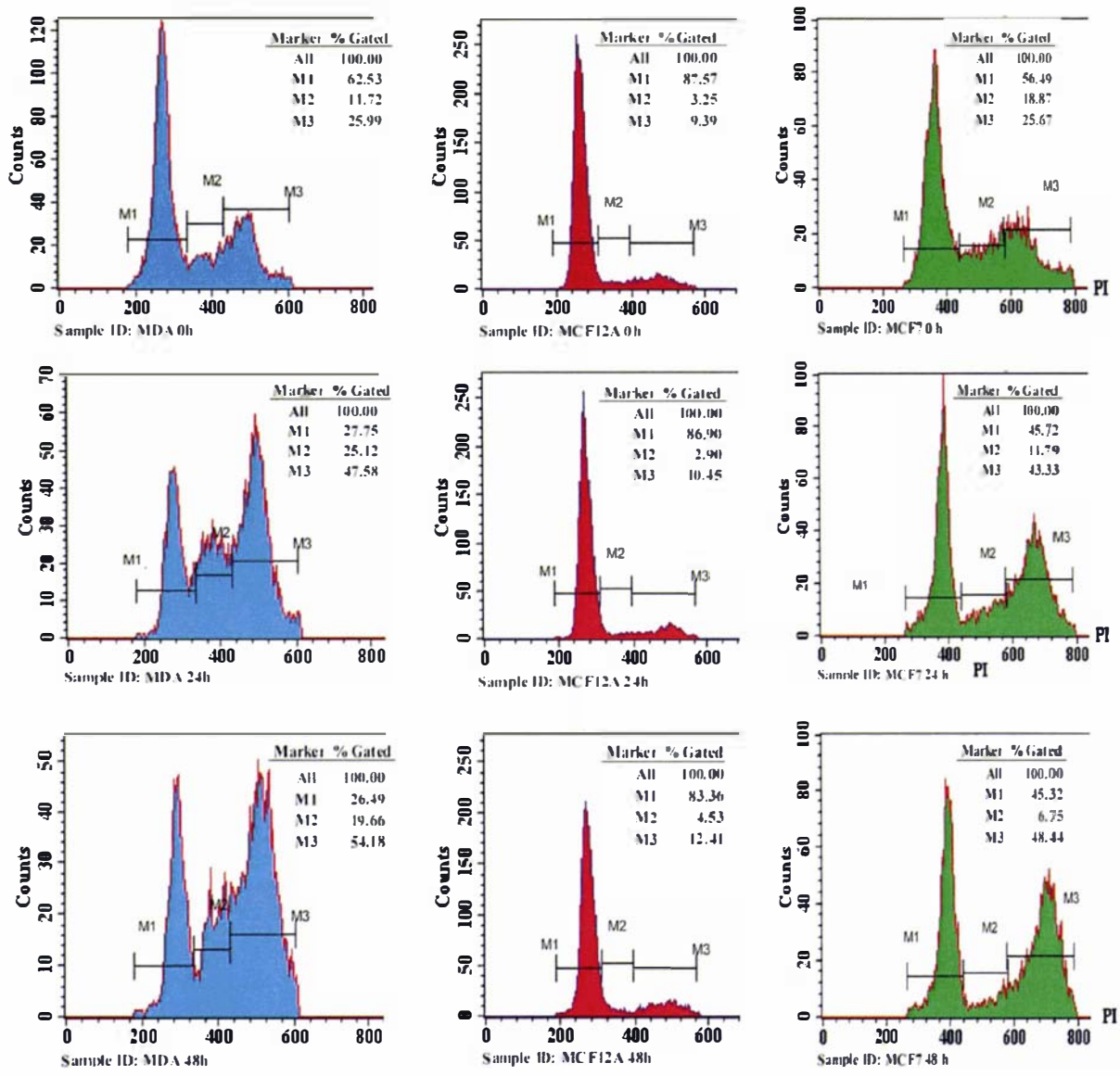

Fig. 6.7: FACS results

Graphs show cell cycle distribution of MDA MB 231, MCF12A, and MCF7 cell lines 0, 24, and 48 h after 3 μM doxorubicin treatment. All FACS experiments were repeated with a different batch of cells to ensure reproducibility. The number of cells in G1- (M1), S- (M2), and G2/M-phase (M3) of the cell cycle are indicated. The intervals M1, M2, and M3 which were used to distinguish between different cell cycle stages are identical for all samples of the same cell line. The results are representative of two experiments.

6.8.2 Synchronization of MDA, MCF7 and MCF12A Cells

The cellular addition of thymidine leads to the depletion of intracellular dCTP pools, and as a consequence drastically slows down the replication process. This results in an accumulation

of cells at the transition from G1- into S-phase of the cell cycle (Bjursell and Reichard, 1973). Once the cells are released from the imposed thymidine block they should traverse through the cell cycle synchronously. In an attempt to mimic the MDA MB 231 cell cycle distribution 24 h after doxorubicin exposure, cells were subjected to a double thymidine block. Cells were initially blocked 24 h after passaging by adding 2 mM thymidine to the growth media. 16 h after blocking, cells were released for 10 hours before repeating the thymidine-block, again for 16 h. The cells were then harvested 0, 3, 6, 7.5, 9, and 24 h after being released from the second block, to determine at what point the cell cycle distribution profile was most similar to that seen 24 h after doxorubicin exposure in the respective cell lines. FACS profiles of MDA MB 231 cells treated with 3 μM doxorubicin looked most similar to cells 6 h after release from the thymidine block (Fig. 6.8). Ultimately, this approach did not succeed in producing a cell cycle distribution profile of sufficient similarity to that of drug exposed cells, to allow confident comparison of cell cycle state and protein expression. Therefore, cell cycle-independent expression of Rad51 and topo II alpha could not be confirmed in MDA MB 231 in these experiments.

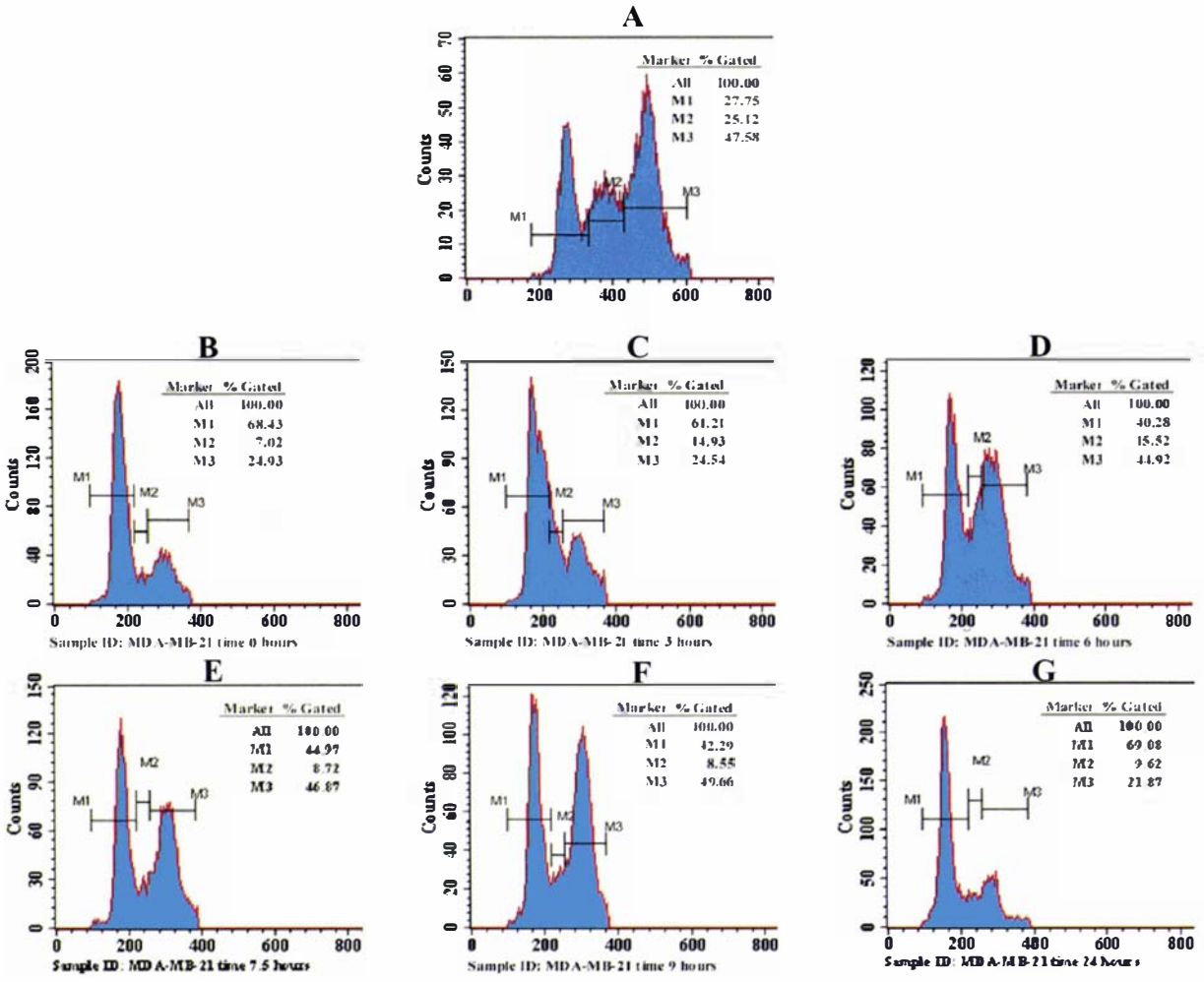

Fig. 6.8: Double thymidine block of MDA MB 231 cells

FACS profile of cells 0, 3, 6, 7.5, 9, and 24 h (B through G) after release from thymidine block compared to (A) 24 h after treatment with 3 μM doxorubicin.

6.8.3 Drug Dosage Effect

Cells were treated with moderate to low (0.6 μM), moderate to high (3 μM) and high concentrations (15 μM) of doxorubicin to investigate the dosage-dependent response of MDA MB 231, MCF12A, and MCF7 cell lines. Furthermore, cell viability was determined using the above mentioned doxorubicin concentrations over a period of 7 days, employing erythrosine B to distinguish between viable and dead cells as described in section 2.2.1.5. These drug concentrations were chosen relative to the drug sensitivity of MDA MB 231 cells, which were the most sensitive of the 3 cell lines used (Fig. 6.9).

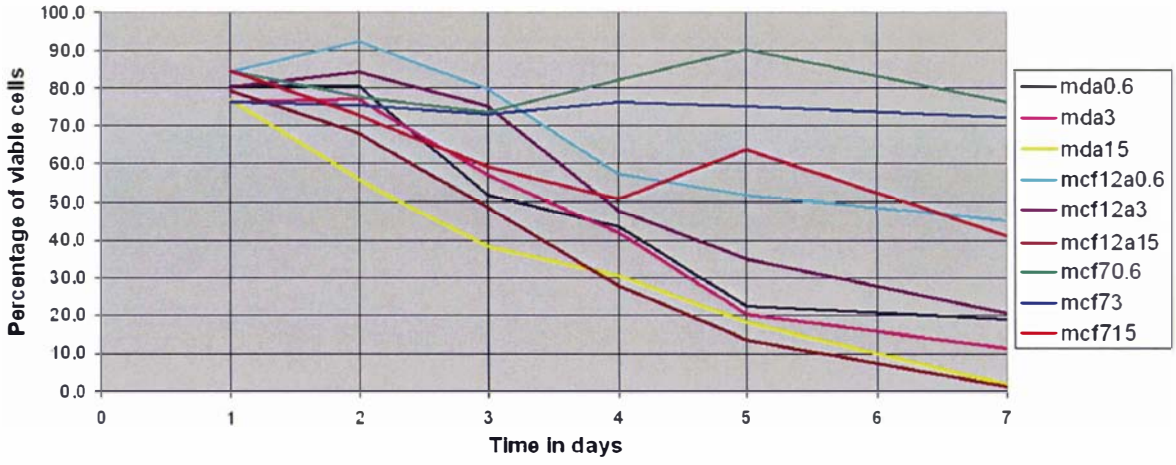

Fig. 6.9: Cell viability assay

The impact of drug treatment on MDA MB 231, MCF12A, and MCF7 cell survival using 0, 0.6, 3, and 15 μM doxorubicin, was monitored over 1 week with samples taken every 24 h after initial exposure. No sample was taken on day 6. Results are averages of duplicate (in some cases triplicate) counts of two, independently grown and identically treated, samples.

Both FACS analysis and immunoblotting were performed using the same sample, which was collected 24 h after drug exposure, as changes in protein expression were most significant at this point during the time course experiments. As in the time course experiments, DNA-PKcs levels remained largely unaltered across all concentrations of doxorubicin as compared to the unexposed control (Fig. 6.10). In MCF7 cells DNA-PK levels appeared elevated due to one experiment showing unusually low levels of DNA-PK in the control (0 h) (Fig. 6.11). A third experiment which could not be included for statistical purposes as it was only available on x-ray film, confirmed the trends seen in the first experiment suggesting DNA-PK levels to remain unaltered after treatment (data not shown). Rad51 and topo II alpha expression in both MDA MB 231 and MCF12A cells, was markedly increased in response to 0.6 μM and 3 μM doxorubicin. Indeed all cell lines displayed significantly higher topo II alpha levels 24 h after exposure to 0.6 μM doxorubicin compared to the control. A dosage of 15 μM appeared to reduce topo II alpha levels compared to that observed at the lower doses. Interestingly, in MCF7 cells Rad51 levels exhibited a completely opposite response, as they declined significantly with increasing drug concentration. Hence the Rad51 response of the ER positive MCF7 cells is contrary to that seen in the ER negative MDA MB 231 cell line. On the other

hand, topo II alpha levels concur with those seen in MDA and MCF12A cells with 0.6 μM doxorubicin.

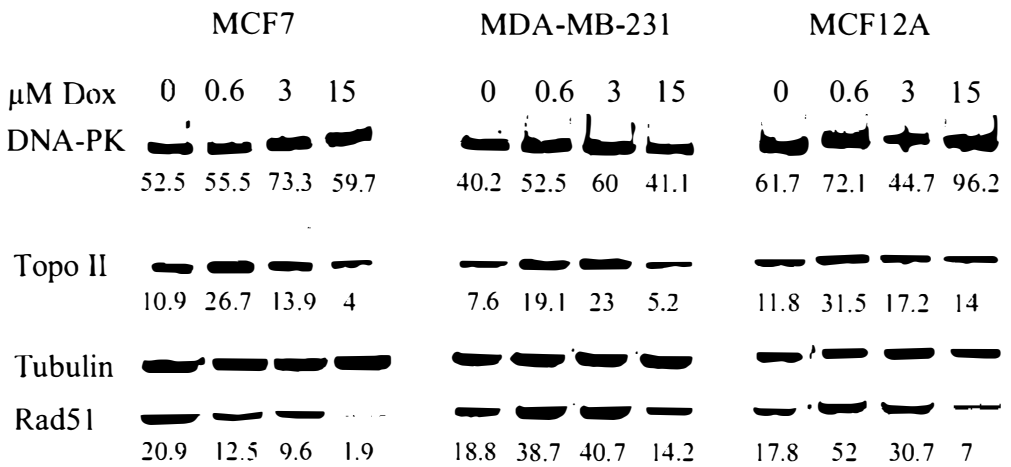

Fig. 6.10: Immunoblot of MDA MB 231, MCF12A, and MCF7 cell protein extract

20 μg of total protein were separated on a 5-10% polyacrylamide gel to investigate a drug-dosage response of DNA-PK, topo II alpha, alpha tubulin and Rad51 to 0, 0.6, 3, and 15 μM doxorubicin in the cell lines tested. Numbers indicate signal intensity as a percent relative to tubulin (100%) of the same lane. The results are representative of 3 experiments.

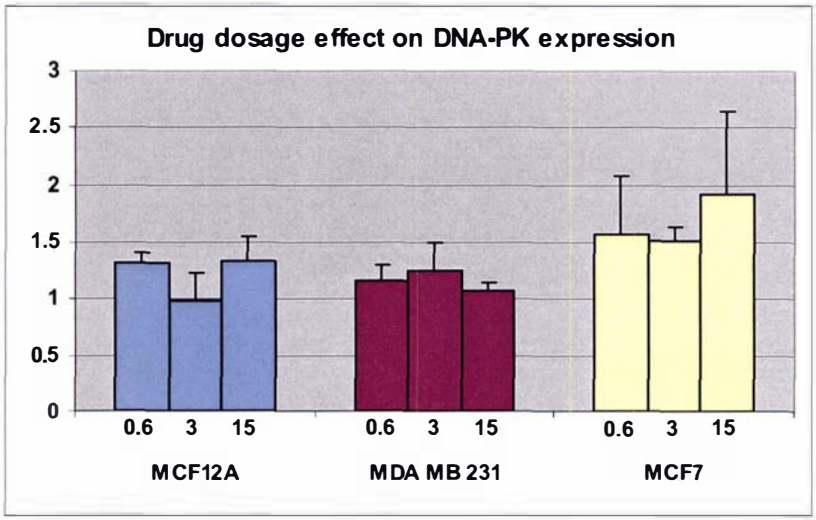

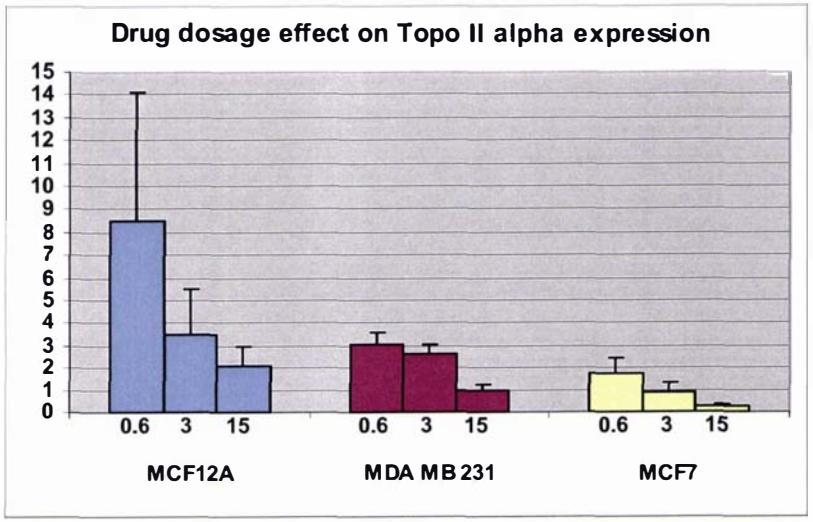

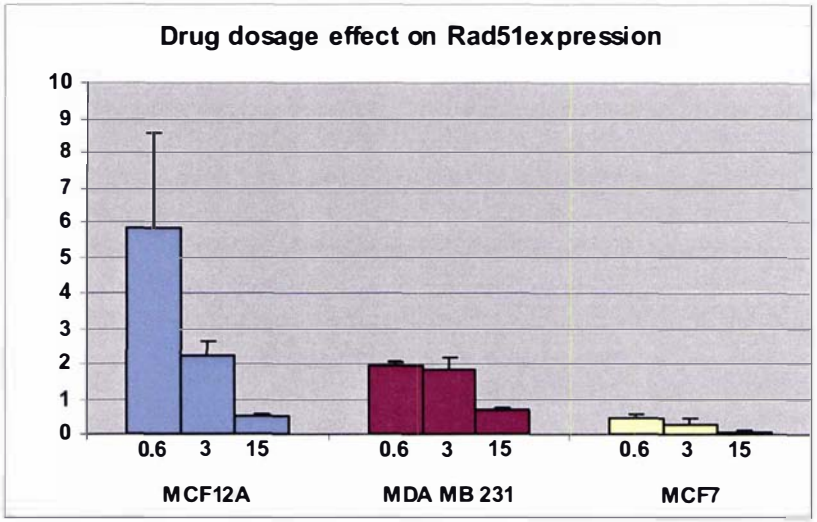

Fig. 6.11: Statistical analysis of dosage-dependent changes in protein expression

Graphs show mean levels of DNA-PKcs, Topo II alpha, and Rad51 levels in the cell lines tested 24 hours after 0, 0.6, 3 and 15 μM doxorubicin treatment compared to the mean of the control (0 h) which was set to a value of 1. Error bars indicate standard error of means for 2 experiments. Rad51 downregulation after 15 μM doxorubicin treatment of MCF 7 cells was statistically significant ($p=0.02$). All other changes in protein expression did not reach statistical significance ($p<0.05$).

6.8.4 Dosage-Dependent FACS Analysis

FACS analysis of samples used in the experiment to test effect of drug dosage revealed that neither MCF7 nor MCF12A cells showed any significant changes in cell cycle distribution 24 h after exposure to varying amounts of doxorubicin (Fig. 6.12). Hence, the changes in Rad51 and topo II alpha expression in these cell lines were not cell cycle state specific, but appeared to be a genuine response to drug exposure, confirming the observations made during time course analysis. The results seen in MDA MB 231 cells were harder to interpret. A similar response was observed in cells exposed to 0.6 μM and 3 μM of doxorubicin, with the latter containing 50% more cells in G1. If Rad51 expression was indeed restricted to the late stages of the cell cycle, this should have resulted in a much weaker signal in samples treated with 3 μM compared to 0.6 μM doxorubicin, but in fact the observed signal was actually slightly stronger. Hence, it seems likely that changes in Rad51 and topo II alpha protein levels in MDA MB 231 cells are also independent of cell cycle distribution, under these conditions.

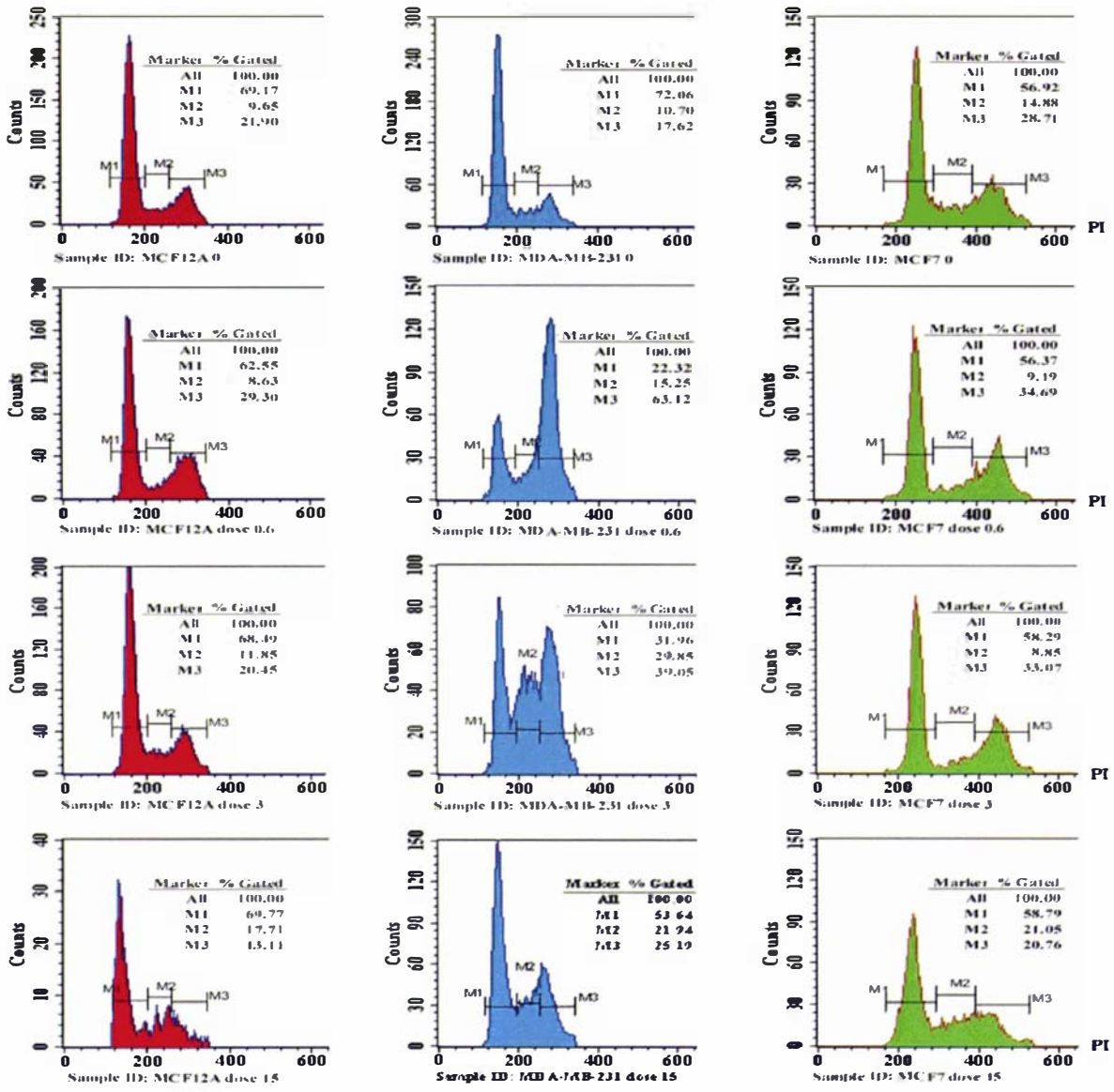

Fig. 6.12: FACS profiles for time course experiment

A total of 10^5 cells were counted for each sample, with the exception of MCF12A cells treated with 15 μM, as not enough cells were present in that sample (note the change in scale of y-axis). The number of cells in G1- (M1), S- (M2), and G2/M-phase (M3) of the cell cycle are indicated. The intervals M1, M2, and M3 which were used to distinguish between different cell cycle stages are identical for all samples of the same cell line. The experiment was repeated once with similar results.

6.9 Breast Cancer Immunohistochemistry

Although both Rad51 and DNA-PK are essential in DNA-DSB repair, their precise role in malignant transformation and resistance to ionising radiation/chemotherapy remains unclear. Not surprisingly, Rad51 levels have previously been shown to be differentially regulated between normal and malignant human tissues, including breast (Moll *et al.*, 1999; Maacke *et al.*, 2000; Maacke *et al.*, 2000). On the other hand, expression of the DNA-protein kinase catalytic subunit (DNA-PKcs) which forms part of the functional DNA-PK protein complex, together with the Ku70 and Ku80 heterodimer, did not show any significant differences between different normal and malignant human tissues, including breast tissue. It seems that DNA-PKcs mRNA levels remain largely unaltered across a range of different types of tissue, while protein expression levels are cell and tissue specific, coinciding with Ku80 levels. Furthermore, expression levels in several cancerous tissues were paralleled by those in normal tissue. Interestingly, invasive carcinoma of the breast lacked consistent DNA-PKcs and Ku80 expression, while lactating breast epithelium cells showed strong nuclear expression of both proteins, indicating that altered protein expression may coincide with pathological changes (Moll *et al.*, 1999).

Unchanged DNA-PKcs levels have also been reported between normal colon tissue, colon adenomas, and colon carcinomas (Rigas *et al.*, 2001). Another group however, refutes this, claiming colorectal tumours show significantly higher levels of mRNA and protein of DNA-PKcs, as well as Ku70 and 80, and an increase in DNA-PK activity, compared to normal tissue (Hosoi *et al.*, 2004). Differences in the expression of DNA-PKcs have also been reported between different states of lymphoid malignancies (Holgersson *et al.*, 2004).

Rad51, which is a BRCA1 interactive protein, has been reported to be down-regulated in about 30% of sporadic, hereditary and BRCA1-mutated breast carcinomas, while exhibiting high expression in normal mammary epithelial cells (Yoshikawa *et al.*, 2000). In contrast, another study reported that the histological grading of sporadic invasive ductal breast cancer was correlated with the over-expression of wild–type Rad51, which may be permissive for tumour progression (Maacke *et al.*, 2000).

Expression profiles in malignant breast tissue, and more importantly in relapse patients having developed resistance to chemotherapy, is limited and inconclusive. No previous studies have investigated a correlation between deregulated DNA-PK and/or Rad51 expression and patient

survival, in general or after treatment. In order to determine the feasibility of such an investigation, a pilot study was designed. For this purpose, tissue samples of 10 randomly chosen patients, prior to chemotherapeutic treatment, were selected from the Palmerston North Hospital tissue bank, and analysed for the expression of Rad51 and DNA-PKcs, and potential consequences such as patient survival.

6.9.1 Staining of MDA MB 231 Cells

The purpose of this experiment was to ensure that the antibodies against Rad51 and DNA-PKcs could be used for immunohistological staining of cells, and to ensure the protein specificity of the antibodies. MDA MB 231 cells were harvested, either untreated (0 h), or 2 h and 24 h after exposure to 3 μM doxorubicin, and fixed in 10 % formalin. The samples were then transferred to Dr Bruce Lockett at the Palmerston North Hospital, where the cells were prepared as cell blocks for immunohistochemical analysis (section 2.2.7). The cells were probed with DNA-PKcs and Rad51 antibody and analysed by light microscopy (Fig. 6.13).

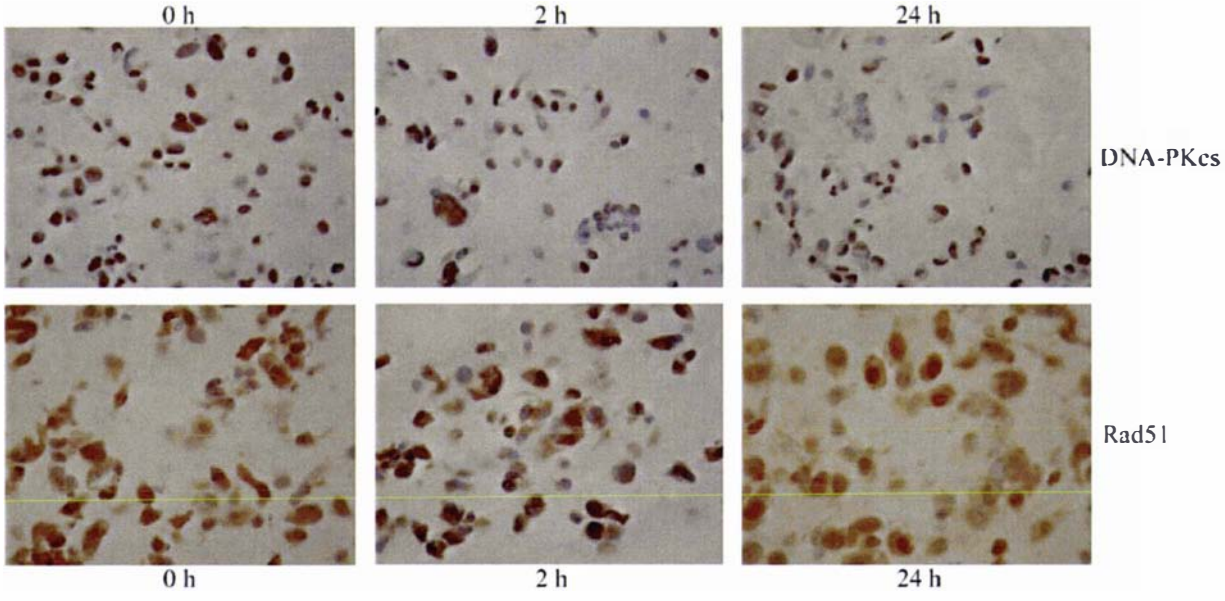

Fig. 6.13: Immunohistochemical analysis of Rad51 and DNA-PKcs expression in MDA MB 231 cell blocks

Blocks of MDA MB 231 cells which were harvested 0, 2, and 24 h after drug treatment, were probed with Rad51 and DNA-PKcs primary antibodies and are shown above at 400x magnification. While DNA-PKcs (top row) was primarily detected within the nucleus, Rad51 (bottom row) produced strong cytoplasmic signals exceeding the intensity of nuclear staining.

To assess the overall intensity of staining, which was determined manually, a scoring system was implemented which ranged from 0 (no staining) to 3 (strongest staining) (McCarty *et al.*, 1985). Nuclear and cytoplasmic staining were scored separately to detect any drug-induced translocation effect of Rad51 or DNA-PKcs (Table 6.1), and results summarised (Table 6.2)

MDA MB 231, 0 h

	DNA-PKcs						Rad51				
Staining Intensity (Nuclear)	0	1	2	3	total		0	1	2	3	total
	27	38	25	10	H-score		53	39	8	0	H-score
	0	38	50	30	**118**		0	39	16	0	**55**
Staining Intensity (Cytoplasmic)	0	1	2	3	total		0	1	2	3	total
	86	12	1	0	H-score		9	63	19	9	H-score
	0	12	2	0	**14**		0	63	38	27	**128**

MDA MB 231, 2 h

	DNA-PKcs						Rad51				
Staining Intensity (Nuclear)	0	1	2	3	total		0	1	2	3	total
	9	29	42	20	H-score		30	44	17	9	H-score
	0	29	84	60	**173**		0	44	34	27	**105**
Staining Intensity (Cytoplasmic)	0	1	2	3	total		0	1	2	3	total
	75	24	2	0	H-score		7	23	63	7	H-score
	0	24	4	0	**28**		0	23	126	21	**170**

MDA MB 231, 24 h

	DNA-PKcs						Rad51				
Staining Intensity (Nuclear)	0	1	2	3	total		0	1	2	3	total
	18	30	41	11	H-score		46	40	10	4	H-score
	0	30	82	33	**145**		0	40	20	12	**72**
Staining Intensity (Cytoplasmic)	0	1	2	3	total		0	1	2	3	total
	97	3	0	0	H-score		10	70	20	0	H-score
	0	3	0	0	**3**		0	70	40	0	**110**

Table 6.1: Nuclear and cytoplasmic staining of DNA-PKcs and Rad51 in MDA MB 231 cells
To assess the intensity of histological staining (H-score), 100 cells from each sample (0, 2, 24 h) were categorised according to the observed staining intensity (0 to 3). The number of cells in each category was then multiplied by the intensity value (0 to 3) of that category, and the sum of all four categories resulted in the final H-score. For example: DNA-PKcs 0 h featured 10 cells that showed the maximum staining intensity and therefore fell into category number 3. This resulted in a sum of 30 (3 x 10). The total H-score of all categories for DNA-PKcs was 118. DNA-PKcs and Rad51 primary antibodies were used at concentrations of 1:1200 and 1:90, respectively.

	H-score	0 h	2 h	24 h
DNA-PKcs	Nuclear	118	173	145
	Cytoplasmic H Score	14	28	3
Rad51	Nuclear	55	105	72
	Cytoplasmic H Score	128	170	110

Table 6.2: Summary of H-scores of MDA MB 231 cells

The staining intensity for DNA-PKcs and Rad51 was at its strongest 2 h after drug exposure. While DNA-PKcs showed almost exclusive nuclear staining, Rad51 was predominantly present in the cytoplasm. Interestingly, 24 h after doxorubicin exposure nuclear Rad51 staining increased while cytoplasmic staining decreased compared to the control. Hence, Rad51 possibly shows a protein translocation effect after drug treatment.

Both DNA-PKcs and Rad51 antibodies successfully stained MDA MD 231 cells, which confirmed their suitability for the subsequent analysis of tumour tissue.

6.9.2 Tumour Sample Analysis

As a first step, control samples containing different types of tissue were used to assess the ability of the DNA-PKcs and Rad51 antibodies to differentially stain tumour and normal tissue, and to determine the appropriate dilution of the antibodies for histological analysis (Fig. 6.14).

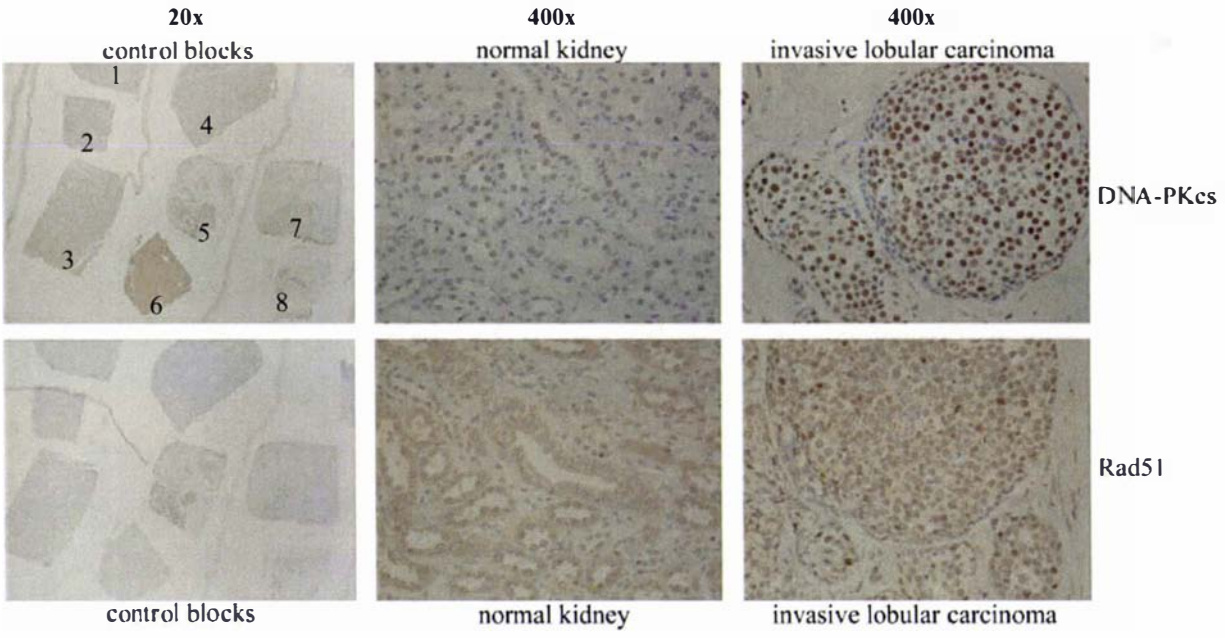

Fig. 6.14: Control blocks used for testing DNA-PKcs and Rad51 primary antibodies

Control blocks containing different tissues, such as metastatic invasive ductal carcinoma (1), invasive ductal carcinoma (2), normal kidney (3), metastatic invasive lobular carcinoma (4), invasive lobular carcinoma (5), normal liver (6), invasive ductal carcinoma (grade 1) (7), and fibroadenoma (8) were tested for the expression of Rad51 (bottom row) and DNA-PKcs (top row). DNA-PKcs showed strong nuclear staining in several cases, including normal kidney and invasive lobular carcinoma tissue. Rad51 produced weaker signals in most control tissues compared to DNA-PKcs signals, but showed strong cytoplasmic staining in kidney tissue, as well as strong nuclear and cytoplasmic staining in breast tumour.

After successfully staining control tissues and establishing an immunostaining protocol using a primary antibody concentration of 1:2000 for DNA-PKcs and 1:100 for Rad51, respectively, 10 breast tumour samples from the Palmerston North Hospital tissue bank were randomly selected and analysed for differentially expressed DNA-PKcs and Rad51 protein levels (Fig. 6.15, 6.16, and 6.17). The immunohistochemical results of the 10 tested specimens were summarised and analysed for any obvious patterns, for example DNA-PKcs or Rad51 expression and time of survival (Table 6.3).

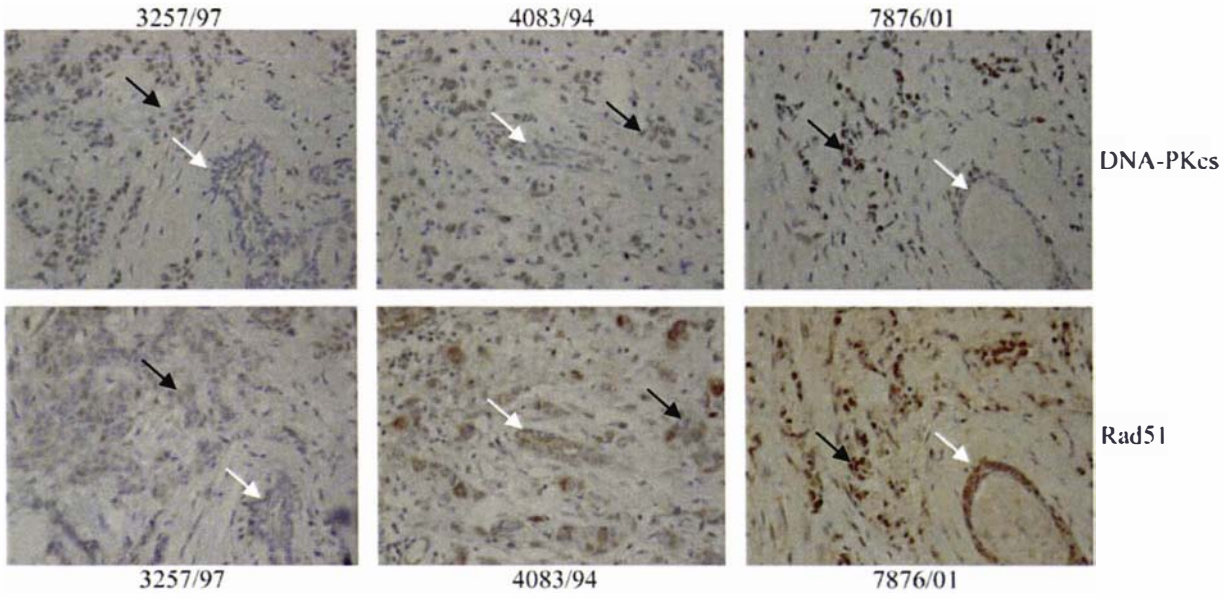

Fig. 6.15: Patient tissue samples probed against DNA-PKcs and Rad51 protein

Normal (white arrows) and cancerous (black arrows) breast tissues from three different patients, 3257/97, 4083/94, and 7876/01 were analysed for expression of DNA-PKcs (top row) and Rad51 (bottom row) and are shown at 400x magnification. There were no striking differences in the expression of either protein in samples from patient 3257/97. In the case of patient 4083/94, no apparent differences in DNA-PKcs expression were distinguishable between normal and tumour tissue. Rad51 however, was in fact more strongly expressed in normal epithelial cells than in tumour cells. Patient 7876/01 featured intense staining for both proteins. However, only the levels of Rad51 were dramatically higher in tumour tissue compared to the normal tissue, with both nuclear and cytoplasmic staining being observed.

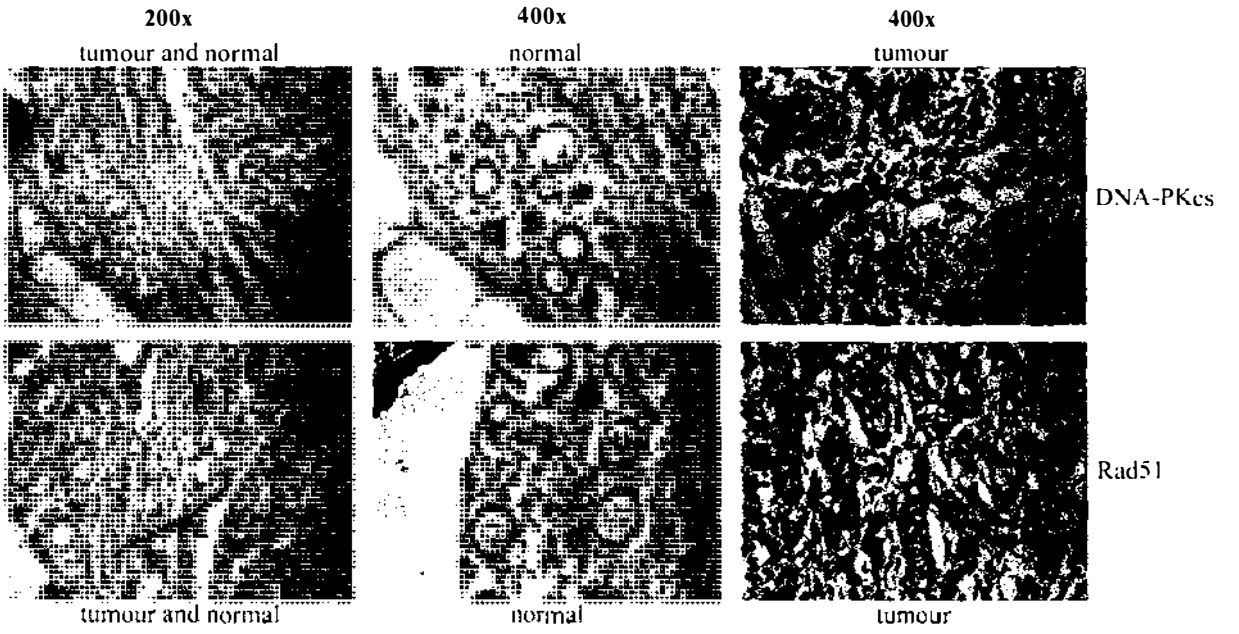

Fig. 6.16: Immunohistochemical staining of normal and tumour tissue

DNA-PKcs (top row) and Rad51 (bottom row) expression were analysed for patient 18800/00. Sections of both normal and tumour tissue were magnified from the whole sample to illustrate differences between the two tissues. In the case of patient 18800/00, DNA-PKcs levels in the tumour tissues were drastically higher than those in normal tissue, while Rad51 levels remained unaltered.

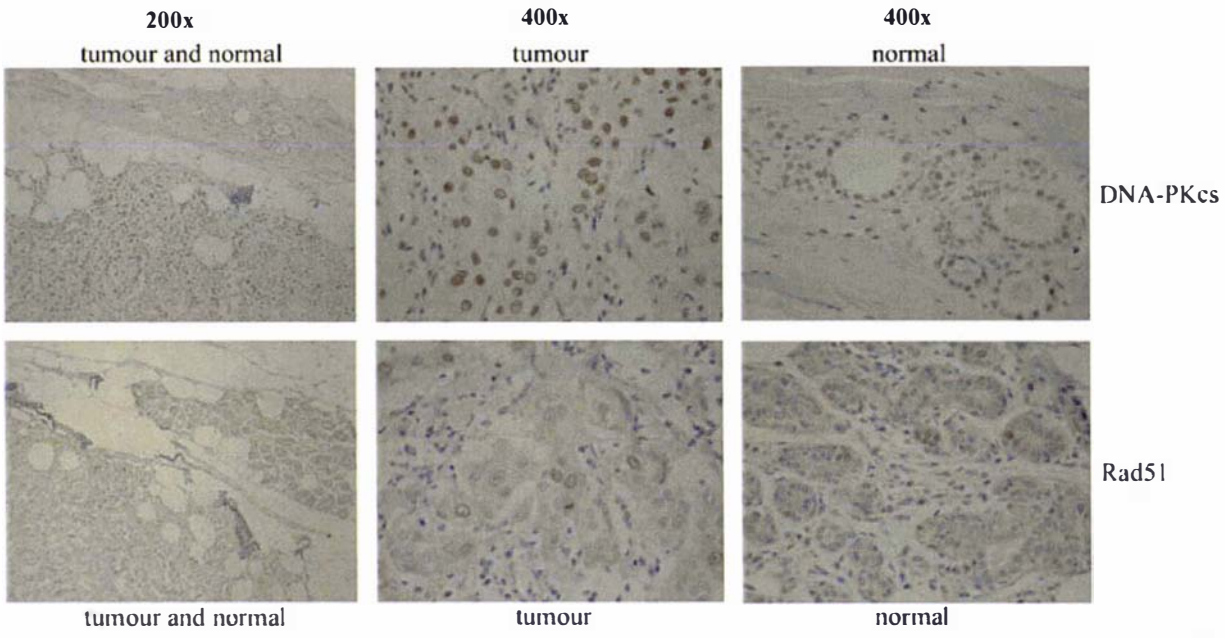

Fig. 6.17: Rad51 and DNA-PKcs expression in specimen 17641/00G

Specimen 17641/00G is shown at 200x magnification, while the tumour and normal epithelial tissue is shown at 400x magnification. The immunohistochemical staining of sample 17641/00G revealed drastically increased levels of DNA-PKcs (top row) in tumour tissue compared to normal epithelium. Rad51 levels (bottom row) were found to be higher in normal epithelial cells than in tumour tissue. The immunological analysis of Rad51 also exhibited higher background levels, unlike DNA-PKcs detection which was virtually free of background noise.

Case#	Tumour DNA-PKcs H-Score	Adj. Normal Epithelium DNA-PKcs H H-Score	Tumour RAD-51 H H-Score	Adj. Normal Epithelium RAD-51 H H-Score	Age at diagnosis	ER/PR status	Therapy	Health
4083/94	= 139	158	↓19	37	42	positive	tamoxifen	alive
18800/00	↑ 170	80	= 47	47	45	negative	chemo	alive
3257/97	= 62	81	= 50	57	43	positive		relapsed/dead
6081/98	↑ 192	122	↑ 151	89	86	positive	tamoxifen	dead
17641/00 B	↑ 191	128	↓ 13	33	59	negative	chemo	alive
17641/00 G	↑ 220	99	= 21	22	59	negative	chemo	alive
22089/01	= 154	140	↑ 170	57	44	positive	chemo	alive
7876/01	↑ 154	123	↑ 198	41	57	positive	chemo	alive
9778/99	= 70	68	= 29	35	53	positive		relapsed/alive
1996/96	↑ 124	91	= 19	24	84	positive	tamoxifen	relapsed/alive

Table 6.3: Summary of immunohistological staining of Rad51 and DNA-PKcs of 10 different tissue specimens

In addition to recording the staining intensities for DNA-PKcs and Rad51 in the individual specimens, statistically relevant information such as age, estrogen (ER) and progesterone receptor (PR) status, type of therapy, and status of health, was also collected in order to identify any potential patterns. Unfortunately, in some cases not all information was available. Interestingly, DNA-PKcs levels in tumours were either up-regulated (↑) or close to the levels of the adjacent normal epithelial tissue (=), but never clearly down-regulated (↓). Rad51 levels on the other hand, were found to be clearly up- or down-regulated in tumour samples.

The results revealed that both DNA-PKcs and Rad51 were differentially regulated in some breast tumours, while in others levels similar to those of normal tissue were observed. The results also showed different levels of these repair proteins when individual tissue samples were compared. There was neither a correlation between differentially regulated protein levels of DNA-PKcs and Rad51, nor of protein expression and patient survival.

6.10 Discussion

Proteins involved in DNA repair pathways have been widely proposed as targets for selectively sensitising tumour cells to radio- and chemotherapy. A better understanding of the response to chemotherapeutic agents of two key proteins in NHEJ and HR, DNA-PKcs and Rad51, respectively, would help determine the feasibility of this approach. Rad51 in particular is overexpressed in many tumours compared to normal tissue, leading to increased levels of resistance (Maacke *et al.*, 2000; Henning and Sturzbecher, 2003). Hence, it has been professed as one of the most suitable targets. There have been conflicting reports however, as to whether or not Rad51 is radiation- or drug-inducible (Bishop *et al.*, 1998; Russell *et al.*, 2003). The results presented here show that Rad51 levels are altered upon doxorubicin treatment in cancerous and normal cells and that this response is cell cycle-independent as well as cell line specific. MDA MB 231 and MCF12A cells showed increased Rad51 levels upon drug exposure 24 h and 48 h after treatment. It seems plausible that to repair the DSB lesions Rad51 expression is likely to be increased, especially if NHEJ is saturated. The availability of DNA-PK is likely to be a limiting factor for NHEJ, as this is not increased upon drug-induced DSB (Boldogh *et al.*, 2003). Although DNA-PKcs analysis showed some inconsistencies, no significant alterations due to drug exposure were found, which is in accordance with these observations.

Down-regulation of Rad51 however, as seen in MCF7 is not easily explained. One of the most striking differences between MCF7 and MDA MB 231 cells is that the latter express a mutant p53, a mutant TGF-ß and are ER negative. In particular, p53 (Sturzbecher *et al.*, 1996; Marmorstein *et al.*, 1998; Kanamoto *et al.*, 2002; Linke *et al.*, 2003) and TGF-ß (Kanamoto *et al.*, 2002) act as regulators of Rad51-mediated DNA repair. BRCA2 (Marmorstein *et al.*, 1998) and c-Abl (Kharbanda *et al.*, 1998; Yuan *et al.*, 1998) are also known to interact with Rad51, but the exact mechanisms of Rad51 regulation are not yet fully understood. An imbalance and/or dysfunction of p53 and TGF-ß could influence Rad51 expression, as a response to increased need for DNA repair. On the other hand MCF12A cells express normal

p53 and TGF- ß, but respond to doxorubicin treatment in a similar manner to that observed in MDA MB 231 cells, suggesting an alternative mechanism is likely to be associated with increased Rad51 protein expression in response to chemotherapeutic treatment.

Indeed, the down-regulation of Rad51 in MCF7 cells implies that HR may not play a critical role in repair of doxorubicin-induced DNA damage. One consequence of this down-regulation would be a decrease in the ability of the cell to perform chromosomal recombination. Overexpression of Rad51 is seen in immortalized human cell lines (Xia *et al.*, 1997) and in tumour cells (Maacke *et al.*, 2000), and has been shown to have a dominant negative effect on cell survival (Flygare *et al.*, 2001; Kim *et al.*, 2001). Indeed, MCF7 cells overexpress Rad51 (Raderschall *et al.*, 1999), but according to the current data MCF12A showed an even greater elevation of expression, and MDA MB 231 displayed the highest level of expression out of the cell lines tested. A further increase, as a response to DSB, could possibly be more harmful leading to hyperrecombination and/or increased apoptosis. In this respect the down-regulation of Rad51 may enhance doxorubicin tolerance, concomitantly distributing DNA repair duties to other Rad51-independent pathways. In fact, MCF7 cells are the most doxorubicin tolerant cell line tested in this study. This suggests that Rad51-mediated HR may not play an important role in contributing to increased resistance towards doxorubicin. Moreover, NHEJ has been suggested to be the predominant repair pathway for topo II poison-induced DNA lesions (Adachi *et al.*, 2003). Further studies in chicken cells (DT 40) have indicated the contribution of HRR to the removal of IR-induced DNA DSBs to be marginal. This group also suggests a model in which HRR may not be involved in the repair of DSBs until after the breaks have been sealed (Wang *et al.*, 2001).

The results presented here illustrate that Rad51 expression is cell line-dependent which is in agreement with a study by Russell and co-workers who found Rad51 expression inducible in glioma tumour cells, but not in normal fibroblasts (Russell *et al.*, 2003). Furthermore, the results of this study have also shown that topo II alpha is up-regulated in a cell cycle-independent manner 24 h after exposure to low to moderate drug concentrations in all cell lines used. It is possible that topo II alpha levels are elevated to compensate for drug bound topo II alpha protein or due to an increased need for topological rearrangement and maintenance triggered by DNA DSB repair. Hence Rad51, as well as topo II alpha appeared to be doxorubicin "inducible" in MDA MB 231 and MCF12A cell lines resulting in higher protein levels when using low to moderate concentrations of drug.

In other studies, low levels of topo II alpha have been associated with doxorubicin resistance in drug resistant cell lines (Tanoguchi *et al.*, 1998). Differential regulation of topo II alpha levels observed in the current study however, represents an initial response to doxorubicin treatment of drug sensitive cells. In addition, low levels of topo II alpha were observed after treatment with a high dose (15 μM) of doxorubicin. This effect was more likely to be caused by mechanisms which do not contribute to drug resistance. The use of high drug concentrations resulted in fewer viable cells and a higher number of cells with an abnormal morphology compared to cells which had received lower drug concentrations (data not shown). One possible explanation could be that higher amounts of drug may result in more cells undergoing necrosis or apoptosis more quickly, which may impair protein synthesis as well as decrease levels of certain proteins, such as Rad51 and topo II alpha, due to proteolysis.

It has previously been suggested that protein levels of DNA-PK, including DNA-PKcs could possibly be altered as a consequence of pathological changes (Moll *et al.*, 1999). Rad51 has been reported to be differentially regulated in tumour cells including breast tissue (Moll *et al.*, 1999; Maacke *et al.*, 2000). The research described here has also shown Rad51 to be differentially regulated in human breast cancer cell lines in response to doxorubicin exposure. To determine the feasibility of an in depth investigation into the relationship of changing levels of the DNA repair proteins DNA-PKcs and Rad51 in response to chemotherapy, immunohistochemical analysis of 10 randomly selected breast tumour samples was performed as a pilot study.

Initially, MDA MB 231 cells were immunostained using DNA-PKcs and Rad51 primary antibodies to evaluate the ability of these antibodies to detect protein in human tissues. Immunohistochemistry results showed an overall increase, as well as specific increase in nuclear staining of DNA-PKcs and Rad51 after doxorubicin treatment. It is important to bear in mind that this experiment was carried out only once and was performed simply to assess the feasibility of the antibodies for use in immunohistochemical staining of whole cells, and not for correlating with results from western blots. Hence, the results underscored the usefulness of these primary antibodies, as differential regulation of DNA-PKcs and Rad51 was detected in response to doxorubicin treatment.

Although the statistical relevance of analysing a small number of samples was limited, it provided convincing evidence that not only were DNA-PKcs and Rad51 levels altered in some tumour cases compared to adjacent normal epithelial, but that the antibodies used in this study could be successfully used for further, large-scale, immunohistochemical analysis of tumour tissues with statistical relevance.

This was the first time that DNA-PKcs and Rad51 levels have been examined concomitantly. In contrast to previously published data (Moll *et al.*, 1999), the results obtained in this research show DNA-PKcs protein levels to be significantly altered between tumour and normal breast tissue in some patients. The results also suggest that protein expression levels of Rad51 can be either up- or down-regulated in tumour tissue compared to normal tissue, which is in agreement with previous reports (Maacke *et al.*, 2000; Yoshikawa *et al.*, 2000). There was no apparent correlation in the expression of these two DNA repair proteins.

While increased activity of DNA-PKcs has been reported in many tumours and tumour cell lines, and seems to be indicative of chemo-resistance and patient prognosis, the impact of elevated protein levels remains unclear. Increased DNA-PKcs activity has been associated with an increase in radiation and drug resistance (Boldogh *et al.*, 2003; Shintani *et al.*, 2003). DNA-PKcs protein levels prior to treatment however, did not show any correlation with cellular resistance. It was only after radiation therapy that surviving cells displayed increased DNA-PKcs levels (Shintani *et al.*, 2003).

In other studies, increased levels of DNA-PKcs were reported to be associated with metastatic state and chemo-resistance (Um *et al.*, 2004). Increased protein levels and increased protein activity were also shown to be much higher in some drug resistant cell lines than in their parental counterparts. The drug resistant cells however, were very susceptible to wortmannin, a DNA-PK inhibitor, resulting in increased drug sensitivity while the parental cells remained unaffected (Kim *et al.*, 2000).

Overexpression of Rad51, which protects against DNA damaged-induced apoptosis (Raderschall *et al.*, 2002), as well as resulting in enhanced IR and drug resistance of cultured tumour cell lines (Vispe *et al.*, 1998; Yanagisawa *et al.*, 1998; Yanez and Porter, 1999; Hansen *et al.*, 2003; Hansen *et al.*, 2003), has been reported for many tumour cell lines (Raderschall *et al.*, 2002). In a different report however, no correlation between Rad51 protein

levels and drug resistance in epithelial tumours could be found (Wang *et al.*, 2001). Moreover, Rad51 knock-down studies have shown reduced Rad51 protein levels to result in significantly increased drug and IR sensitivity (Taki *et al.*, 1996; Ohnishi *et al.*, 1998; Collis *et al.*, 2001; Raderschall *et al.*, 2002). Increasing Rad51 protein levels have also been reported after drug treatment (Christodoulopoulos *et al.*, 1999).

Overall, the consequences of elevated DNA-PKcs and Rad51 protein levels are not very well defined and there have been contradictory reports in the literature. It is also not clear if indeed an increase in protein levels necessarily results in increased function, for example an increase in Rad51 expression should result in enhanced DNA repair capabilities, but there may be other factors involved contributing to cellular resistance or DNA repair.

Given the current data, an investigation into the alteration of the levels of DNA repair proteins prior to chemotherapy and post-treatment could be helpful in generating new information on treatment efficacy and patient prognosis. In general, biopsies are performed on patients prior to any treatment, as was the case in this study. Specimens are obtained after initial therapy only in patients that have suffered a relapse of disease. These cases are notoriously more difficult to treat and suffer a high mortality rate. It would be of particular interest to investigate whether increased levels of DNA-PKcs and/or Rad51 do indeed result in increased DNA-damage repair, and therefore render tumours overexpressing these proteins drug resistant. If this was the case both proteins could be used as prognostic markers. It would also be of interest to investigate any alterations in DNA-PKcs and/or Rad51 protein levels in relapsed patients as a result of therapy. Hence, investigating any correlation of the aberrant expression of DNA repair proteins in these tumours to time of survival could provide valuable information, as this may have implications for further treatment options.

Clearly, more information is needed to unravel the complex regulatory mechanisms involved in Rad51 expression and the precise role it plays in response to chemotherapeutic treatment. However, the results produced by this study have useful implications for tumour therapy, since both topo II alpha and Rad51 were inducible at certain doxorubicin concentrations in particular cell lines. It is therefore possible that combination of treatments including a Rad51 inhibitor may be more potent in killing susceptible tumour cells than current procedures. Nevertheless, these results also highlight the fact that sensitising tumour cells by targeting Rad51 as a key component of the HR repair pathway may not be universally applicable and

that IR and/or drug response need to be determined first if such an approach is to be successful.

Chapter Seven
Summary and Discussion

7.1 Project Aims

The aim of this project was to detect proteins which were differentially regulated, in normal and tumour cell lines, in response to doxorubicin exposure, as this could elucidate mechanisms involved in the development of cellular drug resistance. This goal was pursued by investigating the temporal response of global changes in protein expression after drug treatment, as well as targeting specific proteins potentially involved in damage management. Surface-enhanced laser desorption ionisation mass spectrometry (SELDI-MS) and two dimensional gel electrophoresis (2DGE) were utilized for global protein expression analysis, in an attempt to discover candidate proteins exhibiting significant changes in protein levels in response to doxorubicin treatment. In addition, the expression levels of Rad51 and the DNA-dependent protein kinase catalytic subunit (DNA-PKcs) were specifically monitored, using western blots, as these proteins are key factors in two independent pathways concerned with the repair of doxorubicin-mediated DNA damage. An increased capacity for DNA damage repair may be associated with increased Rad51 and DNA-PKcs protein levels, leading to cellular drug resistance. Therefore a number of breast tumour specimens were analysed by employing immunohistochemistry for deregulated levels of these repair proteins.

7.2 Project Results

SELDI-MS was used successfully to detect seven potential candidate proteins differentially regulated in cells after doxorubicin treatment. Unfortunately, SELDI-MS had to be discontinued as it was offered for promotional purposes only, and hence further candidates could not be determined and results could not be confirmed. Nevertheless, the mass of one candidate matched that of Caveolin-2, a protein which has previously been shown to exhibit altered expression in response to doxorubicin treatment.

2DGE was employed to confirm SELDI-MS results and to detect additional candidate proteins. Initially, changes were made to the standard 2D protocol, leading to improved sensitivity and robustness and resulting in high quality 2D protein expression patterns. In order to increase the number of proteins that could be analysed, samples were prefractionated using RP-HPLC. This protocol did not deliver reproducible results however, and therefore was discontinued. In an alternative approach, protein patterns were successfully simplified

and protein resolution improved by replacing broad pH range focusing strips with narrow range strips. Manual comparison of 2D gels however, could not reproducibly detect proteins genuinely differentially regulated after drug treatment. In order to obtain greater data objectivity, Phoretix 2D Evolution, a 2D gel software analysis program, was used to analyse protein expression and spot patterns on the 2D gels. This analysis confirmed the observations made during manual 2D gel analysis.

Immunoblotting results of the two DNA double-strand break repair proteins, Rad51 and DNA-PKcs, showed Rad51 to be differentially regulated in human breast and breast cancer cells in response to doxorubicin exposure, while DNA-PKcs levels remained largely unchanged. Results also showed that Rad51 appears to be regulated in a cell line-dependent-, and dosage-dependent manner. Topo II alpha, the target of doxorubicin, was up-regulated in all cell lines, in a dosage-dependent manner. Results obtained using fluorescence activated cell sorting (FACS) demonstrated that these changes were not due to cell cycle arrest-induced alterations in cell cycle distribution in cells, but a genuine response to doxorubicin exposure. Furthermore, in a pilot study using tissue specimens from the Palmerston North tissue bank, Rad51 and DNA-PKcs were found to be independently overexpressed in some breast tumours. These results suggest that DNA-PKcs and Rad51 may be potential candidates for targeted chemotherapy, but that the feasibility for combinational chemotherapy with doxorubicin would depend on the type of tumour to be treated.

7.3 Surface Enhanced Laser Desorption Ionisation Mass Spectrometry (SELDI-MS)

SELDI-MS was used for detecting differentially regulated proteins in normal breast and breast cancer cell lines after doxorubicin treatment, and to assess the likelihood of detecting such candidates using 2DGE. SELDI-MS is a technology which combines protein fractionation using chromatographic surfaces, with mass spectrometric analysis. This approach allows the analysis of whole proteins, rather than peptides, which can be an advantage when investigating possible changes, such as post-translational modifications. Although SELDI-MS technology has been proposed for the analysis of proteins of up to 500 kDa in size, the results of this project indicate that this technology is likely to be optimal for analysing proteins of up to approximately 30-40 kDa. The sensitivity for larger proteins is significantly reduced as these are much harder to ionize and to introduce into the gas phase, making detection very difficult (McCracken, Ciphergen, personal communication). Because sample preparation and analysis are fairly straight forward procedures compared to other

techniques, SELDI-MS is very fast and allows numerous repeats. This is aided by the requirement for only small sample volumes, making this technology ideal for analysing proteins of moderate size.

SELDI-MS was successfully utilized to discover seven differentially regulated proteins in response to doxorubicin treatment. The molecular weight of one of these proteins (16.828 kDa), corresponded to Caveolin-2, a protein which may play a role in tumour progression (Sagara *et al.*, 2004). It is likely that more candidate proteins would have been detected using this procedure had it been freely available, given the similar responses of two proteins (16.828 kDa and 20.223 kDa) in MDA MB 231 and MCF12A cells. The method would have been limited however, since proteins of up to only 30-40 kDa can be detected with high sensitivity. The data obtained using SELDI-MS illustrated the usefulness of this technology for the current project. It also illustrated that doxorubicin treatment did result in alterations of protein profiles in the cell lines tested and that similar changes might be detectable using 2DGE.

7.4 Two Dimensional Gel Electrophoresis (2DGE)

2DGE was used to find additional candidates, as well as to confirm the SELDI-MS results, and had the added advantage of being relatively sensitive over a wide range of protein masses. The results obtained using 2DGE however, exhibited strong variations between different batches of cells used, and lacked sensitivity overall. These findings were confirmed utilizing 2D Phoretix Evolution software for gel analysis.

The major obstacles encountered in this study using a standard 2DGE protocol were insufficient scope and unreliable loading references. When analysing whole cell extracts, the total number of proteins which can be separated on a 2D gel is usually limited to ~1500, when using silver staining. The vast majority of proteins detected however, are high abundance proteins which are usually of limited interest to the researcher (Gygi *et al.*, 2000). The scope and sensitivity of 2DGE is restricted by the loading capacity of the IPG strips used for IEF, which is claimed to be up to 2 mg of protein (Amersham Biosciences). The experience from this research project shows however, that protein loads of 400 μg result in loss of resolution due to excessive amounts of protein and possibly higher concentrations of substances interfering with silver staining (data not shown). Hence, loading of 2 mg of protein seems feasible only for samples of limited complexity, which is not typically the case when analysing crude cell extracts, as performed in this project.

7.5 Sample Prefractionation Strategies

7.5.1 Liquid Chromatography

In order to overcome the problem of low loading capacity, to increase the sensitivity of the 2D protocol used in this study, an approach employing RP-HPLC originally developed by Badock et al. (2001) was adopted. This protocol used a urea based sample buffer very similar to the one used in the current project. The protocol successfully improved the sensitivity of the standard protocol, but unfortunately sample loading and subsequent sample concentration were unreliable and therefore this approach was not implemented.

Alternatively, ion exchange high performance liquid chromatography (Butt *et al.*, 2001) could have been used for prefractionating protein samples in order to increase the sensitivity of detecting low abundance proteins. In theory, the most important advantage of both of these chromatographic techniques is their ability to separate significant amounts of protein using separation conditions which are readily adjustable, and which result in customized protein fractions. This approach has the potential to analyse a total of 2 mg (or more) of protein by separating suitable sample fractions on 2D gels. In this scenario, a roughly 10-20 fold increase in sensitivity would have been obtained in comparison to the original 2D procedure, which used a maximum of only 75-150 µg of whole cell extract and did not involve fractionation.

In retrospect, the use of ion exchange chromatography may have provided a more straight forward alternative for fractionating protein samples. Because proteins are eluted in salts or buffers, samples could easily have been precipitated to concentrate proteins after fractionation. This would have been a major advantage over post RP-HPLC concentrating procedures, as the organic solvent used to elute proteins off the column severely interfered with protein precipitation. One disadvantage of ion exchange chromatography is however, that fractions are not as easily customized and hence offers less flexibility than RP-HPLC procedures.

7.5.2 Multi Compartment Electrophoresis

During the course of this research, other prefractionation techniques have been developed that could have helped in providing increased sensitivity to the protocol used in this study, and hence the detection of less abundant proteins. The use of multi compartment electrophoresis (MCE) in particular has rapidly become very popular as a fractionation method for 2D gel based proteomic studies. Samples are fractionated by separating proteins according to their pI,

much like the initial IEF step of 2D electrophoresis. For this procedure several interconnected chambers are divided by pH specific membranes, allowing the focusing of a protein within a pH range matching its isoelectric point value (Fig. 7.1).

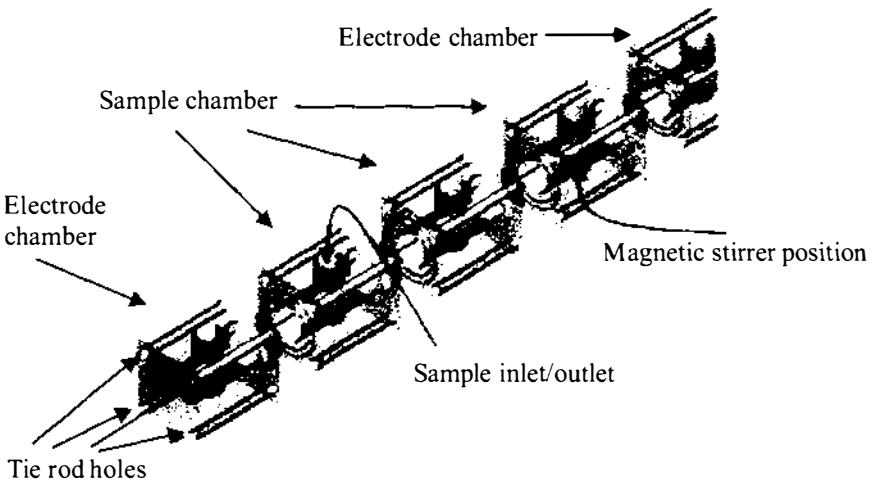

Fig. 7.1: Multi compartment electrophoresis

Several different chambers are assembled through rod holes, resulting in a tube like structure. Electrode chambers, an anode chamber at the low pH end, and a cathode chamber at the alkaline pH end, complete the assembly. Samples are loaded/removed through an inlet/outlet opening and sample circulation maintained using a magnetic stirrer. Protein samples are separated depending on the pH of immobilized membranes (not shown) placed between the chambers. (Taken from Hamdan and Righetti, 2003)

This technology also allows focusing of high abundance proteins, such as albumins, which can subsequently be eliminated from any further analysis (Simpson, 2003). A further increase in protein sensitivity is obtained by using narrow pH immobiline dry strips for IEF, which are usually available in the same pH range as the isoelectric membranes used for MCE. Since MCE technology typically allows the fractionation of proteins within less than 1 pH unit, for example between pH 4.6-5.4, the sensitivity of detection of low abundance proteins is increased tremendously. The major advantages of MCE are that the protein sample remains in the same buffer at all times, high abundance proteins can be eliminated, and higher loading capacity is achieved.

In this project, the use of MCE would have been ideal for sample prefractionation, as fractions can be directly separated using 2DGE without the need for protein concentration or buffer exchange. Furthermore, MCE would have offered a reasonable capacity for customizing

fractions by using different isoelectric membranes, and combining them with the appropriate immobiline IEF strips. In this study, pH 4-7 strips have been demonstrated to be superior to pH 3-10 strips with regard to protein resolution, when whole cell extracts were used (section 4.6). It is very likely that this improvement in protein resolution would have been even more dramatic, had samples been fractionated and separated using MCE in addition to narrow pH strips, such as pH 4.5 – 5.5. This would have substantially increased the sensitivity of the protocol and consequently the chances of finding any candidate proteins. The combination of these features would have allowed the analysis of a considerably larger amount of protein, hence increasing the overall sensitivity of the protocol and the chance of finding candidate proteins. Unfortunately, acquiring this technology would have cost approximately NZ$30,000 and hence was beyond the budget of this project.

7.6 Protein Visualisation and Staining Methods

This study utilized standard two dimensional gel electrophoresis procedures for detecting differentially expressed proteins. Equal amounts of protein from different samples were loaded onto 2D gels, silver stained, and subsequently analysed for differentially regulated proteins. Unlike (semi-) quantitative techniques, such as immunoblotting, 2DGE does not commonly use loading controls, and hence these were also omitted from this project. Feasible loading controls such as alpha tubulin however, may have helped to determine variability between different samples and hence improved data quality.

The variation in staining intensity between gels not silver stained concomitantly was another major difficulty encountered in this study. As a result spot intensities appeared to vary due to different degrees of staining rather than differences in protein concentration. Additionally, the narrow dynamic range of silver staining was also a drawback of this protocol. As a result, silver staining lacked the necessary robustness required for an optimal proteomic staining protocol. The absence of genuine loading controls for 2D gels and in proteomic studies in general, in addition to the susceptibility of silver staining to variations, made it very difficult to reliably detect differentially regulated proteins in this project.

In the meantime, modern staining techniques such as Sypro Ruby, Cy dye, and Deep purple have been developed which have the potential to circumvent the described short comings of silver staining procedures, as these staining methods are robust and sensitive because they are end point stains. In addition, they are also compatible with mass spectrometry (MS)

(Simpson, 2003). The emergence of fluorescent dyes, such as Sypro Ruby and Cy dyes has indeed revolutionized 2DGE. Cy dyes in particular, have now made it possible to reliably quantify differences in protein concentration between two different samples, and also to use a loading control. This technique was first introduced by Unlu et al. (1997), and has since been developed into a differential gel electrophoresis (DIGE) system which allows the simultaneous analysis of two different samples in addition to a control (a mixture of equal parts of the two samples which are to be analysed), all of which are labelled with different Cy dyes ($Cy^{TM}2$, $Cy^{TM}3$, or $Cy^{TM}5$). Because, each of the three dyes are detected at different wave lengths, and all samples are run on the same gel (unlike silver staining), it is possible to quantify any differences in protein expression between samples, thereby avoiding variations typical of samples run on separate gels. The control sample acts as an internal standard and assists in assessing the reproducibility of any observed differences, when different batches are analysed (Gharbi *et al.*, 2002; Friedman *et al.*, 2004; Liang *et al.*, 2005).

As the current project investigated changes in protein expression at various time points, DIGE would have been the gel electrophoretic method of choice, had it been available. This methodology would have significantly improved the reliability of comparative gel analysis, as the typical variabilities associated with silver staining would have been avoided. Furthermore, DIGE would have allowed the analysis of more samples in the same amount of time, resulting in higher throughput. The increased reproducibility of DIGE may well have resulted in the detection of candidate proteins, which could then have been analysed in more detail using a more targeted approach, such as immunoblotting. Acquiring both the dyes as well as the necessary software for gel analysis however, would have cost approximately NZ$100,000 and hence was beyond the budget of this project.

7.7 Statistical Analysis

Technical and biological variations cause alterations in protein levels which are commonly encountered during sample analysis. In order to discriminate genuine changes in protein levels from general variability, statistical analysis of data can be performed. To this end the Student t-test is the most commonly employed method for determining statistical significance of differential protein expression in proteomic research and for western blots, as used in this project. Nevertheless, certain statistics software is proposed to be superior to t-tests, such as the significance analysis of microarrays method. There is however, no general agreement on statistical data processing of proteomic data derived from 2D. Furthermore, it is nowadays

standard to analyse gel images or mass spectrometry data using instrument specific data analysis software and depending on the type of analysis method/software used, results can vary significantly (Meunier *et al.*, 2005; Maurer *et al.*, 2005; Molloy *et al.*, 2003).

With regard to the 2DGE data produced in this project, conducting statistical analysis would have been ineffective. This is mainly due to dynamic limitations of silver staining and the encountered variation in overall staining intensity between different gels. To determine the statistical significance of altered protein expression using silver staining, protein levels of specific candidates are usually analysed using immunoblotting in an additional step (Chen *et al.*, 2002). Since the data from the 2D gels did not yield any candidates for further analysis by immunoblotting, statistical analysis was not carried out.

7.8 Alternative Methods for Proteome Analysis

Some of the main drawbacks of the 2DGE procedure, encountered in general as well as in this research, are its very time-consuming nature and lack of high throughput capacity. With this in mind, any additional steps incorporated into the standard 2DGE protocol striving to add sensitivity by using prefractionation and narrow pH range IEF strips, inevitably result in a dramatic increase in the work load. For example, if a whole cell extract, as used in this project, was separated into two pH range specific fractions prior to 2DGE using MCE, this would immediately double the number of gels required for sample analysis.

Techniques based on liquid chromatography (LC) principles, coupled with a mass spectrometer (MS) or tandem MS (MS/MS), could have helped in overcoming these 2DGE associated problems, as these strategies offer high-throughput, as well as sensitive and immediate protein or peptide analysis. Although there are many different forms of LC-MS/MS, the multidimensional protein identification technology (MudPIT) represents one of the most potent systems. Unfortunately, acquiring such technology was beyond the budget of this research.

7.8.1 Multidimensional Protein Identification Technology (MudPIT)

MudPIT procedures use reversed-phase and strong cation exchange resins packed into the same column, coupled to an electro spray ionisation (ESI) tandem mass spectrometer, which effectively allows a two dimensional separation of a complex protein mixture (Fig. 7.2). Unlike 2DGE however, proteins and peptides are separated according to hydrophobicity and

ionic interaction. Because the digested proteins are eluted off the two columns directly into the tandem MS/MS, a protein can successfully be identified by analysing only one of its peptides, making this a much more reliable identification procedure than peptide mass finger printing, which is used with matrix-assisted laser desorption ionisation mass spectrometry.

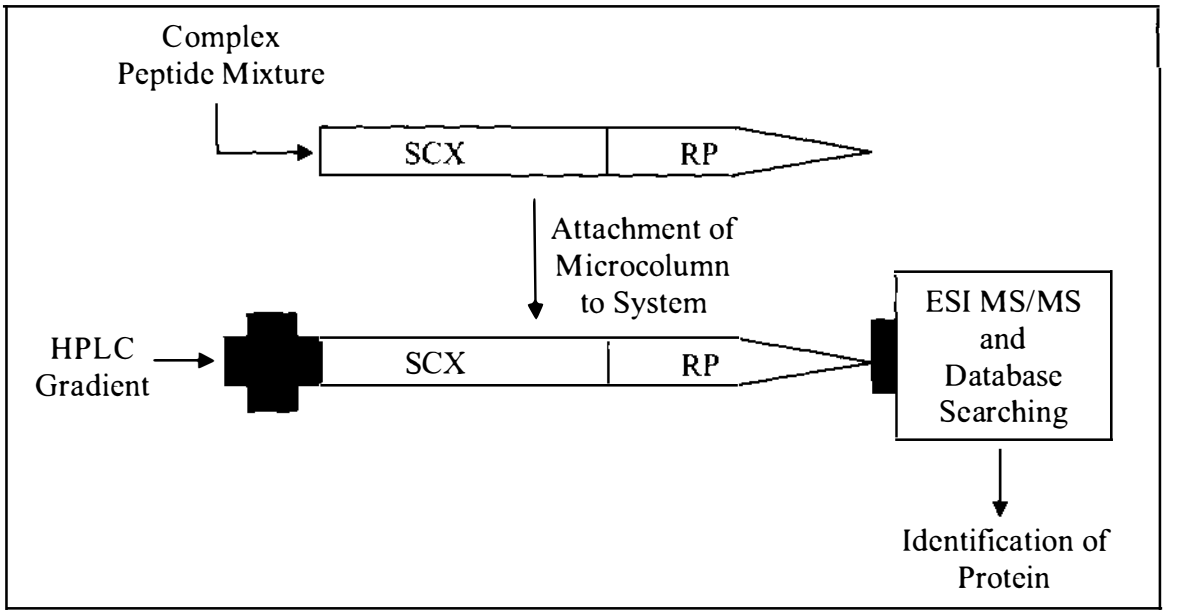

Fig. 7.2: Multi dimensional protein identification technology

A peptide mixture is loaded onto a strong cation exchange (SCX) and reversed-phase (RP) column and eluted using an HPLC gradient. The HPLC system is combined with an electro spray ionisation tandem mass spectrometer (ESI-MS/MS) allowing online peptide sequencing and identification. (Modified from Simpson, 2003)

This technology is superior to 2DGE in terms of high throughput and protein identification and therefore would have offered a more potent approach to this study. Much like 2DGE however, it does not use any loading controls, and as a result data reproducibility may be compromised. On the other hand, MudPIT would have offered the possibility of repeated analysis of samples to increase the confidence in data, which could have partially ameliorated this problem.

7.8.2 Isotope-Coded Affinity Tagging (ICAT)

One strategy which may have been able to overcome most problems associated with the use of 2DGE encountered in this research, such as the lack of suitable loading controls, high-throughput and sensitivity, is ICAT. In this method, different tags are used to label cysteine containing peptides of two different samples. The tagging of these peptides allows the

quantification of a protein in each sample and any discrepancies in expression between the two samples. The main advantage of this approach is the ability to use fractionated samples, which are analysed and identified at the same time. This means that certain proteins could be used as loading controls. Generally, the tags consist of three functional moieties: a cysteine reactive moiety, a linker with either eight hydrogens (light) or eight deuterium (heavy) atoms, and a biotin moiety (affinity tag). The tags only attach to cysteine residues, theoretically allowing them to bind approximately 92% of all human cysteine containing proteins (Miseta and Csutora, 2000). After tagging, protein samples are digested and affinity purified, thereby dramatically simplifying the complexity of the peptide mixture. After affinity purification, the peptides of two differently labelled samples are loaded onto a RP-HPLC column and eluted directly into an MS/MS for analysis (Fig. 7.3). Quantification is achieved by comparing intensities of the light and the heavy peptide peaks, which will be 8 mass/charge (m/z) units apart due to the difference in weight of hydrogen and deuterium (Fig. 7.4).

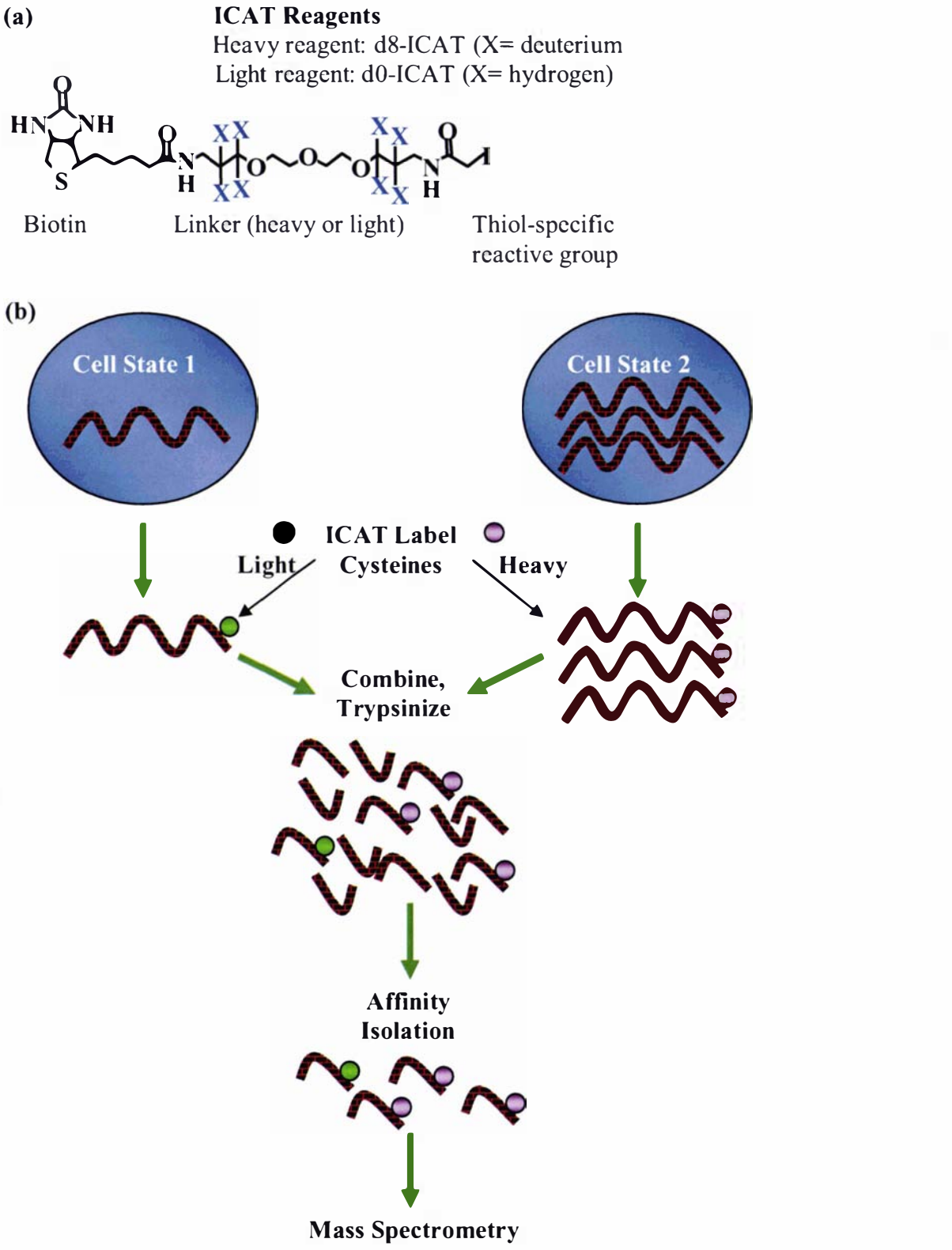

Fig. 7.3: Isotope-coded affinity tagging

This schematic depicts the principles of ICAT which was first introduced by (Gygi *et al.*, 1999). Hydrogen or deuterium are used to generate a light and a heavy form of the

linker molecule (a). Two samples labelled either with a light or heavy tag are prepared for quantitative MS analysis (b). (Modified from Simpson, 2003)

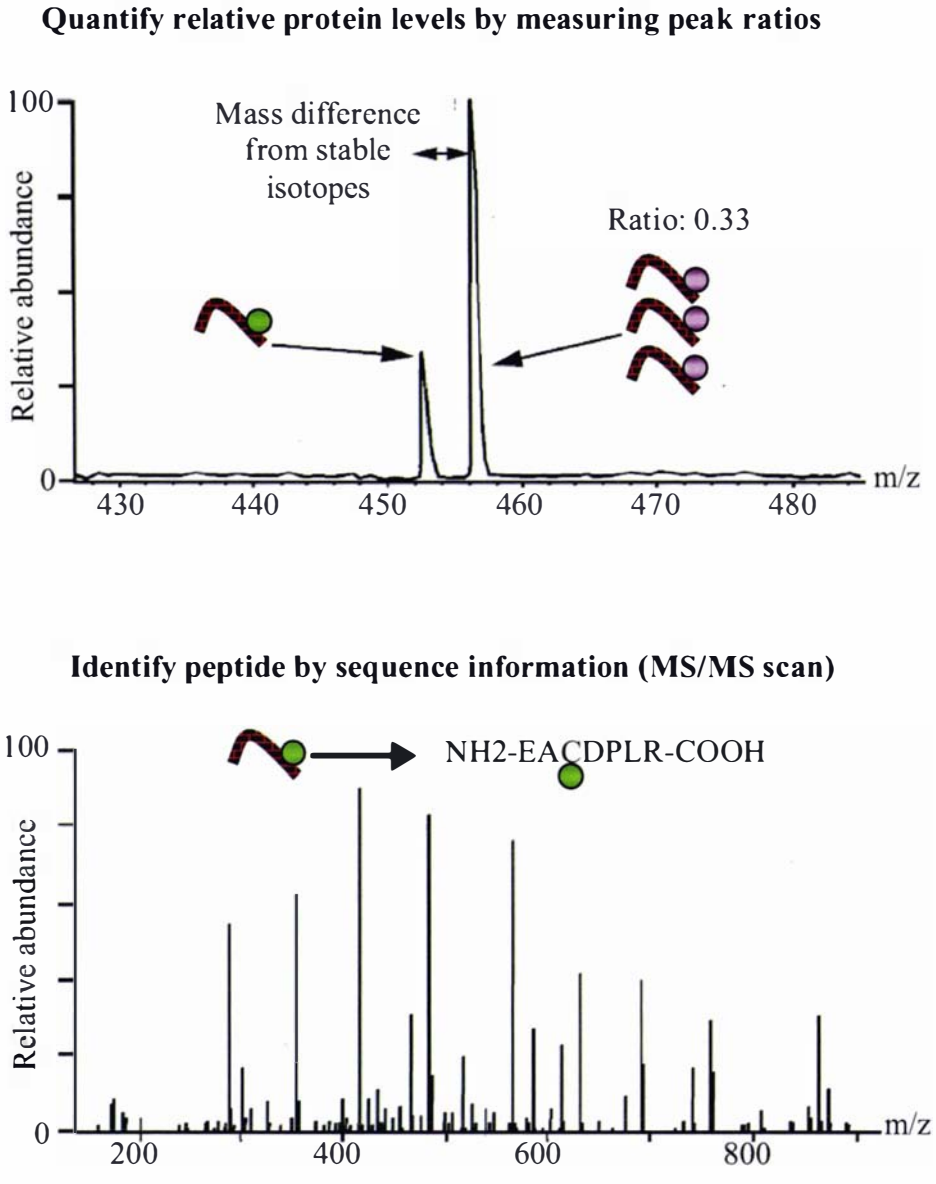

Fig. 7.4: Peptide quantification and identification using MS/MS

Identical peptides from two different samples are separated by 8 m/z units and quantified according to the individual peak height (A). Peptides are then identified by MS/MS (B). The peptide sequence deduced from MS/MS data indicates the cysteine residue labelled with a light tag (green dot). (Modified from Simpson, 2003)

ICAT would have been the non-electrophoretic method of choice for this research project, had it been available. It would have allowed the comparison and concomitant analysis of two samples, and therefore improved overall data quality. As proteins can be identified immediately after elution from a RP-HPLC column, this also allows the identification of

proteins which remain unchanged in all samples, and hence can be used as loading controls, as in the case of alpha tubulin. The possibility of using these loading controls would have allowed the detection of more subtle differences in protein expression than was possible with 2DGE. Because ICAT analysis is also much less time consuming than 2DGE, it would have been possible to repeatedly run samples in order to gain greater statistical confidence. Furthermore, ICAT protein identification offers superior sensitivity and robustness, as additional handling steps which are typical for post 2DGE identification procedures and often lead to peptide losses and decreasing sensitivity, are avoided.

7.9 The Future of "Old Fashioned" 2DGE and Proteomics

Ideally the investigation of changes occurring in cells in response to doxorubicin treatment would analyse and identify all proteins present. In reality however, no single method or technique exists which alone can achieve this goal. Consequently, all currently available methods suffer from inherent limitations associated with the instrumentation and/or methodology being utilized, and therefore can only render an incomplete picture of the events occurring after drug treatment.

Ultimately, the aim of any proteomic study is to achieve a level of sensitivity allowing the detection of low abundance proteins. These include proteins regulating expression and pathway activation which are likely to be part of the cellular stress response to doxorubicin treatment. Such proteins are often present at only 10 copies per cell, and consequently are below the detection limits of standard protocols, regardless of the analysis technique being employed. In such cases, large amounts of starting material have to be available and appropriately fractionated, to obtain a sample which may be investigated for such low abundance proteins. When growing adherent cells such as those used in this research, space requirements and high cost strongly limits the potential of possible scale-up procedures. Indeed, not all settings will be amenable for such a scale-up procedure and therefore may manifest a natural barrier for proteomic analysis at this time (Fig. 7.5).

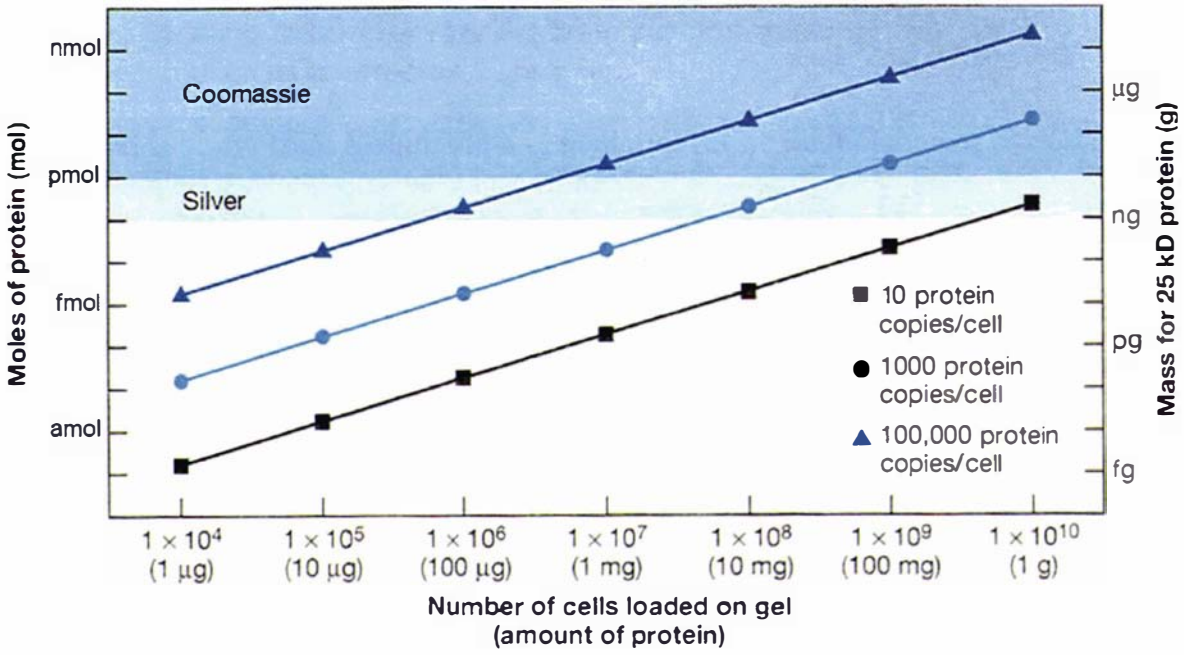

Fig. 7.5: Detection limits for a 25 kDa protein

The schematic shows the detection limit for a 25 kDa protein using silver and Coomassie blue staining, indicating the moles (mol) and mass (g) depending on the copy number and number of cells (or their estimated total weight). (Modified from Simpson, 2003)

Differences in protein expression due to environmental change or stress, as mentioned above, are likely to involve low abundance proteins, such as transcription factors. As evident from the results of this study, the traditional approach of using 2DGE however, is not sensitive enough to detect such proteins, and it is also not possible to quantify them. 2DGE is routinely used to separate proteins of 10–100 kDa in size, as larger proteins are unable to consistently enter the IPG gel strips. Silver staining procedures like the one employed in this study will only detect proteins of, for example 25 kDa, if they have a copy number of 10^5 per cell, when approximately 100 µg (75 µg/gel were loaded in this study) of protein extract is used (Fig. 7.5). Hence even a ten fold increase in sensitivity using appropriate fractionation procedures would still not be sensitive enough to detect proteins of relatively few copy numbers. As a matter of fact, to detect a low copy number (10 copies/cell) protein of 25 kDa using 2DGE and silver staining, 1 g of whole protein extract would be required (Fig. 7.5). Protein yields from tissue cultures in this study were roughly 0.1 mg/cm^2. Hence it would have been necessary to grow cultures covering an area of approximately 100 m^2 in order to obtain 1 g of total protein. Consequently, 2DGE is impractical for the analysis of low abundance proteins.

Due to the issues mentioned above, future studies endeavouring to elucidate drug treatment-induced changes in mammalian cells will be compelled to offer several features: a) high sensitivity, which will likely be a combination of sophisticated prefractionation strategies and sensitive protein detection in the femto to atto mol region; b) high throughput, since prefractionation will be inevitable and dramatically increase the number of fractions that are required to be analysed for one sample; c) automated data assessment (bioinformatics), because a huge amount of data will be generated.

Because 2DGE approaches fail to provide the degree of sensitivity, high throughput capacity, and online protein identification required, it is quite likely that future studies similar to this project will employ either liquid chromatography or liquid electrophoresis (for example free flow electrophoresis), or a combination of both separation techniques, coupled to MS/MS, allowing sensitive protein analysis and online identification.

7.10 Post-Translational Modifications

In the current study, post-translational changes, in particular changes in phosphorylation status, would be likely to occur in response to doxorubicin-induced DNA damage. It is well established that proteins involved in DNA damage signalling, including p53, ATR, ATM, and c-Abl, can be phosphorylated and/or phosphorylate other proteins (Khanna and Jackson, 2001; Lee and Paull, 2005). In theory, any post-translational modifications of a protein that result in a change of the isoelectric point value and/or molecular weight, such as phosphorylation, can be detected using 2DGE. If such a modification was unique to drug treated samples, a horizontal shift of the modified protein relative to the protein's position on the control gel would be expected, as a consequence of the change in isoelectric point value. Changes such as these were not observed using 2DGE in this project.

In general, 2DGE is not the preferred method to study post-translational changes of proteins, such as alterations in phosphorylation status, for several reasons. The labile nature of post-translational modifications and presence of phosphatases make it very difficult to maintain these protein alterations during sample preparation. Moreover, the dynamic range of protein phosphorylation is low, as a protein kinase phosphorylates only 5-10% of its target protein on average (Simpson, 2003). Hence it is almost impossible to detect such changes in less abundant proteins without sophisticated isolation and enrichment steps, such as immunoprecipitation or immobilized metal affinity chromatography. Therefore the study of

global changes in phosphorylation in a cell, also referred to as phosphoproteome, differs significantly from proteomic based approaches which simply monitor changes in expression patterns. Hence the use of 2DGE in phosphoproteomic studies is usually limited to the separation of proteins prior to immunoblotting procedures using phospho-specific antibodies.

7.11 Drug Treatment

There are two basic approaches for treating mammalian tissue culture cells in order to investigate cellular response to drug treatment as attempted in this study. One strategy is to maintain cells under continuous drug exposure. Usually the drug concentrations are initially quite low (sub μM), and are then increased if drug tolerant cells are selected to study potential resistance mechanisms (Batist *et al.*, 1986). Some researchers however, question the usefulness of such an experimental setup, as it does not reflect the clinical reality (Isaacs, personal communication).

A second strategy is to transiently expose cells to a relatively high concentration (~1-5 μM) of the drug only once or in intervals, which more accurately simulates the clinical situation. This approach has already successfully been implemented in previous studies, including research done in this laboratory studying drug-induced changes in protein expression (Allen *et al.*, 2004). Hence, a similar strategy was adopted for this project, monitoring short (2 h), mid (24 h), and long term (48 h) changes in protein expression after doxorubicin treatment. Unfortunately, genuine changes in global protein expression were not detectable due to the lack of sensitivity of 2DGE. The drug treatment protocol itself was sound however, as it allowed the successful monitoring of changes in protein expression when a more sensitive technique for protein analysis was employed, such as SELDI-MS and immunoblotting.

7.12 DNA Repair Proteins

Doxorubicin targets the DNA-bound topoisomerase II alpha enzyme which can lead to the breakage of both DNA strands when the DNA replication machinery collides with the drug bound DNA-protein complex. There are two main mechanisms present in mammalian cells which are involved in the repair of such DNA double-strand break (DSB) lesions. These are non-homologous end joining (NHEJ) in which DNA-PKcs is a key player, and homologous recombination repair (HRR), in which Rad51 plays a key role. Normal and cancerous breast cells were analysed for changes in the amounts of these DNA repair proteins and topo II alpha at various times after exposure, and also using different dosages. Furthermore, protein levels

of Rad51 and DNA-PKcs were also investigated in normal and malignant breast tissue from primary tumours.

Topo II alpha protein levels were found to be elevated in a time-dependent and doxorubicin dosage-dependent manner, while DNA-PKcs levels largely remained unaltered under all conditions in the cell lines tested. Rad51 was expressed in a cell specific and drug dosage-dependent manner with higher protein levels found in the drug sensitive cell lines. Moreover, both DNA-PKcs and Rad51 exhibited altered protein levels independent of each other, in some clinical specimens.

7.12.1 Rad51

Although Rad51 is known to play a key role in homologous recombination and repair, this is likely to be only one of its functions. Rad51 is also known to interact with other DNA damage repair signalling proteins, such as BRCA1, BRCA2, p53, and c-Abl, the latter controlling Rad51 phosphorylation (section 6.4). The consequences of these interactions however, remain to be elucidated. Moreover, to function as part of the DNA recombination machinery, Rad51 has to be transported into the nucleus, as it is also found in the cytoplasm. Hence, protein localization may have functional consequences, as well.

Naturally one would assume that higher levels of Rad51 protein would confer increased drug resistance due to enhanced DNA repair capacity. The results of this project however, suggest that certain levels of Rad51 may be more indicative of cell death than cell survival, consistent with observations made by others (Flygare *et al.*, 2001; Yoo and McKee, 2004). At this stage it is unclear what exactly the functional consequences of differentially regulated Rad51 levels are. Hence, the next step would be to determine whether drug-induced changes in Rad51 protein expression result in altered DNA repair capacity.

One way of assessing DNA repair is by using comet assays. In this scenario, broken and degraded DNA would result in a smear on a stained agarose gel. Initially one would expect to see an increase in smearing after drug treatment of the cells. As the levels of Rad51 increase however, the degree of smearing should be reduced if DNA repair takes place. If increased Rad51 levels are present in apoptotic cells only however, DNA repair procedures may have been aborted. Hence Rad51 levels may not be indicative of DNA repair capacity and cell survival.

If indeed the up-regulation of Rad51 results in increased DNA repair capacity, this increase should be measurable in an assay. For this purpose the DNA repair rate of unexposed cells would have to be compared to those showing increased Rad51 levels after drug exposure. Because Rad51 functions by facilitating DNA strand exchange during homologous recombination repair, the exchange rate can be measured. For this purpose, the incorporation of radio-labelled oligonucleotides into double-stranded homologous DNA can be radiographically measured after gel electrophoretic separation of the DNA (Morrison *et al.*, 1999). In the case of increased Rad51 functionality, this should result in a stronger signal as more radio-labelled oligonucleotides would have been incorporated into the homologous DNA strand.

Tyrosine phosphorylation of Rad51 is known to be regulated by c-Abl (Henning and Sturzbecher, 2003). Because the DNA binding properties of Rad51 are determined by its tyrosine phosphorylation status (section 6.4), and hence determine its functionality in the DNA repair process, it would be important to investigate any changes in phosphorylation as a response to drug treatment. One possible approach would be to use phosphotyrosine antibodies in a western blotting procedure to investigate any correlation between increased Rad51 levels and increase in tyrosine phosphorylation, since Rad51 has two tyrosine residues which are known to be phosphorylated. An MS/MS approach would be the easiest way to determine the individual phosphorylation status of these tyrosine residues.

Rad51 is known to form nuclear foci with other proteins such as BRCA2 in the event of DNA repair (Yuan *et al.*, 1999; Tarsounas *et al.*, 2003). Since DNA repair is confined to the nucleus, cellular localization or distribution of Rad51 after drug treatment may provide insights into any additional roles Rad51 may have. The immunohistochemistry results obtained from MDA MB 231 cells in this study have already indicated potential re-localization of Rad51, from the cytoplasm into the nucleus due to drug treatment. If in addition, antibodies which specifically target the phosphorylated tyrosine residues of Rad51 were used, this could help to understand the consequences of these post-translational modifications on protein localization.

Determining whether Rad51 up-regulation after drug treatment is due to increased transcriptional activity, or if post-transcriptional regulation is responsible, may be important as well, as this could have implications for treatment options. Such options include for

example the use of interfering RNA, which has already been successfully employed to target DNA-PKcs, and thereby sensitising tumour cells to chemo/radio therapy (Peng *et al.*, 2002; Collis *et al.*, 2003). An experiment could be designed using cyclohexamide, a protein synthesis inhibitor, and actinomycin D or alpha amanitin, which are mRNA synthesis inhibitors, in order to determine the mode of Rad51 regulation in response to drug treatment.

Doxorubicin is assumed to predominantly cause DNA damage, but also produces oxygen free radicals which can be lethal as well. To investigate whether Rad51 expression is in any way linked to apoptosis, cellular changes indicative of apoptotic onset could be examined. Such investigations could, for example, monitor the translocation of Bax, a pro-apoptotic protein, from the cytosol to the mitochondrial membrane; the cytosolic increase in cytochrome c levels, or the activation of caspases, to name a few candidates (Smaili *et al.*, 2003). Bax and cytochrome c translocation could be monitored using specific primary antibodies. A fluorescent secondary antibody could then be used to determine the protein location by fluorescence microscopy (Chiang-Ting *et al.*, 2005). Furthermore, caspase activity could be monitored by a method such as FACS, using a fluorescence emitting peptide linker which contains caspase cleavage sites (He *et al.*, 2004). Upon caspase-mediated cleavage of the linker, the fluorescence signal would be lost. Hence the loss of fluorescence would be relative to caspase activity.

Doxorubicin, representing one of the most commonly used chemotherapeutic drugs, was utilized in this study. In a clinical setting however, different drugs are usually combined for more effective therapy. Hence, other commonly used drugs such as, for example, etoposide or cyclophosphamide, albeit inducing DNA damage by a different mechanism of action, may also lead to altered levels in Rad51. Hence testing the potential of different drugs to induce Rad51 expression, either as sole agents or in combination, may provide valuable information for targeted therapy.

7.12.2 DNA-Dependent Catalytic Subunit (DNA-PKcs)

As a key component of the active DNA-PK complex, the DNA-PK catalytic subunit (DNA-PKcs) has been shown to require autophosphorylation to function in the DNA repair processes (Burma and Chen, 2004). Because DNA-PK responds to DNA damage by increased activity, rather than elevated protein levels, it is conceivable that post-translational modifications of the catalytic subunit mediate changes in the activity state of DNA-PK (Boldogh *et al.*, 2003).

Similar to phosphorylation events of Rad51, a tandem MS based approach would be best to analyse post-translational modifications of DNA-PKcs after drug exposure and its consequences for DNA repair. Determining the presence of any modifications in tumour specimens overexpressing DNA-PKcs, and any affect these may have on proteins involved in DNA damage response pathways, such as BRCA1, may also provide relevant information.

7.13 Cell Cycle

Fluorescence activated cell sorting (FACS) results suggested that the observed changes in protein levels were independent of cell cycle state in MCF12A and MCF7 and were a genuine response to doxorubicin treatment. It is very likely that the changes seen in MDA MB 231 are also independent of the cell cycle, but FACS analysis results were not entirely conclusive. Hence, cell cycle synchronization using thymidine was employed in an attempt to mimic the cell cycle distribution profile seen in drug treated MDA MB 231 cells and to monitor cell cycle specific protein expression. These protein expression data could then have been compared to the protein levels observed in response to drug treatment. Thymidine treatment however, did not succeed in providing meaningful data. More conclusive data could be obtained by determining the specific protein levels at different stages of the cell cycle. This could be achieved using synchronization agents which arrest cells at different stages of the cell cycle such as aphidicolin (G1/S-phase), hydroxyurea (S-phase), or nocodazole (G2/M-phase). Alternatively, cells could be synchronized in G1 by serum depletion. After the subsequent addition of fresh serum the cells could be analysed for cell cycle specific protein expression, as they are traversing the cell cycle. Elevated Rad51 and topo II alpha protein levels in MDA MB 231 cells would indeed be independent of cell cycle state if the levels of both proteins were higher in drug exposed cells than at any cell cycle stage in each of the synchronized cultures.

7.14 Clinical Aspects

Both Rad51 and DNA-PKcs overexpression in tumours have been reported to be involved in enhancing resistance to certain therapeutic drugs. Furthermore, the results presented here show that at least one DNA double-strand repair protein, Rad51, is differentially regulated in response to doxorubicin treatment and could play an important role in the cellular response to such lesions. In addition, immunoblotting and immunohistochemistry results obtained in this study suggest that Rad51 and DNA-PKcs concentrations in patients' tumours vary and that alterations in Rad51 levels in response to chemotherapy are tumour-dependent, and are likely

to vary significantly as well. Because normal and malignant tissue may experience opposite effects with regard to Rad51 levels, which may actually be down-regulated in tumours and up-regulated in normal or benign tissue due to drug treatment, targeting Rad51 in combination with doxorubicin may be problematic. Consequently, any therapy targeting Rad51 would first have to assess its relative abundance and expected response in tumour and normal cells to determine the feasibility of such an approach.

If indeed Rad51 and/or DNA-PKcs are overexpressed in tumour tissue compared to normal tissue there are two possibilities for utilizing these proteins in therapeutic treatment and as a prognostic marker. For prognostic purposes a large group of samples, likely using hundreds of specimens, would have to be analysed for any correlations between protein expression and patient specific factors, such as those used in the current pilot study. Any relevant correlations between protein expression and clinical response could hence be used as prognostic markers. Monitoring other proteins known to interact with both Rad51 and DNA-PKcs, such as p53 and c-Abl in case of Rad51 and BRCA1 and Ku70/80 in case of DNA-PKcs, may also reveal important information. Such information may include a causal relationship between interacting proteins, as the phosphorylated form of Rad51 may only be present if c-Abl levels are also elevated for example. Or they may include synergetic effects on clinical response and outcome if more than one protein is aberrantly expressed. Differences in post-translational modification and particularly phosphorylation status are also worth analysing, because they are important in terms of protein activity and are likely to influence clinical outcome as well.

If targeting Rad51 and/or DNA-PKcs for therapeutic purposes one option would be to use a specific drug or inhibitor causing more destructive effects in cells that overexpress the proteins. A second approach would be to design a drug which targets Rad51 or DNA-PKcs, in order to reach a specific destination, but which acts on a different protein. Hence, the proteins would function as a pathfinder or anchor.

7.15 Conclusions

This project was a pilot study striving to elucidate cellular response mechanisms to chemotherapy which may lead to increased levels of resistance, and to discover candidate proteins which may be targeted to improve current clinical procedures. This study demonstrated the limitations of using standard 2DGE for sensitive detection of protein alterations in normal and cancerous breast cells in response to drug treatment. Furthermore,

limitations of combining 2DGE procedures with other technologies, such as reversed-phase high performance liquid chromatography, to achieve increased sensitivity have also been demonstrated. Using more sensitive immunodetection, Rad51 and topo II alpha were identified as differentially regulated proteins in response to chemotherapy while DNA-PKcs levels remained largely unchanged. Furthermore, Rad51 and DNA-PKcs, which are both involved in DNA damage repair, were found to be overexpressed in some tumour cells, making them excellent candidates for targeted chemotherapy under certain conditions. In conclusion, these results provide a promising starting point for future investigations into understanding the cellular response to DNA double-strand break-inducing drug treatment and devising more potent strategies for chemotherapy.

References

Abal, M., Andreu, J. M. and Barasoain, I. (2003). Taxanes: microtubule and centrosome targets, and cell cycle dependent mechanisms of action. *Curr Cancer Drug Targets* **3**(3): 193-203.

Adachi, N., Suzuki, H., Iiizumi, S. and Koyama, H. (2003). Hypersensitivity of nonhomologous DNA end-joining mutants to VP-16 and ICRF-193: implications for the repair of topoisomerase II-mediated DNA damage. *J Biol Chem* **278**(38): 35897-902.

Adam, B. L., Qu, Y., Davis, J. W., Ward, M. D., Clements, M. A., Cazares, L. H., Semmes, O. J., Schellhammer, P. F., Yasui, Y., Feng, Z. and Wright, G. L., Jr. (2002). Serum protein fingerprinting coupled with a pattern-matching algorithm distinguishes prostate cancer from benign prostate hyperplasia and healthy men. *Cancer Res* **62**(13): 3609-14.

Agrawal, M., Abraham, J., Balis, F. M., Edgerly, M., Stein, W. D., Bates, S., Fojo, T. and Chen, C. C. (2003). Increased 99mTc-sestamibi accumulation in normal liver and drug-resistant tumors after the administration of the glycoprotein inhibitor, XR9576. *Clin Cancer Res* **9**(2): 650-6.

Allen, K. A. (2003). An investigation into the regulation of the topisomerase II alpha promoter in breast cancer cells exposed to doxorubincin. Palmerston North, Massey University.

Allen, K. A., Williams, A. O., Isaacs, R. J. and Stowell, K. M. (2004). Down-regulation of human topoisomerase IIalpha correlates with altered expression of transcriptional regulators NF-YA and Sp1. *Anticancer Drugs* **15**(4): 357-62.

Badock, V., Steinhusen, U., Bommert, K. and Otto, A. (2001). Prefractionation of protein samples for proteome analysis using reversed-phase high-performance liquid chromatography. *Electrophoresis* **22**(14): 2856-64.

Batist, G., Tulpule, A., Sinha, B. K., Katki, A. G., Myers, C. E. and Cowan, K. H. (1986). Overexpression of a novel anionic glutathione transferase in multidrug-resistant human breast cancer cells. *J Biol Chem* **261**(33): 15544-9.

Belanger, M. M., Roussel, E. and Couet, J. (2003). Up-regulation of caveolin expression by cytotoxic agents in drug-sensitive cancer cells. *Anticancer Drugs* **14**(4): 281-7.

Berkelman, T. and Stenstedt, T. (1998). 2-D Electrophoresis: Using immobilized pH gradients, Principles & Methods. Amersham Pharmaciea Biotech Inc.

Bianchi, F., Hu, J., Pelosi, G., Cirincione, R., Ferguson, M., Ratcliffe, C., Di Fiore, P. P., Gatter, K., Pezzella, F. and Pastorino, U. (2004). Lung cancers detected by screening with spiral computed tomography have a malignant phenotype when analyzed by cDNA microarray. *Clin Cancer Res* **10**(18 Pt 1): 6023-8.

Bishop, D. K., Ear, U., Bhattacharyya, A., Calderone, C., Beckett, M., Weichselbaum, R. R. and Shinohara, A. (1998). Xrcc3 is required for assembly of Rad51 complexes in vivo. *J Biol Chem* **273**(34): 21482-8.

Bjursell, G. and Reichard, P. (1973). Effects of thymidine on deoxyribonucleoside triphosphate pools and deoxyribonucleic acid synthesis in Chinese hamster ovary cells. *J Biol Chem* **248**(11): 3904-9.

Boldogh, I., Roy, G., Lee, M. S., Bacsi, A., Hazra, T. K., Bhakat, K. K., Das, G. C. and Mitra, S. (2003). Reduced DNA double strand breaks in chlorambucil resistant cells are related to high DNA-PKcs activity and low oxidative stress. *Toxicology* **193**(1-2): 137-52.

Bourgarel-Rey, V., El Khyari, S., Rimet, O., Bordas, B., Guigal, N., Braguer, D., Seree, E., Barra, Y. and Briand, C. (2000). Opposite effects of antimicrotubule agents on c-myc oncogene expression depending on the cell lines used. *Eur J Cancer* **36**(8): 1043-9.

Brown, K. J. and Fenselau, C. (2004). Investigation of doxorubicin resistance in MCF-7 breast cancer cells using shot-gun comparative proteomics with proteolytic 18O labeling. *J Proteome Res* **3**(3): 455-62.

Burger, H., Foekens, J. A., Look, M. P., Meijer-van Gelder, M. E., Klijn, J. G., Wiemer, E. A., Stoter, G. and Nooter, K. (2003). RNA expression of breast cancer resistance protein, lung resistance-related protein, multidrug resistance-associated proteins 1 and 2, and multidrug resistance gene 1 in breast cancer: correlation with chemotherapeutic response. *Clin Cancer Res* **9**(2): 827-36.

Burma, S. and Chen, D. J. (2004). Role of DNA-PK in the cellular response to DNA double-strand breaks. *DNA Repair (Amst)* **3**(8-9): 909-18.

Butt, A., Davison, M. D., Smith, G. J., Young, J. A., Gaskell, S. J., Oliver, S. G. and Beynon, R. J. (2001). Chromatographic separations as a prelude to two-dimensional electrophoresis in proteomics analysis. *Proteomics* **1**(1): 42-53.

Castellanos-Serra, L. and Paz-Lago, D. (2002). Inhibition of unwanted proteolysis during sample preparation: evaluation of its efficiency in challenge experiments. *Electrophoresis* **23**(11): 1745-53.

Chen, S. T., Pan, T. L., Tsai, Y. C. and Huang, C. M. (2002). Proteomics reveals protein profile changes in doxorubicin--treated MCF-7 human breast cancer cells. *Cancer Lett* **181**(1): 95-107.

Chen, Y. N., Mickley, L. A., Schwartz, A. M., Acton, E. M., Hwang, J. L. and Fojo, A. T. (1990). Characterization of adriamycin-resistant human breast cancer cells which display overexpression of a novel resistance-related membrane protein. *J Biol Chem* **265**(17): 10073-80.

Chevalier, F., Rofidal, V., Vanova, P., Bergoin, A. and Rossignol, M. (2004). Proteomic capacity of recent fluorescent dyes for protein staining. *Phytochemistry* **65**(11): 1499-506.

Chiang-Ting, C., Tzu-Ching, C., Ching-Yi, T., Song-Kuen, S. and Ming-Kuen, L. (2005). Adenovirus-Mediated bcl-2 Gene Transfer Inhibits Renal Ischemia/Reperfusion Induced Tubular Oxidative Stress and Apoptosis. *Am J Transplant* **5**(6): 1194-203.

Christodoulopoulos, G., Malapetsa, A., Schipper, H., Golub, E., Radding, C. and Panasci, L. C. (1999). Chlorambucil induction of HsRad51 in B-cell chronic lymphocytic leukemia. *Clin Cancer Res* **5**(8): 2178-84.

Chu, E., Grever, M.R., Chabner, A.C. (2001). Pharmacology of Cancer Chemotherapy. Cancer: Principles and Practive of Oncology, 6th edition. V. T. J. Devita, S. Hellaman and S. A. Rosenberg, Lippincott Williams & Wilkins.

Ciocca, D. R., Fuqua, S. A., Lock-Lim, S., Toft, D. O., Welch, W. J. and McGuire, W. L. (1992). Response of human breast cancer cells to heat shock and chemotherapeutic drugs. *Cancer Res* **52**(13): 3648-54.

Collis, S., Swartz, M. and DeWeese, T. (2003a). siRNA-silencing of DNA repair factors results in enhanced radiation and chemotherapy-mediated killing of human cancer cells. *Int J Radiat Oncol Biol Phys* **57**(2 Suppl): S144.

Collis, S. J., Swartz, M. J., Nelson, W. G. and DeWeese, T. L. (2003). Enhanced radiation and chemotherapy-mediated cell killing of human cancer cells by small inhibitory RNA silencing of DNA repair factors. *Cancer Res* **63**(7): 1550-4.

Collis, S. J., Tighe, A., Scott, S. D., Roberts, S. A., Hendry, J. H. and Margison, G. P. (2001). Ribozyme minigene-mediated RAD51 down-regulation increases radiosensitivity of human prostate cancer cells. *Nucleic Acids Res* **29**(7): 1534-8.

Deffie, A. M., Batra, J. K. and Goldenberg, G. J. (1989). Direct correlation between DNA topoisomerase II activity and cytotoxicity in adriamycin-sensitive and -resistant P388 leukemia cell lines. *Cancer Res* **49**(1): 58-62.

DiBiase, S. J., Zeng, Z. C., Chen, R., Hyslop, T., Curran, W. J., Jr. and Iliakis, G. (2000). DNA-dependent protein kinase stimulates an independently active, nonhomologous, end-joining apparatus. *Cancer Res* **60**(5): 1245-53.

Dickson, R. B. and Stancel, G. M. (2000). Estrogen receptor-mediated processes in normal and cancer cells. *J Natl Cancer Inst Monogr*(27): 135-45.

Diestra, J. E., Scheffer, G. L., Catala, I., Maliepaard, M., Schellens, J. H., Scheper, R. J., Germa-Lluch, J. R. and Izquierdo, M. A. (2002). Frequent expression of the multi-drug resistance-associated protein BCRP/MXR/ABCP/ABCG2 in human tumours detected by the BXP-21 monoclonal antibody in paraffin-embedded material. *J Pathol* **198**(2): 213-9.

Doyle, L. A., Yang, W., Abruzzo, L. V., Krogmann, T., Gao, Y., Rishi, A. K. and Ross, D. D. (1998). A multidrug resistance transporter from human MCF-7 breast cancer cells. *Proc Natl Acad Sci U S A* **95**(26): 15665-70.

Duffy, M. J. (2005). Predictive markers in breast and other cancers: a review. *Clin Chem* **51**(3): 494-503.

Dummer, R., Bergh, J., Karlsson, Y., Horowitz, J. A., Mulder, N. H., Huinink, D. T. B., Burg, G., Hofbauer, G. and Osanto, S. (2000). Biological activity and safety of adenoviral vector-expressed wild-type p53 after intratumoral injection in melanoma and breast cancer patients with p53-overexpressing tumors. *Cancer Gene Ther* **7**(7): 1069-76.

Dutt, M. J. and Lee, K. H. (2000). Proteomic analysis. *Curr Opin Biotechnol* **11**(2): 176-9.

Dwek, M. V., Ross, H. A. and Leathem, A. J. (2001). Proteome and glycosylation mapping identifies post-translational modifications associated with aggressive breast cancer. *Proteomics* **1**(6): 756-62.

Eriksson, A., Lewensoh, R., Larsson, R. and Nilsson, A. (2002). DNA-dependent protein kinase in leukaemia cells and correlation with drug sensitivity. *Anticancer Res* **22**(3): 1787-93.

Evans, C. D., Mirski, S. E., Danks, M. K. and Cole, S. P. (1994). Reduced levels of topoisomerase II alpha and II beta in a multidrug-resistant lung-cancer cell line. *Cancer Chemother Pharmacol* **34**(3): 242-8.

Faneyte, I. F., Kristel, P. M., Maliepaard, M., Scheffer, G. L., Scheper, R. J., Schellens, J. H. and van de Vijver, M. J. (2002). Expression of the breast cancer resistance protein in breast cancer. *Clin Cancer Res* **8**(4): 1068-74.

Feldhoff, P. W., Mirski, S. E., Cole, S. P. and Sullivan, D. M. (1994). Altered subcellular distribution of topoisomerase II alpha in a drug-resistant human small cell lung cancer cell line. *Cancer Res* **54**(3): 756-62.

Ferrero, J. M., Etienne, M. C., Formento, J. L., Francoual, M., Rostagno, P., Peyrottes, I., Ettore, F., Teissier, E., Leblanc-Talent, P., Namer, M. and Milano, G. (2000). Application of an original RT-PCR-ELISA multiplex assay for MDR1 and MRP, along with p53 determination in node-positive breast cancer patients. *Br J Cancer* **82**(1): 171-7.

Filipits, M., Suchomel, R. W., Dekan, G., Haider, K., Valdimarsson, G., Depisch, D. and Pirker, R. (1996). MRP and MDR1 gene expression in primary breast carcinomas. *Clin Cancer Res* **2**(7): 1231-7.

Flygare, J., Benson, F. and Hellgren, D. (1996). Expression of the human RAD51 gene during the cell cycle in primary human peripheral blood lymphocytes. *Biochim Biophys Acta* **1312**(3): 231-6.

Flygare, J., Falt, S., Ottervald, J., Castro, J., Dackland, A. L., Hellgren, D. and Wennborg, A. (2001). Effects of HsRad51 overexpression on cell proliferation, cell cycle progression, and apoptosis. *Exp Cell Res* **268**(1): 61-9.

Friedman, D. B., Hill, S., Keller, J. W., Merchant, N. B., Levy, S. E., Coffey, R. J. and Caprioli, R. M. (2004). Proteome analysis of human colon cancer by two-dimensional difference gel electrophoresis and mass spectrometry. *Proteomics* **4**(3): 793-811.

Galvani, M., Hamdan, M., Herbert, B. and Righetti, P. G. (2001). Alkylation kinetics of proteins in preparation for two-dimensional maps: a matrix assisted laser desorption/ionization-mass spectrometry investigation. *Electrophoresis* **22**(10): 2058-65.

Galvani, M., Rovatti, L., Hamdan, M., Herbert, B. and Righetti, P. G. (2001a). Protein alkylation in the presence/absence of thiourea in proteome analysis: a matrix assisted laser desorption/ionization-time of flight-mass spectrometry investigation. *Electrophoresis* **22**(10): 2066-74.

Gaudiano, G., Koch, T. H., Lo Bello, M., Nuccetelli, M., Ravagnan, G., Serafino, A. and Sinibaldi-Vallebona, P. (2000). Lack of glutathione conjugation to adriamycin in human breast cancer MCF-7/DOX cells. Inhibition of glutathione S-transferase p1-1 by glutathione conjugates from anthracyclines. *Biochem Pharmacol* **60**(12): 1915-23.

Gehrmann, M. L., Fenselau, C. and Hathout, Y. (2004). Highly altered protein expression profile in the adriamycin resistant MCF-7 cell line. *J Proteome Res* **3**(3): 403-9.

Gehrmann, M. L., Hathout, Y. and Fenselau, C. (2004a). Evaluation of metabolic labeling for comparative proteomics in breast cancer cells. *J Proteome Res* **3**(5): 1063-8.

Getz, E. B., Xiao, M., Chakrabarty, T., Cooke, R. and Selvin, P. R. (1999). A comparison between the sulfhydryl reductants tris(2-carboxyethyl)phosphine and dithiothreitol for use in protein biochemistry. *Anal Biochem* **273**(1): 73-80.

Gharahdaghi, F., Weinberg, C. R., Meagher, D. A., Imai, B. S. and Mische, S. M. (1999). Mass spectrometric identification of proteins from silver-stained polyacrylamide gel: a method for the removal of silver ions to enhance sensitivity. *Electrophoresis* **20**(3): 601-5.

Gharbi, S., Gaffney, P., Yang, A., Zvelebil, M. J., Cramer, R., Waterfield, M. D. and Timms, J. F. (2002). Evaluation of two-dimensional differential gel electrophoresis for proteomic expression analysis of a model breast cancer cell system. *Mol Cell Proteomics* **1**(2): 91-8.

Godovac-Zimmermann, J., Kleiner, O., Brown, L. R. and Drukier, A. K. (2005). Perspectives in spicing up proteomics with splicing. *Proteomics* **5**(3): 699-709.

Graus-Porta, D., Beerli, R. R., Daly, J. M. and Hynes, N. E. (1997). ErbB-2, the preferred heterodimerization partner of all ErbB receptors, is a mediator of lateral signaling. *Embo J* **16**(7): 1647-55.

Grus, F. H., Joachim, S. C. and Pfeiffer, N. (2003). Analysis of complex autoantibody repertoires by surface-enhanced laser desorption/ionization-time of flight mass spectrometry. *Proteomics* **3**(6): 957-61.

Gusterson, B. A., Gelber, R. D., Goldhirsch, A., Price, K. N., Save-Soderborgh, J., Anbazhagan, R., Styles, J., Rudenstam, C. M., Golouh, R., Reed, R. and et al. (1992). Prognostic importance of c-erbB-2 expression in breast cancer. International (Ludwig) Breast Cancer Study Group. *J Clin Oncol* **10**(7): 1049-56.

Gygi, S. P., Corthals, G. L., Zhang, Y., Rochon, Y. and Aebersold, R. (2000). Evaluation of two-dimensional gel electrophoresis-based proteome analysis technology. *Proc Natl Acad Sci U S A* **97**(17): 9390-5.

Gygi, S. P., Rist, B., Gerber, S. A., Turecek, F., Gelb, M. H. and Aebersold, R. (1999). Quantitative analysis of complex protein mixtures using isotope-coded affinity tags. *Nat Biotechnol* **17**(10): 994-9.

Hamdan, M. and Righetti, P. G. (2003). Assessment of protein expression by means of 2-D gel electrophoresis with and without mass spectrometry. *Mass Spectrom Rev* **22**(4): 272-84.

Hansen, L. T., Lundin, C., Helleday, T., Poulsen, H. S., Sorensen, C. S., Petersen, L. N. and Spang-Thomsen, M. (2003). DNA repair rate and etoposide (VP16) resistance of tumor cell subpopulations derived from a single human small cell lung cancer. *Lung Cancer* **40**(2): 157-64.

Hansen, L. T., Lundin, C., Spang-Thomsen, M., Petersen, L. N. and Helleday, T. (2003a). The role of RAD51 in etoposide (VP16) resistance in small cell lung cancer. *Int J Cancer* **105**(4): 472-9.

Hanstein, B., Djahansouzi, S., Dall, P., Beckmann, M. W. and Bender, H. G. (2004). Insights into the molecular biology of the estrogen receptor define novel therapeutic targets for breast cancer. *Eur J Endocrinol* **150**(3): 243-55.

Harker, W. G., Slade, D. L., Parr, R. L., Feldhoff, P. W., Sullivan, D. M. and Holguin, M. H. (1995). Alterations in the topoisomerase II alpha gene, messenger RNA, and subcellular protein distribution as well as reduced expression of the DNA topoisomerase II beta enzyme in a mitoxantrone-resistant HL-60 human leukemia cell line. *Cancer Res* **55**(8): 1707-16.

Hathout, Y., Gehrmann, M. L., Chertov, A. and Fenselau, C. (2004). Proteomic phenotyping: metastatic and invasive breast cancer. *Cancer Lett* **210**(2): 245-53.

Hathout, Y., Riordan, K., Gehrmann, M. and Fenselau, C. (2002). Differential protein expression in the cytosol fraction of an MCF-7 breast cancer cell line selected for resistance toward melphalan. *J Proteome Res* **1**(5): 435-42.

He, L., Wu, X., Meylan, F., Olson, D. P., Simone, J., Hewgill, D., Siegel, R. and Lipsky, P. E. (2004). Monitoring caspase activity in living cells using fluorescent proteins and flow cytometry. *Am J Pathol* **164**(6): 1901-13.

Henning, W. and Sturzbecher, H. W. (2003). Homologous recombination and cell cycle checkpoints: Rad51 in tumour progression and therapy resistance. *Toxicology* **193**(1-2): 91-109.

Herbert, B., Galvani, M., Hamdan, M., Olivieri, E., MacCarthy, J., Pedersen, S. and Righetti, P. G. (2001). Reduction and alkylation of proteins in preparation of two-dimensional map analysis: why, when, and how? *Electrophoresis* **22**(10): 2046-57.

Holbro, T., Civenni, G. and Hynes, N. E. (2003). The ErbB receptors and their role in cancer progression. *Exp Cell Res* **284**(1): 99-110.

Holgersson, A., Nilsson, A., Lewensohn, R. and Kanter, L. (2004). Expression of DNA-PKcs and Ku86, but not Ku70, differs between lymphoid malignancies. *Exp Mol Pathol* **77**(1): 1-6.

Holm, C., Goto, T., Wang, J. C. and Botstein, D. (1985). DNA topoisomerase II is required at the time of mitosis in yeast. *Cell* **41**(2): 553-63.

Hopfner, K. P., Putnam, C. D. and Tainer, J. A. (2002). DNA double-strand break repair from head to tail. *Curr Opin Struct Biol* **12**(1): 115-22.

Hosoi, Y., Watanabe, T., Nakagawa, K., Matsumoto, Y., Enomoto, A., Morita, A., Nagawa, H. and Suzuki, N. (2004). Up-regulation of DNA-dependent protein kinase activity and Sp1 in colorectal cancer. *Int J Oncol* **25**(2): 461-8.

Ismail, I. H., Martensson, S., Moshinsky, D., Rice, A., Tang, C., Howlett, A., McMahon, G. and Hammarsten, O. (2004). SU11752 inhibits the DNA-dependent protein kinase and DNA double-strand break repair resulting in ionizing radiation sensitization. *Oncogene* **23**(4): 873-82.

Ito, K., Fujimori, M., Nakata, S., Hama, Y., Shingu, K., Kobayashi, S., Tsuchiya, S., Kohno, K., Kuwano, M. and Amano, J. (1998). Clinical significance of the increased multidrug resistance-associated protein (MRP) gene expression in patients with primary breast cancer. *Oncol Res* **10**(2): 99-109.

Jackson, S. P. (2002). Sensing and repairing DNA double-strand breaks. *Carcinogenesis* **23**(5): 687-96.

Jin, X., Chen, Y., Lubman, D. M., Misek, D. and Hanash, S. M. (1999). Capillary electrophoresis/tandem mass spectrometry for analysis of proteins from two-dimensional sodium dodecyl sulfate polyacrylamide gel electrophoresis. *Rapid Commun Mass Spectrom* **13**(23): 2327-34.

Jordan, V. C. and Morrow, M. (1999). Tamoxifen, raloxifene, and the prevention of breast cancer. *Endocr Rev* **20**(3): 253-78.

Kanamoto, T., Hellman, U., Heldin, C. H. and Souchelnytskyi, S. (2002). Functional proteomics of transforming growth factor-beta1-stimulated Mv1Lu epithelial cells: Rad51 as a target of TGFbeta1-dependent regulation of DNA repair. *Embo J* **21**(5): 1219-30.

Kellner, U., Sehested, M., Jensen, P. B., Gieseler, F. and Rudolph, P. (2002). Culprit and victim -- DNA topoisomerase II. *Lancet Oncol* **3**(4): 235-43.

Khanna, K. K. and Jackson, S. P. (2001). DNA double-strand breaks: signaling, repair and the cancer connection. *Nat Genet* **27**(3): 247-54.

Kharbanda, S., Yuan, Z. M., Weichselbaum, R. and Kufe, D. (1998). Determination of cell fate by c-Abl activation in the response to DNA damage. *Oncogene* **17**(25): 3309-18.

Kim, C. H., Park, S. J. and Lee, S. H. (2002). A targeted inhibition of DNA-dependent protein kinase sensitizes breast cancer cells following ionizing radiation. *J Pharmacol Exp Ther* **303**(2): 753-9.

Kim, C. K., Choi, E. J., Choi, S. H., Park, J. S., Haider, K. H. and Ahn, W. S. (2003). Enhanced p53 gene transfer to human ovarian cancer cells using the cationic nonviral vector, DDC. *Gynecol Oncol* **90**(2): 265-72.

Kim, P. M., Allen, C., Wagener, B. M., Shen, Z. and Nickoloff, J. A. (2001). Overexpression of human RAD51 and RAD52 reduces double-strand break-induced homologous recombination in mammalian cells. *Nucleic Acids Res* **29**(21): 4352-60.

Kim, S. H., Um, J. H., Dong-Won, B., Kwon, B. H., Kim, D. W., Chung, B. S. and Kang, C. D. (2000). Potentiation of chemosensitivity in multidrug-resistant human leukemia CEM cells by inhibition of DNA-dependent protein kinase using wortmannin. *Leuk Res* **24**(11): 917-25.

Kim, S. T., Lim, D. S., Canman, C. E. and Kastan, M. B. (1999). Substrate specificities and identification of putative substrates of ATM kinase family members. *J Biol Chem* **274**(53): 37538-43.

Knowles, M. R., Cervino, S., Skynner, H. A., Hunt, S. P., de Felipe, C., Salim, K., Meneses-Lorente, G., McAllister, G. and Guest, P. C. (2003). Multiplex proteomic analysis by two-dimensional differential in-gel electrophoresis. *Proteomics* **3**(7): 1162-71.

Kornmann, M., Arber, N. and Korc, M. (1998). Inhibition of basal and mitogen-stimulated pancreatic cancer cell growth by cyclin D1 antisense is associated with loss of tumorigenicity and potentiation of cytotoxicity to cisplatinum. *J Clin Invest* **101**(2): 344-52.

Kornmann, M., Danenberg, K. D., Arber, N., Beger, H. G., Danenberg, P. V. and Korc, M. (1999). Inhibition of cyclin D1 expression in human pancreatic cancer cells is associated with increased chemosensitivity and decreased expression of multiple chemoresistance genes. *Cancer Res* **59**(14): 3505-11.

Kudoh, K., Ramanna, M., Ravatn, R., Elkahloun, A. G., Bittner, M. L., Meltzer, P. S., Trent, J. M., Dalton, W. S. and Chin, K. V. (2000). Monitoring the expression profiles of doxorubicin-induced and doxorubicin-resistant cancer cells by cDNA microarray. *Cancer Res* **60**(15): 4161-6.

Kussmann, M., Lassing, U., Sturmer, C. A., Przybylski, M. and Roepstorff, P. (1997). Matrix-assisted laser desorption/ionization mass spectrometric peptide mapping of the neural cell adhesion protein neurolin purified by sodium dodecyl sulfate polyacrylamide gel electrophoresis or acidic precipitation. *J Mass Spectrom* **32**(5): 483-93.

Landry, F., Lombardo, C. R. and Smith, J. W. (2000). A method for application of samples to matrix-assisted laser desorption ionization time-of-flight targets that enhances peptide detection. *Anal Biochem* **279**(1): 1-8.

Lebedeva, S., Bagdasarova, S., Tyler, T., Mu, X., Wilson, D. R. and Gjerset, R. A. (2001). Tumor suppression and therapy sensitization of localized and metastatic breast cancer by adenovirus p53. *Hum Gene Ther* **12**(7): 763-72.

Lee, J. H. and Paull, T. T. (2005). ATM activation by DNA double-strand breaks through the Mre11-Rad50-Nbs1 complex. *Science* **308**(5721): 551-4.

Lees-Miller, S. P. and Meek, K. (2003). Repair of DNA double strand breaks by non-homologous end joining. *Biochimie* **85**(11): 1161-73.

Leslie, E. M., Deeley, R. G. and Cole, S. P. (2005). Multidrug resistance proteins: role of P-glycoprotein, MRP1, MRP2, and BCRP (ABCG2) in tissue defense. *Toxicol Appl Pharmacol* **204**(3): 216-37.

Liang, C. R., Leow, C. K., Neo, J. C., Tan, G. S., Lo, S. L., Lim, J. W., Seow, T. K., Lai, P. B. and Chung, M. C. (2005). Proteome analysis of human hepatocellular carcinoma tissues by two-dimensional difference gel electrophoresis and mass spectrometry. *Proteomics* **5**(8): 2258-71.

Linke, S. P., Sengupta, S., Khabie, N., Jeffries, B. A., Buchhop, S., Miska, S., Henning, W., Pedeux, R., Wang, X. W., Hofseth, L. J., Yang, Q., Garfield, S. H., Sturzbecher, H. W. and Harris, C. C. (2003). p53 interacts with hRAD51 and hRAD54, and directly modulates homologous recombination. *Cancer Res* **63**(10): 2596-605.

Litman, T., Druley, T. E., Stein, W. D. and Bates, S. E. (2001). From MDR to MXR: new understanding of multidrug resistance systems, their properties and clinical significance. *Cell Mol Life Sci* **58**(7): 931-59.

Longley, D. B., Harkin, D. P. and Johnston, P. G. (2003). 5-fluorouracil: mechanisms of action and clinical strategies. *Nat Rev Cancer* **3**(5): 330-8.

Looi, L. M., Cheah, P. L. and Yap, S. F. (1997). Correlation between histological grade and c-erbB2 oncoprotein overexpression in infiltrating ductal carcinoma of breast. *Malays J Pathol* **19**(1): 35-9.

Luker, K. E., Pica, C. M., Schreiber, R. D. and Piwnica-Worms, D. (2001). Overexpression of IRF9 confers resistance to antimicrotubule agents in breast cancer cells. *Cancer Res* **61**(17): 6540-7.

Maacke, H., Jost, K., Opitz, S., Miska, S., Yuan, Y., Hasselbach, L., Luttges, J., Kalthoff, H. and Sturzbecher, H. W. (2000). DNA repair and recombination factor Rad51 is over-expressed in human pancreatic adenocarcinoma. *Oncogene* **19**(23): 2791-5.

Maacke, H., Opitz, S., Jost, K., Hamdorf, W., Henning, W., Kruger, S., Feller, A. C., Lopens, A., Diedrich, K., Schwinger, E. and Sturzbecher, H. W. (2000a). Over-expression of wild-type Rad51 correlates with histological grading of invasive ductal breast cancer. *Int J Cancer* **88**(6): 907-13.

Marmorstein, L. Y., Ouchi, T. and Aaronson, S. A. (1998). The BRCA2 gene product functionally interacts with p53 and RAD51. *Proc Natl Acad Sci U S A* **95**(23): 13869-74.

Marsh, K. L., Willmore, E., Tinelli, S., Cornarotti, M., Meczes, E. L., Capranico, G., Fisher, L. M. and Austin, C. A. (1996). Amsacrine-promoted DNA cleavage site determinants for the two human DNA topoisomerase II isoforms alpha and beta. *Biochem Pharmacol* **52**(11): 1675-85.

Martensson, S., Nygren, J., Osheroff, N. and Hammarsten, O. (2003). Activation of the DNA-dependent protein kinase by drug-induced and radiation-induced DNA strand breaks. *Radiat Res* **160**(3): 291-301.

Maurer MH, Feldmann RE Jr, Bromme JO, Kalenka A. (2005). Comparison of statistical approaches for the analysis of proteome expression data of differentiating neural stem cells. *J Proteome Res* **4**(1):96-100.

McCarty, K. S., Jr., Miller, L. S., Cox, E. B., Konrath, J. and McCarty, K. S., Sr. (1985). Estrogen receptor analyses. Correlation of biochemical and immunohistochemical methods using monoclonal antireceptor antibodies. *Arch Pathol Lab Med* **109**(8): 716-21.

Meden, H., Marx, D., Roegglen, T., Schauer, A. and Kuhn, W. (1998). Overexpression of the oncogene c-erbB-2 (HER2/neu) and response to chemotherapy in patients with ovarian cancer. *Int J Gynecol Pathol* **17**(1): 61-5.

Meunier B, Bouley J, Piec I, Bernard C, Picard B, Hocquette JF. (2005). Data analysis methods for detection of differential protein expression in two-dimensional gel electrophoresis. *Anal Biochem* **340**(2):226-30.

Mian, S., Ball, G., Hornbuckle, J., Holding, F., Carmichael, J., Ellis, I., Ali, S., Li, G., McArdle, S., Creaser, C. and Rees, R. (2003). A prototype methodology combining surface-enhanced laser desorption/ionization protein chip technology and artificial neural network algorithms to predict the chemoresponsiveness of breast cancer cell lines exposed to Paclitaxel and Doxorubicin under in vitro conditions. *Proteomics* **3**(9): 1725-37.

Ministry of Health, New Zealand, Cancer Trends and Projections, Breast cancer 2002

Miseta, A. and Csutora, P. (2000). Relationship between the occurrence of cysteine in proteins and the complexity of organisms. *Mol Biol Evol* **17**(8): 1232-9.

Moll, U., Lau, R., Sypes, M. A., Gupta, M. M. and Anderson, C. W. (1999). DNA-PK, the DNA-activated protein kinase, is differentially expressed in normal and malignant human tissues. *Oncogene* **18**(20): 3114-26.

Moller, A., Malerczyk, C., Volker, U., Stoppler, H. and Maser, E. (2002). Monitoring daunorubicin-induced alterations in protein expression in pancreas carcinoma cells by two-dimensional gel electrophoresis. *Proteomics* **2**(6): 697-705.

Molloy MP, Brzezinski EE, Hang J, McDowell MT, VanBogelen RA. (2003). Overcoming technical variation and biological variation in quantitative proteomics. *Proteomics* **3**(10):1912-9.

Morrison, C., Shinohara, A., Sonoda, E., Yamaguchi-Iwai, Y., Takata, M., Weichselbaum, R. R. and Takeda, S. (1999). The essential functions of human Rad51 are independent of ATP hydrolysis. *Mol Cell Biol* **19**(10): 6891-7.

Mortz, E., Krogh, T. N., Vorum, H. and Gorg, A. (2001). Improved silver staining protocols for high sensitivity protein identification using matrix-assisted laser desorption/ionization-time of flight analysis. *Proteomics* **1**(11): 1359-63.

Mujoo, K., Maneval, D. C., Anderson, S. C. and Gutterman, J. U. (1996). Adenoviral-mediated p53 tumor suppressor gene therapy of human ovarian carcinoma. *Oncogene* **12**(8): 1617-23.

Nakashima, T. and Clayman, G. L. (2000). Antisense inhibition of cyclin D1 in human head and neck squamous cell carcinoma. *Arch Otolaryngol Head Neck Surg* **126**(8): 957-61.

Nilsson, A., Sirzen, F., Lewensohn, R., Wang, N. and Skog, S. (1999). Cell cycle-dependent regulation of the DNA-dependent protein kinase. *Cell Prolif* **32**(4): 239-48.

Nooter, K., Brutel de la Riviere, G., Look, M. P., van Wingerden, K. E., Henzen-Logmans, S. C., Scheper, R. J., Flens, M. J., Klijn, J. G., Stoter, G. and Foekens, J. A. (1997). The prognostic significance of expression of the multidrug resistance-associated protein (MRP) in primary breast cancer. *Br J Cancer* **76**(4): 486-93.

Nooter, K., Westerman, A. M., Flens, M. J., Zaman, G. J., Scheper, R. J., van Wingerden, K. E., Burger, H., Oostrum, R., Boersma, T., Sonneveld, P. and et al. (1995). Expression of the multidrug resistance-associated protein (MRP) gene in human cancers. *Clin Cancer Res* **1**(11): 1301-10.

Norbury, C. J. and Zhivotovsky, B. (2004). DNA damage-induced apoptosis. *Oncogene* **23**(16): 2797-808.

Oesterreich, S., Weng, C. N., Qiu, M., Hilsenbeck, S. G., Osborne, C. K. and Fuqua, S. A. (1993). The small heat shock protein hsp27 is correlated with growth and drug resistance in human breast cancer cell lines. *Cancer Res* **53**(19): 4443-8.

O'Farrell, P. H. (1975). High resolution two-dimensional electrophoresis of proteins. *J Biol Chem* **250**(10): 4007-21.

Ohnishi, T., Taki, T., Hiraga, S., Arita, N. and Morita, T. (1998). In vitro and in vivo potentiation of radiosensitivity of malignant gliomas by antisense inhibition of the RAD51 gene. *Biochem Biophys Res Commun* **245**(2): 319-24.

Pastink, A., Eeken, J. C. and Lohman, P. H. (2001). Genomic integrity and the repair of double-strand DNA breaks. *Mutat Res* **480-481**: 37-50.

Peer, D., Dekel, Y., Melikhov, D. and Margalit, R. (2004). Fluoxetine inhibits multidrug resistance extrusion pumps and enhances responses to chemotherapy in syngeneic and in human xenograft mouse tumor models. *Cancer Res* **64**(20): 7562-9.

Pegram, M. D., Pienkowski, T., Northfelt, D. W., Eiermann, W., Patel, R., Fumoleau, P., Quan, E., Crown, J., Toppmeyer, D., Smylie, M., Riva, A., Blitz, S., Press, M. F., Reese, D., Lindsay, M. A. and Slamon, D. J. (2004). Results of two open-label, multicenter phase II studies of docetaxel, platinum salts, and trastuzumab in HER2-positive advanced breast cancer. *J Natl Cancer Inst* **96**(10): 759-69.

Peng, Y., Zhang, Q., Nagasawa, H., Okayasu, R., Liber, H. L. and Bedford, J. S. (2002). Silencing expression of the catalytic subunit of DNA-dependent protein kinase by small interfering RNA sensitizes human cells for radiation-induced chromosome damage, cell killing, and mutation. *Cancer Res* **62**(22): 6400-4.

Perquin, M., Oster, T., Maul, A., Froment, N., Untereiner, M. and Bagrel, D. (2001). The glutathione-related detoxification system is increased in human breast cancer in correlation with clinical and histopathological features. *J Cancer Res Clin Oncol* **127**(6): 368-74.

Pucci, S., Mazzarelli, P., Rabitti, C., Giai, M., Gallucci, M., Flammia, G., Alcini, A., Altomare, V. and Fazio, V. M. (2001). Tumor specific modulation of KU70/80 DNA binding activity in breast and bladder human tumor biopsies. *Oncogene* **20**(6): 739-47.

Pusztai, L., Wagner, P., Ibrahim, N., Rivera, E., Theriault, R., Booser, D., Symmans, F. W., Wong, F., Blumenschein, G., Fleming, D. R., Rouzier, R., Boniface, G. and Hortobagyi, G. N. (2005). Phase II study of tariquidar, a selective P-glycoprotein inhibitor, in patients with chemotherapy-resistant, advanced breast carcinoma. *Cancer*.

Rabilloud, T. (1998). Use of thiourea to increase the solubility of membrane proteins in two-dimensional electrophoresis. *Electrophoresis* **19**(5): 758-60.

Raderschall, E., Bazarov, A., Cao, J., Lurz, R., Smith, A., Mann, W., Ropers, H. H., Sedivy, J. M., Golub, E. I., Fritz, E. and Haaf, T. (2002). Formation of higher-order nuclear Rad51 structures is functionally linked to p21 expression and protection from DNA damage-induced apoptosis. *J Cell Sci* **115**(Pt 1): 153-64.

Raderschall, E., Golub, E. I. and Haaf, T. (1999). Nuclear foci of mammalian recombination proteins are located at single-stranded DNA regions formed after DNA damage. *Proc Natl Acad Sci U S A* **96**(5): 1921-6.

Raderschall, E., Stout, K., Freier, S., Suckow, V., Schweiger, S. and Haaf, T. (2002a). Elevated levels of Rad51 recombination protein in tumor cells. *Cancer Res* **62**(1): 219-25.

Ramsden, D. A. and Gellert, M. (1998). Ku protein stimulates DNA end joining by mammalian DNA ligases: a direct role for Ku in repair of DNA double-strand breaks. *Embo J* **17**(2): 609-14.

Richardson, C., Stark, J. M., Ommundsen, M. and Jasin, M. (2004). Rad51 overexpression promotes alternative double-strand break repair pathways and genome instability. *Oncogene* **23**(2): 546-53.

Rigas, B., Borgo, S., Elhosseiny, A., Balatsos, V., Manika, Z., Shinya, H., Kurihara, N., Go, M. and Lipkin, M. (2001). Decreased expression of DNA-dependent protein kinase, a DNA repair protein, during human colon carcinogenesis. *Cancer Res* **61**(23): 8381-4.

Robert, J. and Larsen, A. K. (1998). Drug resistance to topoisomerase II inhibitors. *Biochimie* **80**(3): 247-54.

Ross, D. D., Yang, W., Abruzzo, L. V., Dalton, W. S., Schneider, E., Lage, H., Dietel, M., Greenberger, L., Cole, S. P. and Doyle, L. A. (1999). Atypical multidrug resistance: breast cancer resistance protein messenger RNA expression in mitoxantrone-selected cell lines. *J Natl Cancer Inst* **91**(5): 429-33.

Rothkamm, K., Kruger, I., Thompson, L. H. and Lobrich, M. (2003). Pathways of DNA double-strand break repair during the mammalian cell cycle. *Mol Cell Biol* **23**(16): 5706-15.

Russell, J. S., Brady, K., Burgan, W. E., Cerra, M. A., Oswald, K. A., Camphausen, K. and Tofilon, P. J. (2003). Gleevec-mediated inhibition of Rad51 expression and enhancement of tumor cell radiosensitivity. *Cancer Res* **63**(21): 7377-83.

Sagara, Y., Mimori, K., Yoshinaga, K., Tanaka, F., Nishida, K., Ohno, S., Inoue, H. and Mori, M. (2004). Clinical significance of Caveolin-1, Caveolin-2 and HER2/neu mRNA expression in human breast cancer. *Br J Cancer* **91**(5): 959-65.

Sandler, A., Gordon, M., De Alwis, D. P., Pouliquen, I., Green, L., Marder, P., Chaudhary, A., Fife, K., Battiato, L., Sweeney, C., Jordan, C., Burgess, M. and Slapak, C. A. (2004). A Phase I trial of a potent P-glycoprotein inhibitor, zosuquidar trihydrochloride (LY335979), administered intravenously in combination with doxorubicin in patients with advanced malignancy. *Clin Cancer Res* **10**(10): 3265-72.

Scheffer, G. L., Maliepaard, M., Pijnenborg, A. C., van Gastelen, M. A., de Jong, M. C., Schroeijers, A. B., van der Kolk, D. M., Allen, J. D., Ross, D. D., van der Valk, P., Dalton, W. S., Schellens, J. H. and Scheper, R. J. (2000). Breast cancer resistance protein is localized at the plasma membrane in mitoxantrone- and topotecan-resistant cell lines. *Cancer Res* **60**(10): 2589-93.

Schellens, J. H., Maliepaard, M., Scheper, R. J., Scheffer, G. L., Jonker, J. W., Smit, J. W., Beijnen, J. H. and Schinkel, A. H. (2000). Transport of topoisomerase I inhibitors by the breast cancer resistance protein. Potential clinical implications. *Ann N Y Acad Sci* **922**: 188-94.

Sebastiano, R., Citterio, A., Lapadula, M. and Righetti, P. G. (2003). A new deuterated alkylating agent for quantitative proteomics. *Rapid Commun Mass Spectrom* **17**(21): 2380-6.

Shen, H., Schultz, M., Kruh, G. D. and Tew, K. D. (1998). Increased expression of DNA-dependent protein kinase confers resistance to adriamycin. *Biochim Biophys Acta* **1381**(2): 131-8.

Shepard, R. L., Cao, J., Starling, J. J. and Dantzig, A. H. (2003). Modulation of P-glycoprotein but not MRP1- or BCRP-mediated drug resistance by LY335979. *Int J Cancer* **103**(1): 121-5.

Shintani, S., Mihara, M., Li, C., Nakahara, Y., Hino, S., Nakashiro, K. and Hamakawa, H. (2003). Up-regulation of DNA-dependent protein kinase correlates with radiation resistance in oral squamous cell carcinoma. *Cancer Sci* **94**(10): 894-900.

Simpson, R. J. (2003). Proteins and Proteomics, A Laboratory Manual, Cold Spring Harbor Laboratory Press.

Slamon, D. J., Clark, G. M., Wong, S. G., Levin, W. J., Ullrich, A. and McGuire, W. L. (1987). Human breast cancer: correlation of relapse and survival with amplification of the HER-2/neu oncogene. *Science* **235**(4785): 177-82.

Slamon, D. J., Leyland-Jones, B., Shak, S., Fuchs, H., Paton, V., Bajamonde, A., Fleming, T., Eiermann, W., Wolter, J., Pegram, M., Baselga, J. and Norton, L. (2001). Use of chemotherapy plus a monoclonal antibody against HER2 for metastatic breast cancer that overexpresses HER2. *N Engl J Med* **344**(11): 783-92.

Sliwkowski, M. X., Lofgren, J. A., Lewis, G. D., Hotaling, T. E., Fendly, B. M. and Fox, J. A. (1999). Nonclinical studies addressing the mechanism of action of trastuzumab (Herceptin). *Semin Oncol* **26**(4 Suppl 12): 60-70.

Smaili, S. S., Hsu, Y. T., Carvalho, A. C., Rosenstock, T. R., Sharpe, J. C. and Youle, R. J. (2003). Mitochondria, calcium and pro-apoptotic proteins as mediators in cell death signaling. *Braz J Med Biol Res* **36**(2): 183-90.

Sotiriou, C., Powles, T. J., Dowsett, M., Jazaeri, A. A., Feldman, A. L., Assersohn, L., Gadisetti, C., Libutti, S. K. and Liu, E. T. (2002). Gene expression profiles derived from fine needle aspiration correlate with response to systemic chemotherapy in breast cancer. *Breast Cancer Res* **4**(3): R3.

Stastny, J., Prasad, R. and Fosslien, E. (1984). Tissue proteins in breast cancer, as studied by use of two-dimensional electrophoresis. *Clin Chem* **30**(12 Pt 1): 1914-8.

Stearns, V., Davidson, N. E. and Flockhart, D. A. (2004). Pharmacogenetics in the treatment of breast cancer. *Pharmacogenomics J* **4**(3): 143-53.

Sturzbecher, H. W., Donzelmann, B., Henning, W., Knippschild, U. and Buchhop, S. (1996). p53 is linked directly to homologous recombination processes via RAD51/RecA protein interaction. *Embo J* **15**(8): 1992-2002.

Su, F., Hu, X., Jia, W., Gong, C., Song, E. and Hamar, P. (2003). Glutathion S transferase pi indicates chemotherapy resistance in breast cancer. *J Surg Res* **113**(1): 102-8.

Sullivan, D. M., Latham, M. D. and Ross, W. E. (1987). Proliferation-dependent topoisomerase II content as a determinant of antineoplastic drug action in human, mouse, and Chinese hamster ovary cells. *Cancer Res* **47**(15): 3973-9.

Sumner, L. W., Wolf-Sumner, B., White, S. P. and Asirvatham, V. S. (2002). Silver stain removal using H2O2 for enhanced peptide mass mapping by matrix-assisted laser desorption/ionization time-of-flight mass spectrometry. *Rapid Commun Mass Spectrom* **16**(3): 160-8.

Taki, T., Ohnishi, T., Yamamoto, A., Hiraga, S., Arita, N., Izumoto, S., Hayakawa, T. and Morita, T. (1996). Antisense inhibition of the RAD51 enhances radiosensitivity. *Biochem Biophys Res Commun* **223**(2): 434-8.

Tan M, Y. J., Yu D. (1997). Overexpression of the c-erbB-2/neu gene enhanced intrinsic metastatic potential in human breast cancer cells without increasing their transformation abilities. *Cancer Res* **57**: 1199-1205.

Tanoguchi, K., Sasano, H., Yabuki, N., Kikuchi, A., Ito, K., Sato, S. and Yajima, A. (1998). Immunohistochemical and two-parameter flow cytometric studies of DNA topoisomerase II alpha in human epithelial ovarian carcinoma and germ cell tumor. *Mod Pathol* **11**(2): 186-93.

Tarsounas, M., Davies, D. and West, S. C. (2003). BRCA2-dependent and independent formation of RAD51 nuclear foci. *Oncogene* **22**(8): 1115-23.

Taylor, G. P., Ed. (2003). Current Protocols in Protein Science, John Wiley & Sons, Inc.

Terry, D. E. and Desiderio, D. M. (2003). Between-gel reproducibility of the human cerebrospinal fluid proteome. *Proteomics* **3**(10): 1962-79.

Thiebaud, D. and Secrest, R. J. (2001). Selective estrogen receptor modulators: mechanism of action and clinical experience. Focus on raloxifene. *Reprod Fertil Dev* **13**(4): 331-6.

Topcu, Z. (2001). DNA topoisomerases as targets for anticancer drugs. *J Clin Pharm Ther* **26**(6): 405-16.

Ueda, K., Cornwell, M. M., Gottesman, M. M., Pastan, I., Roninson, I. B., Ling, V. and Riordan, J. R. (1986). The mdr1 gene, responsible for multidrug-resistance, codes for P-glycoprotein. *Biochem Biophys Res Commun* **141**(3): 956-62.

Um, J. H., Kwon, J. K., Kang, C. D., Kim, M. J., Ju, D. S., Bae, J. H., Kim, D. W., Chung, B. S. and Kim, S. H. (2004). Relationship between antiapoptotic molecules and metastatic potency and the involvement of DNA-dependent protein kinase in the chemosensitization of metastatic human cancer cells by epidermal growth factor receptor blockade. *J Pharmacol Exp Ther* **311**(3): 1062-70.

Unlu, M., Morgan, M. E. and Minden, J. S. (1997). Difference gel electrophoresis: a single gel method for detecting changes in protein extracts. *Electrophoresis* **18**(11): 2071-7.

Valerie, K. and Povirk, L. F. (2003). Regulation and mechanisms of mammalian double-strand break repair. *Oncogene* **22**(37): 5792-812.

Van den Bergh, G., Clerens, S., Vandesande, F. and Arckens, L. (2003). Reversed-phase high-performance liquid chromatography prefractionation prior to two-dimensional difference gel electrophoresis and mass spectrometry identifies new differentially expressed proteins between striate cortex of kitten and adult cat. *Electrophoresis* **24**(9): 1471-81.

Varadi, A., Szakacs, G., Bakos, E. and Sarkadi, B. (2002). P glycoprotein and the mechanism of multidrug resistance. *Novartis Found Symp* **243**: 54-65; discussion 65-8, 180-5.

Veuger, S. J., Curtin, N. J., Richardson, C. J., Smith, G. C. and Durkacz, B. W. (2003). Radiosensitization and DNA repair inhibition by the combined use of novel inhibitors of DNA-dependent protein kinase and poly(ADP-ribose) polymerase-1. *Cancer Res* **63**(18): 6008-15.

Vispe, S., Cazaux, C., Lesca, C. and Defais, M. (1998). Overexpression of Rad51 protein stimulates homologous recombination and increases resistance of mammalian cells to ionizing radiation. *Nucleic Acids Res* **26**(12): 2859-64.

Vogel, C. L., Cobleigh, M. A., Tripathy, D., Gutheil, J. C., Harris, L. N., Fehrenbacher, L., Slamon, D. J., Murphy, M., Novotny, W. F., Burchmore, M., Shak, S. and Stewart, S. J. (2001). First-line Herceptin monotherapy in metastatic breast cancer. *Oncology* **61 Suppl 2**: 37-42.

Wang, H., Zeng, Z. C., Bui, T. A., Sonoda, E., Takata, M., Takeda, S. and Iliakis, G. (2001a). Efficient rejoining of radiation-induced DNA double-strand breaks in vertebrate cells deficient in genes of the RAD52 epistasis group. *Oncogene* **20**(18): 2212-24.

Wang, Z. M., Chen, Z. P., Xu, Z. Y., Christodoulopoulos, G., Bello, V., Mohr, G., Aloyz, R. and Panasci, L. C. (2001). In vitro evidence for homologous recombinational repair in resistance to melphalan. *J Natl Cancer Inst* **93**(19): 1473-8.

Welcsh, P. L., Lee, M. K., Gonzalez-Hernandez, R. M., Black, D. J., Mahadevappa, M., Swisher, E. M., Warrington, J. A. and King, M. C. (2002). BRCA1 transcriptionally regulates genes involved in breast tumorigenesis. *Proc Natl Acad Sci U S A* **99**(11): 7560-5.

Wen, S. F., Mahavni, V., Quijano, E., Shinoda, J., Grace, M., Musco-Hobkinson, M. L., Yang, T. Y., Chen, Y., Runnenbaum, I., Horowitz, J., Maneval, D., Hutchins, B. and Buller, R. (2003). Assessment of p53 gene transfer and biological activities in a clinical study of adenovirus-p53 gene therapy for recurrent ovarian cancer. *Cancer Gene Ther* **10**(3): 224-38.

Wikman, H., Seppanen, J. K., Sarhadi, V. K., Kettunen, E., Salmenkivi, K., Kuosma, E., Vainio-Siukola, K., Nagy, B., Karjalainen, A., Sioris, T., Salo, J., Hollmen, J., Knuutila, S.

and Anttila, S. (2004). Caveolins as tumour markers in lung cancer detected by combined use of cDNA and tissue microarrays. *J Pathol* **203**(1): 584-93.

Willmore, E., De Caux, S., Sunter, N. J., Tilby, M. J., Jackson, G. H., Austin, C. A. and Durkacz, B. W. (2004). A novel DNA-dependent protein kinase inhibitor NU7026 potentiates the cytotoxicity of topoisomerase II poisons used in the treatment of leukemia. *Blood*.

Withoff, S., De Jong, S., De Vries, E. G. and Mulder, N. H. (1996). Human DNA topoisomerase II: biochemistry and role in chemotherapy resistance (review). *Anticancer Res* **16**(4A): 1867-80.

Woessner, R. D., Mattern, M. R., Mirabelli, C. K., Johnson, R. K. and Drake, F. H. (1991). Proliferation- and cell cycle-dependent differences in expression of the 170 kilodalton and 180 kilodalton forms of topoisomerase II in NIH-3T3 cells. *Cell Growth & Differentiation: The Molecular Biology Journal Of The American Association For Cancer Research* **2**(4): 209-214.

Wulfkuhle, J. D., McLean, K. C., Paweletz, C. P., Sgroi, D. C., Trock, B. J., Steeg, P. S. and Petricoin, E. F., 3rd (2001). New approaches to proteomic analysis of breast cancer. *Proteomics* **1**(10): 1205-15.

Xia, S. J., Shammas, M. A. and Shmookler Reis, R. J. (1997). Elevated recombination in immortal human cells is mediated by HsRAD51 recombinase. *Mol Cell Biol* **17**(12): 7151-8.

Xie, D., Jauch, A., Miller, C. W., Bartram, C. R. and Koeffler, H. P. (2002). Discovery of over-expressed genes and genetic alterations in breast cancer cells using a combination of suppression subtractive hybridization, multiplex FISH and comparative genomic hybridization. *Int J Oncol* **21**(3): 499-507.

Xu, L., Pirollo, K. F. and Chang, E. H. (2001). Tumor-targeted p53-gene therapy enhances the efficacy of conventional chemo/radiotherapy. *J Control Release* **74**(1-3): 115-28.

Yanagisawa, T., Urade, M., Yamamoto, Y. and Furuyama, J. (1998). Increased expression of human DNA repair genes, XRCC1, XRCC3 and RAD51, in radioresistant human KB carcinoma cell line N10. *Oral Oncol* **34**(6): 524-8.

Yanez, R. J. and Porter, A. C. (1999). Gene targeting is enhanced in human cells overexpressing hRAD51. *Gene Ther* **6**(7): 1282-90.

Yang, J., Xu, Z. P., Huang, Y., Hamrick, H. E., Duerksen-Hughes, P. J. and Yu, Y. N. (2004). ATM and ATR: sensing DNA damage. *World J Gastroenterol* **10**(2): 155-60.

Yang, J. M., Chin, K. V. and Hait, W. N. (1995). Involvement of phospholipase C in heat-shock-induced phosphorylation of P-glycoprotein in multidrug resistant human breast cancer cells. *Biochem Biophys Res Commun* **210**(1): 21-30.

Yoo, S. and McKee, B. D. (2004). Overexpression of Drosophila Rad51 protein (DmRad51) disrupts cell cycle progression and leads to apoptosis. *Chromosoma* **113**(2): 92-101.

Yoshikawa, K., Ogawa, T., Baer, R., Hemmi, H., Honda, K., Yamauchi, A., Inamoto, T., Ko, K., Yazumi, S., Motoda, H., Kodama, H., Noguchi, S., Gazdar, A. F., Yamaoka, Y. and Takahashi, R. (2000). Abnormal expression of BRCA1 and BRCA1-interactive DNA-repair proteins in breast carcinomas. *Int J Cancer* **88**(1): 28-36.

Yu, D. and Hung, M. C. (2000). Role of erbB2 in breast cancer chemosensitivity. *Bioessays* **22**(7): 673-80.

Yu, D., Liu, B., Jing, T., Sun, D., Price, J. E., Singletary, S. E., Ibrahim, N., Hortobagyi, G. N. and Hung, M. C. (1998). Overexpression of both p185c-erbB2 and p170mdr-1 renders breast cancer cells highly resistant to taxol. *Oncogene* **16**(16): 2087-94.

Yu, D., Wolf, J. K., Scanlon, M., Price, J. E. and Hung, M. C. (1993). Enhanced c-erbB-2/neu expression in human ovarian cancer cells correlates with more severe malignancy that can be suppressed by E1A. *Cancer Res* **53**(4): 891-8.

Yuan, S. S., Lee, S. Y., Chen, G., Song, M., Tomlinson, G. E. and Lee, E. Y. (1999). BRCA2 is required for ionizing radiation-induced assembly of Rad51 complex in vivo. *Cancer Res* **59**(15): 3547-51.

Yuan, Z. M., Huang, Y., Ishiko, T., Nakada, S., Utsugisawa, T., Kharbanda, S., Wang, R., Sung, P., Shinohara, A., Weichselbaum, R. and Kufe, D. (1998). Regulation of Rad51 function by c-Abl in response to DNA damage. *J Biol Chem* **273**(7): 3799-802.

Zampieri, L., Bianchi, P., Ruff, P. and Arbuthnot, P. (2002). Differential modulation by estradiol of P-glycoprotein drug resistance protein expression in cultured MCF7 and T47D breast cancer cells. *Anticancer Res* **22**(4): 2253-9.

Zhou, J. and Giannakakou, P. (2005). Targeting microtubules for cancer chemotherapy. *Curr Med Chem Anti-Canc Agents* **5**(1): 65-71.